COMPUTATIONAL ASPECTS OF REAL-TIME SIMULATION OF ROTARY-WING AIRCRAFT

By

Jacob Albert Houck

B.S. Aerospace Engineering

North Carolina State University

May 1970

A Thesis submitted to

the Faculty of

The School of Engineering and Applied Science

of The George Washington University in partial satisfaction

of the requirements for the degree of Master of Science

May 1976

Thesis directed by

Dr. Roland L. Bowles

Assistant Professorial Lecturer in Engineering

ABSTRACT

A study was conducted to determine the effects of degrading a rotating blade element rotor mathematical model suitable for real-time simulation of rotorcraft. Three methods of degradation were studied, reduction of number of blades, reduction of number of blade segments, and increasing the integration interval, which has the corresponding effect of increasing blade azimuthal advance angle. The three degradation methods were stucied through static trim comparisons, total rotor force and moment comparisons, single blade force and moment comparisons over one complete revolution, and total vehicle dynamic response comparisons. Recommendations are made concerning model degradation which should serve as a guide for future users of this mathematical model, and in general, they are in order of minimum impact on model validity: 1) reduction of number of blade segments, 2) reduction of number of blades, and 3) increase of integration interval and azimuthal advance angle. Extreme limits are specified beyond which a different rotor mathematical model should be used.

ACKNOWLEDGEMENTS

My deepest appreciation is extended to all those whose efforts contributed to this document. I am indebted to the National Aeronautics and Space Administration for allowing me the time and opportunity to conduct this study. Words of thanks are due to Mr. Roman Lytwyn, Mr. James E. Dieudonne, and Mr. Burnell T. McKissick for their help in the technical editing of the paper. I would also like to thank Mr. Kenneth S. Pollock and Miss Mary M. Browne for their help in computer programing and Ms. Ann Walker in preparing the manuscript. Finally, I am deeply grateful to Dr. Roland L. Bowles, Chairman of my advisory committee, for his advice in organizing the study and for his suggestions in presenting the results.

TABLE OF CONTENTS

LIST OF TABLES

LIST OF FIGURES

LIST OF FIGURES (Cont'd.)

LIST OF FIGURES (Cont'd.)

LIST OF SYMBOLS AND ABBREVIATIONS

b	blades
BR	blade flapping angle, degrees
CDC	Control Data Corporation
IFR	instrument flight rules
NASA	National Aeronautics and Space Administration
PB	body axis roll rate, degrees per second
PBD	body axis roll acceleration, radians per second^2
PHI, ϕ	roll attitude, degrees
s	segments
THET, θ	pitch attitude, degrees
VTOL	vertical take-off and landing
XA	lateral cyclic control position, % of total travel
XB	longitudinal cyclic control position, % of total travel
XC	collective control position, % of total travel
XLAG	blade lagging angle, degrees
XP	tail rotor pedal control position, % of total travel
α	angle of attack, degrees
Δt	integration interval, seconds
$\Delta\Psi$	azimuthal advance angle, degrees

INTRODUCTION

In view of the expanding interest in helicopter research and development in the past decade at the Langley Research Center (LaRC), several real-time man-in-the-loop helicopter simulation programs have been developed. The simulations have been used as analytical tools, for man/vehicle performance evaluation, and in support of flight test programs. These studies have included flight director development, development and evaluation of advanced heads-up computer generated displays, route structure development for intercity transportation, evaluation of terminal area navigation and approach procedures, motion-visual research, and mathematical model research and development. The rotorcraft mathematical models employed in these studies have varied from simple linear perturbation models to full force and moment models including rotating blade element rotor models. Figure 1 presents a chronology of these models and studies.

An initial effort was begun in 1968 to develop a real-time simulation program using a rotor design model similar in scope and complexity to the nonreal-time Bell Helicopter Company C-81 programs, the most recent of which is documented in reference 1. This model proved too complex mathematically and beyond the computational capabilities of the LaRC real-time simulation (RTS) facility (Appendix A). At present this is still true, but should be partially rectified with the acquisition of new computers by mid-1976.

In 1969, a linear perturbation model was developed. The model contained constant derivatives, and therefore, was limited about trim velocities represented by those derivatives. The model contained no rotor representation, however, rotor effects were lumped in the derivatives of the vehicle. The

CHRONOLOGY OF SIMULATION EFFORT

1968 - Initial Effort

Effort To Write Real-Time Program Using A Rotor Design Model

Model too Complex for Real-Time Simulations

1969 - Linear Perturbation Model - No Rotor

Support of CH-46 Automatic Landing Studies

VTOL Flight Director Development

1970 - 71 - Modified Blade Element Model

COBRA - Basic Validation Program

S-61 Instrument Flight Rules - Enroute and Terminal Area Navigation

S-61 Pilot Display - Heads-Up Display Studies

Helicopter/Fighter Evasive Maneuvers

S-61 Motion/Visual Evaluation

1974 - Present Modified Bailey Classical Rotor Model

CH-54 Sling Load Studies

1974 - Present Advanced Research Helicopter Rotating Blade Element Model

Support Research in Rotor Model Simulation

Rotor Systems Research Aircraft Support

Advancing Blade Concept Vehicle

Figure 1

simulation utilized a fixed-base cockpit with the minimum necessary instrumentation to accomplish the tasks undertaken. This simulation was utilized for design and evaluation of VTOL flight directors, (References 2 and 3), evaluation of moving map systems, design and evaluation of graphics displays, and support of the CH-46 Automatic Landing Flight Program which resulted in the first automatic landing of a helicopter to a predetermined point. Presently the simulation is being used to support the NASA VTOL Approach and Landing Technology (VALT) Program.

During 1970 - 1971, another effort was initiated to develop a real-time simulation program containing a rotor mathematical model. It was decided in this effort to use a rotor model (Modified Blade Element) developed by Melpar, Inc. under a U.S. Navy contract (Reference 4), and later applied to a HUEYCOBRA helicopter under a U.S. Army contract by Electronic Associates, Inc. (Reference 5). The mathematical model and computer program were updated and converted to run on the Langley Research Center RTS system (Reference 6). The vehicle model contains nonlinear six-degree-of-freedom rigid body dynamics, nonlinear aerodynamic data for the rotor and body, and a complex stability and control augmentation system. The equations are not constrained to a given flight condition but are valid over the entire flight regime including hover, transition, forward flight, autorotation, etc. This simulation program was then utilized to conduct enroute IFR navigation studies, terminal area IFR navigation and approach studies in the New York metropolitan area, and pilot workload and task performance studies (Reference 7). The simulation utilized a fixed base cockpit containing the navigation equipment necessary to conduct these tests. The simulation when developing pilot displays

and special instrumentation (Reference 8) utilized a visual system representing an airport and a link to a graphics computer to generate heads-up displays for approach and landing aids. These studies supported the NASA VALT program. Two additional studies are presently underway - one to develop and evaluate motion-visual requirements for VTOL simulation, and the second to develop and evaluate helicopter/fighter evasive maneuvers employing the LaRC Differential Maneuvering Simulator.

In 1974, development of a simulation program utilizing a Modified Bailey Classical Rotor model to represent a CH-54 heavy lift helicopter for sling load studies was begun. Primary applications for this on-going study are development and evaluation of load stabilization systems and evaluation of advanced load display systems.

With the advanced rotor research planned at the Langley Research Center, an effort to adapt and evaluate a real-time helicopter/compound mathematical model, including a state-of-the-art rotor model was initiated in 1974. This model was developed by Sikorsky Aircraft (Reference 9) and represents the Rotor Systems Research Aircraft (RSRA). The RSRA is a flying test platform to be used in the evaluation of advanced rotor and control systems. The RSRA mathematical model was derived from Sikorsky's general helicopter simulation model which has been used extensively in nonreal-time in the design of helicopters and compound vehicles. The model is basically a total force, non-linear, large angle representation in six rigid body degrees of freedom. In addition, rotor blade flapping, lagging and hub rotational degrees of freedom are represented. Each simulated component of the aircraft (Figure 2) is modularized within the mathematical model and summed prior to the general equations of motion.

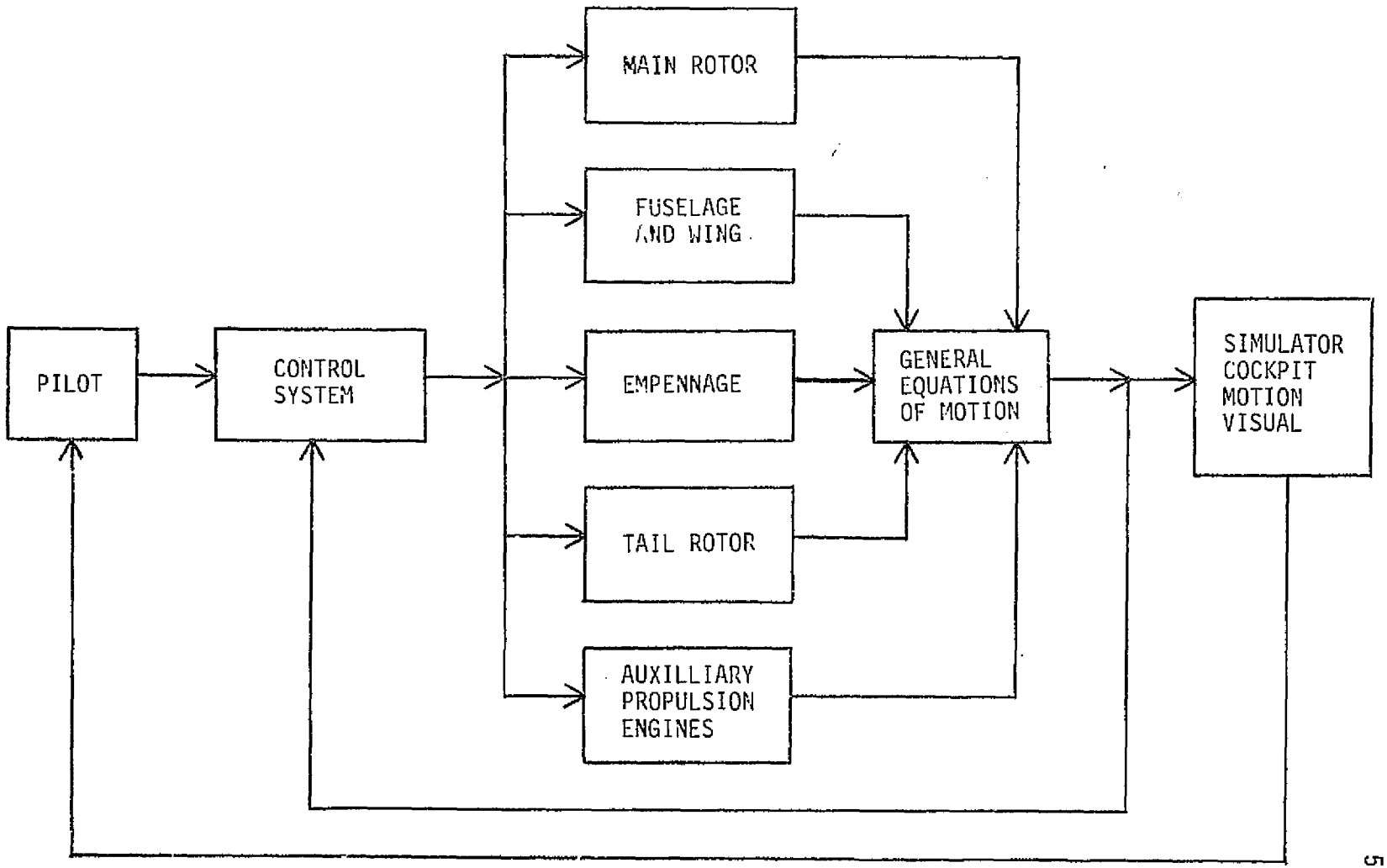

Figure 2.- Simplified Block Diagram of RSRA Mathematical Model.

This characteristic allows easy manipulation of the aircraft's configuration.

Researchers have encountered a major problem when using this mathematical model for real-time man-in-the-loop simulation studies, i.e., obtaining real-time operation while using the full rotor model (actual number of blades and a representative number of segments for each blade). Real-time operation is reached when the computer execution time for the active portion of the program is less than or equal to the prescribed integration time interval. In the past this has been accomplished by degrading the model in various ways. The purpose of this paper is to investigate the various methods of rotor and total vehicle model degradation. This will include the effects due to reducing the number of blades, reducing the number of blade segments, varying the integration interval in size which in turn varies the azimuthal advance angle, and combinations of the three. This study, while similar in scope to limited data presented in References 9 and 10, will provide extensive data on the effects of rotor degradation, total model degradation, and possible solutions to these problems.

ROTOR SYSTEMS RESEARCH AIRCRAFT VEHICLE DESCRIPTION

The following brief description from Reference 9 of the RSRA vehicle (Figure 3) is provided. The RSRA is a versatile flying test platform designed to evaluate various rotor concepts and control systems. It can be flown as a single rotor helicopter, compound helicopter, and as a fixed wing aircraft. The design gross weight in the compound configuration is 11,884 kgs. (26,200 lbs). Flight speeds from hover to 350 knots are possible depending on the configuration. Initially, the 5-bladed, 18.9 m. (62 ft.) diameter Sikorsky H-3 series main rotor system will be installed. This will be driven through a 2500 hp. gearbox by two General Electric T58 shaft turbine engines. An H-3 series tail rotor will be used for main rotor torque reaction. Auxiliary propulsion is provided by two fuselage mounted General Electric TF34 turbofan engines. The RSRA has a 34.37 sq.m. (370 sq.ft.) variable incidence wing which can be positioned in flight at angles between 15^{o} leading edge up and 9^{o} leading edge down. This allows complete unloading of the rotor at speeds down to 120 knots and increased loading of the rotor over most of its operational range. The empennage consists of a variable incidence lower horizontal stabilator with geared elevator linked directly to the wing, a high fixed horizontal stabilizer, and a vertical stabilizer. The aircraft is provided with a full complement of both fixed wing and helicopter primary controls, which in the compound mode are linked through a control phasing unit. This allows the pilot to select variable control power from each surface during flight. In addition, wing flaps and a tail-located drag brake are provided for platform lift and drag modulation, respectively. The fly-by-wire control system from the pilot's control stick has a mechanical

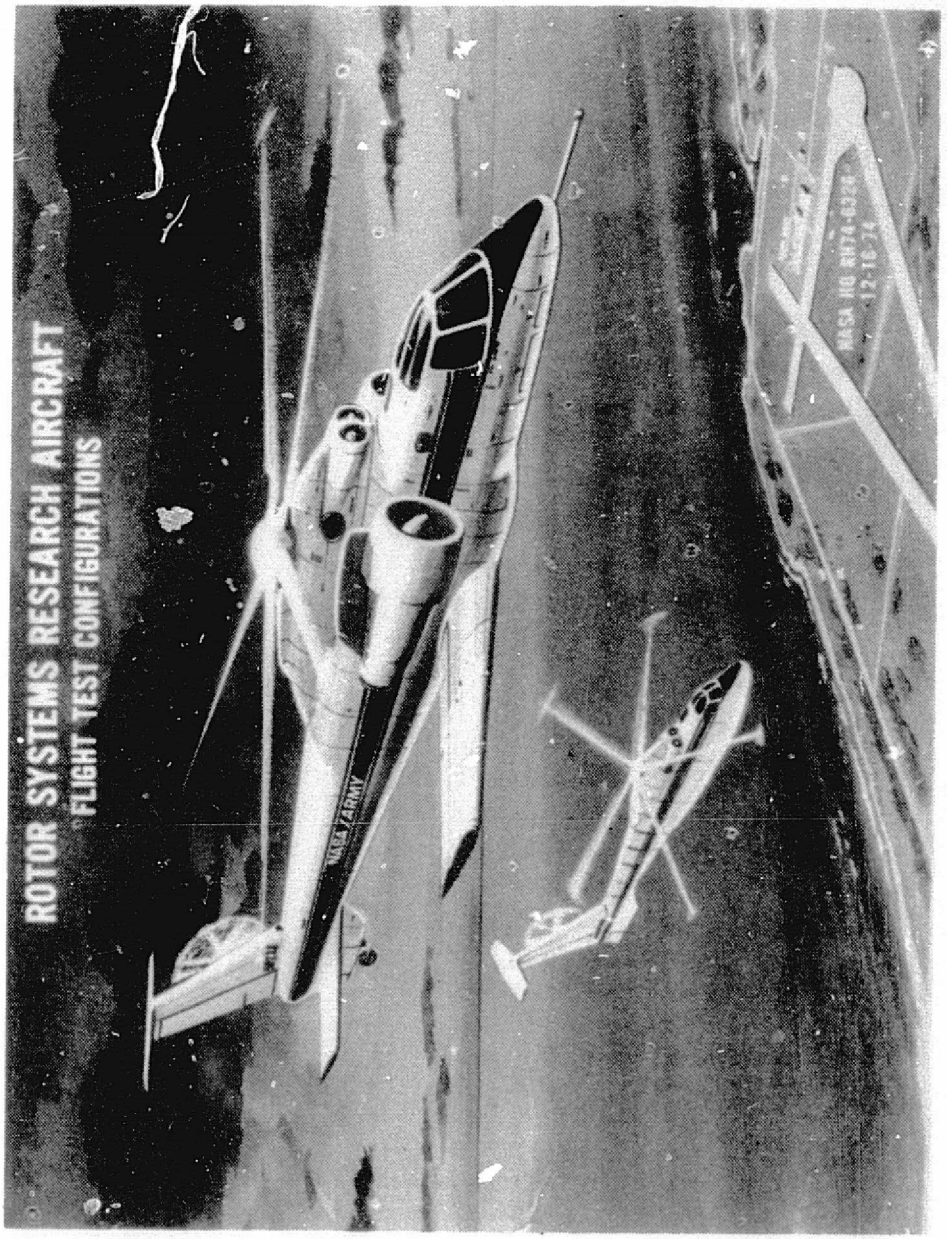

Figure 3.- Rotor Systems Research Aircraft.

backup system from the copilot's stick. The control system incorporates an onboard digital computer which processes the pilot's control movements, generates stability augmentation signals and provides signals to the control stick force augmentation system. Flight during data acquisition runs may be controlled automatically by the digital computer. In addition, it provides the capability for pre-programed testing and variable stability simulation. When the computer is disengaged, stability augmentation is provided by a backup analog system.

ROTOR MODEL DESCRIPTION

The following brief description of the rotor model is provided. The total rotor forces and moments are developed from a combination of the aerodynamic, mass and inertia loads acting on each simulated blade. For each blade simulated, the flapping and lagging degrees of freedom are represented. In addition, when the rotor speed governor is disengaged, the rotor shaft degree of freedom is released. Blade element theory is used to determine the aerodynamic loads. Blade inertia, mass and weight effects are fully accounted for in the model. The elemental aerodynamic loads, dependent on local blade angle of attack and velocity vector, are summed along each blade. The mass and inertia loads, dependent on blade and aircraft motion, are added to the aerodynamic loads for each blade. This summation gives the shear loads on the blade root hinge pins. Total rotor forces are obtained by summing all the blade hinge pin shears with regard to azimuth. Rotor moments result from the offset of the hinge shears from the center of the shaft. Blade flapping and lagging motion is determined from aerodynamics and inertia moments about the hinge pins. Interference airflow from the wing (compound vehicle only) onto the rotor and wash effects from the rotor onto the wing (compound vehicle only), fuselage, and empennage are accounted for. The following basic assumptions are made in the rotor representation:

(1) No account is taken of rotor blade or airframe flexibility.

(2) Air mass flow degree of freedom through the rotor can be represented by applying a simple lag to the calculation of downwash. The only non-uniform flow is due to increases in

forward speed. This causes a redistribution of the uniform flow from the front to the back of the disk.

(3) Simple sweep theory can be applied to determine the aerodynamic effects of yawed flow on the blade element, from unyawed flow blade data.

(4) Quasi-static aerodynamic loads.

(5) Coincident blade hinges.

For a more detailed treatment of the rotor model and computer program structure, the reader is directed to the appropriate sections in Reference 9.

PROBLEM DESCRIPTION

This section provides an insight into the difficulties encountered with the use of this rotor mathematical model, and the methods utilized by previous researchers to overcome these problems. This and the next section describe the detailed study covered in this paper to evaluate these methods in light of the RSRA vehicle.

Other researchers have been hampered in using the rotating blade element model for man-in-the-loop real-time simulation applications due primarily to the inadequate computing bandwidth of current computers. In order to use this model at all, gross degradation of the rotor representation and/or integration interval size were required. This was done so that the computer execution time for the active part of the program would be less than or equal to the desired integration interval, in other words, achieve real-time execution. The mathematical model was programed by Sikorsky Aircraft in a nonreal-time mode to insure validity of the rotor model. In the nonreal-time mode, the rotor is represented by the actual number of blades, a representative number of blade segments to adequately represent the blade loading, the actual rotor rotational rate, and a sufficiently small azimuthal advance angle, i.e., a small integration interval size. Since this type of representation precludes the achievement of real-time execution, various combinations of reduced blades, blade segments, rotor rotational rate, and increased azimuthal advance angle are utilized to fit the model into the available computer cycle time while still retaining "satisfactory" static and dynamic comparisons with the nonreal-time model. The steps necessary in reducing the mathematical model of the rotor, which accounts for a major portion of the computation time, for

real-time operation are not routine, however, some general guidelines do exist (References 9 and 10), and they are used as a starting point for this study. The guidelines are a minimum number of three blades, three blade segments, and a maximum of 30 degrees of azimuthal advance for models with higher elastic blade modes and 55 degrees for models without higher blade modes. An example of the above is provided from References 9 and 10. In this case, the vehicle represented is a Sikorsky S-65 (6 bladed) helicopter, and a maximum azimuthal advance of 50 degrees was chosen. Figure 4 shows the effect of rotor rotational speed and azimuthal update on allowable program execution time for flapping convergence. Several Sikorsky present and future helicopters are provided for comparison. As can be seen the maximum program execution time available for the S-65 helicopter, given a 50 degree azimuthal increase is approximately 46 to 47 milliseconds. This allowable program execution time must now be matched to the computational speed capability of the digital computer being used, in this case, a PDP-10 computer. Figure 5 shows this capability for the PDP-10 computer executing an S-65 helicopter simulation program. Boundaries of minimum blades and blade segments are indicated along with the allowable program execution time established in Figure 4. For this particular aircraft and computer, a solution existed of 4 blades and 5 blade segments which met the user's, Sikorsky Aircraft, requirements, however, situations can arise with higher rotational speed rotors and inadequate computers where the rotor must be "artifically slowed down" in order to simulate the necessary blades and blade segments and to obtain flapping convergence.

The Langley Research Center is confronted with the problem of using this

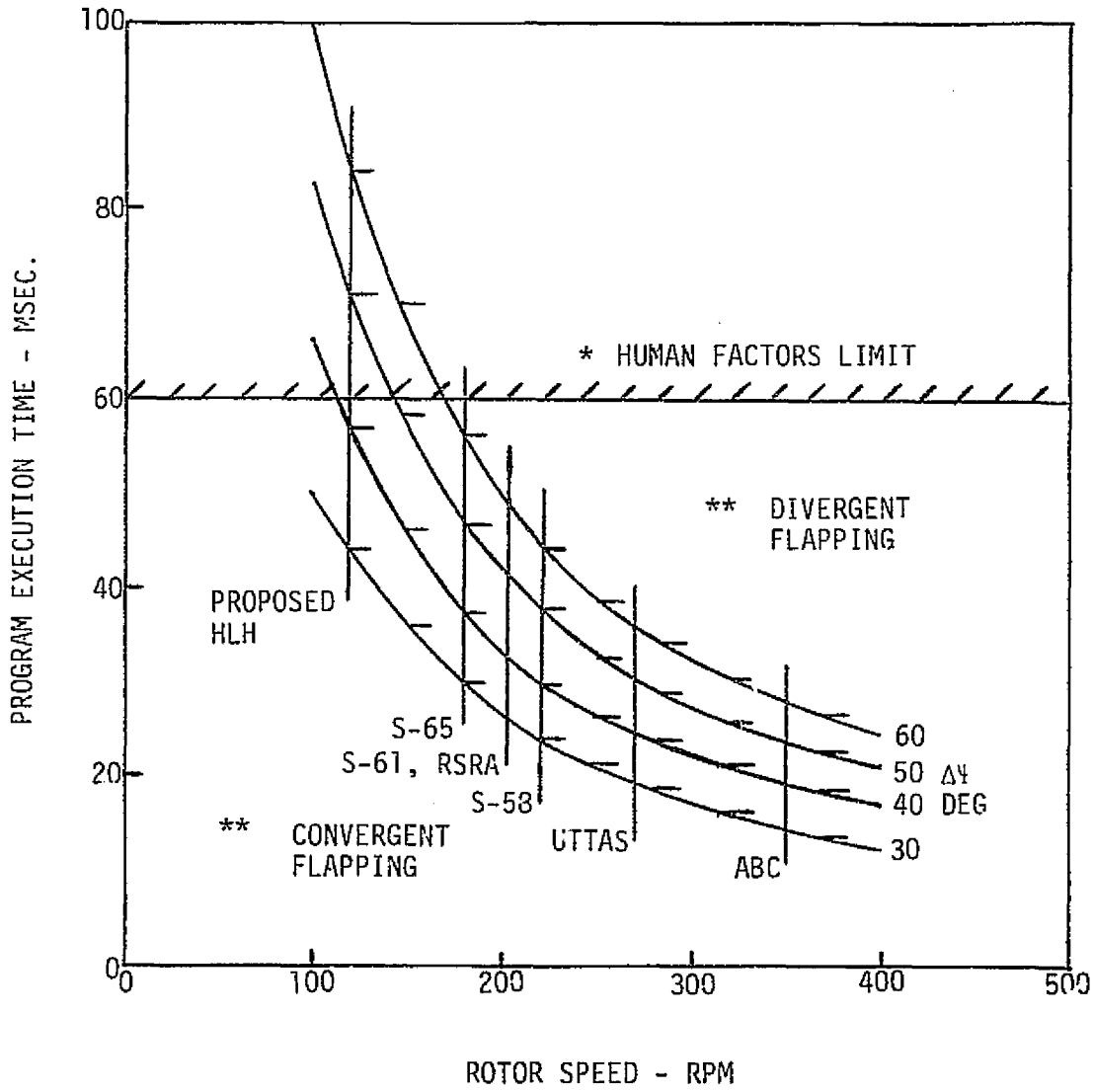

Figure 4.- Effect of Rotor Speed and Azimuthal Update on Allowable Program Execution Time for Flapping Convergence.

* Visual flicker, motion base stepping, instrument flicker, etc. noticeable to pilot.

** Mathematical convergence and divergence.

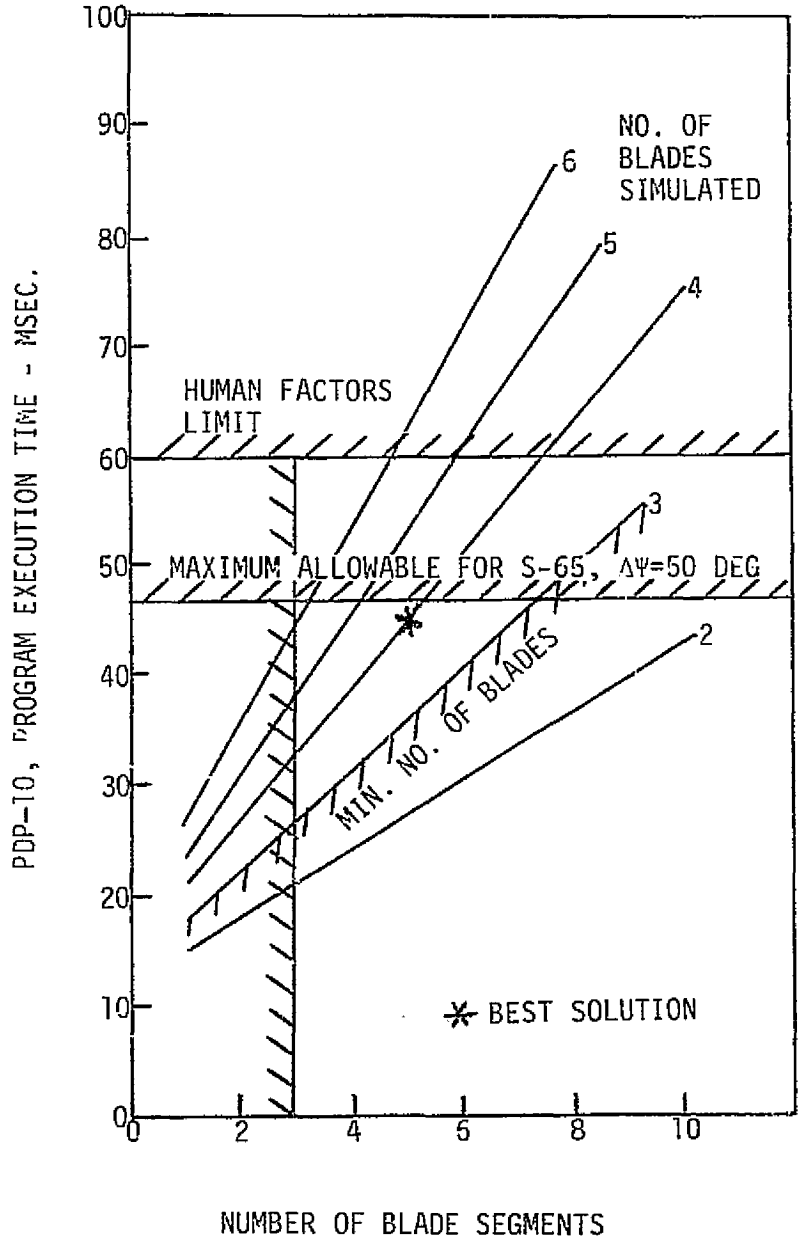

Figure 5.- Program Execution Time for an S-65 Series Simulation on the PDP-10 Computer.

model to represent the RSRA vehicle and candidate advanced rotors and control systems for both objective and subjective man-in-the-loop real-time studies, and a question exists as to whether this can be done with sufficient validity. Presently, the rotor mathematical model is structured to represent the H-3 series main rotor which will be delivered with the vehicle. This consists of 5 blades (actual number), 5 blade segments, and 203.3 RPM (actual rotor rotational rate). The standard LaRC RTS integration interval of 1/32 of a second (31.25 milliseconds) is being used which leads to an azimuthal advance of 38.1 degrees. Once the computer system overhead is subtracted, this leaves some 28 milliseconds of which the RSRA helicopter configuration presently uses approximately 22 milliseconds, however, the RSRA compound configuration requires slightly more than 28 milliseconds and will not achieve real-time status with this integration interval.

Some relief is offered for the future when the Langley Research Center's new computers, CDC CYBER 175's, are delivered. Figure 6 presents a 5-bladed rotor model of 200 RPM rotational rate or essentially the RSRA rotor system as delivered. An azimuthal advance angle of 30 degrees was chosen for illustrative purposes. Program execution time has been normalized to unity for the CDC 6600 computer with the ICOPS RUN compiler. The CDC CYBER 175 with the NOS FTN compiler (optimization enabled) is represented at its tested bandwidth of 3.5 times faster than the CDC 6600. As in Figure 5, minimum blade and blade segment boundaries are presented. The crossed area represents the combinations of blades and blade segments which can be modeled on the CDC 6600. Note that the 5-blade 5-blade segment representation decided upon for the RSRA real-time simulation program cannot be achieved for this azimuthal advance angle, however,

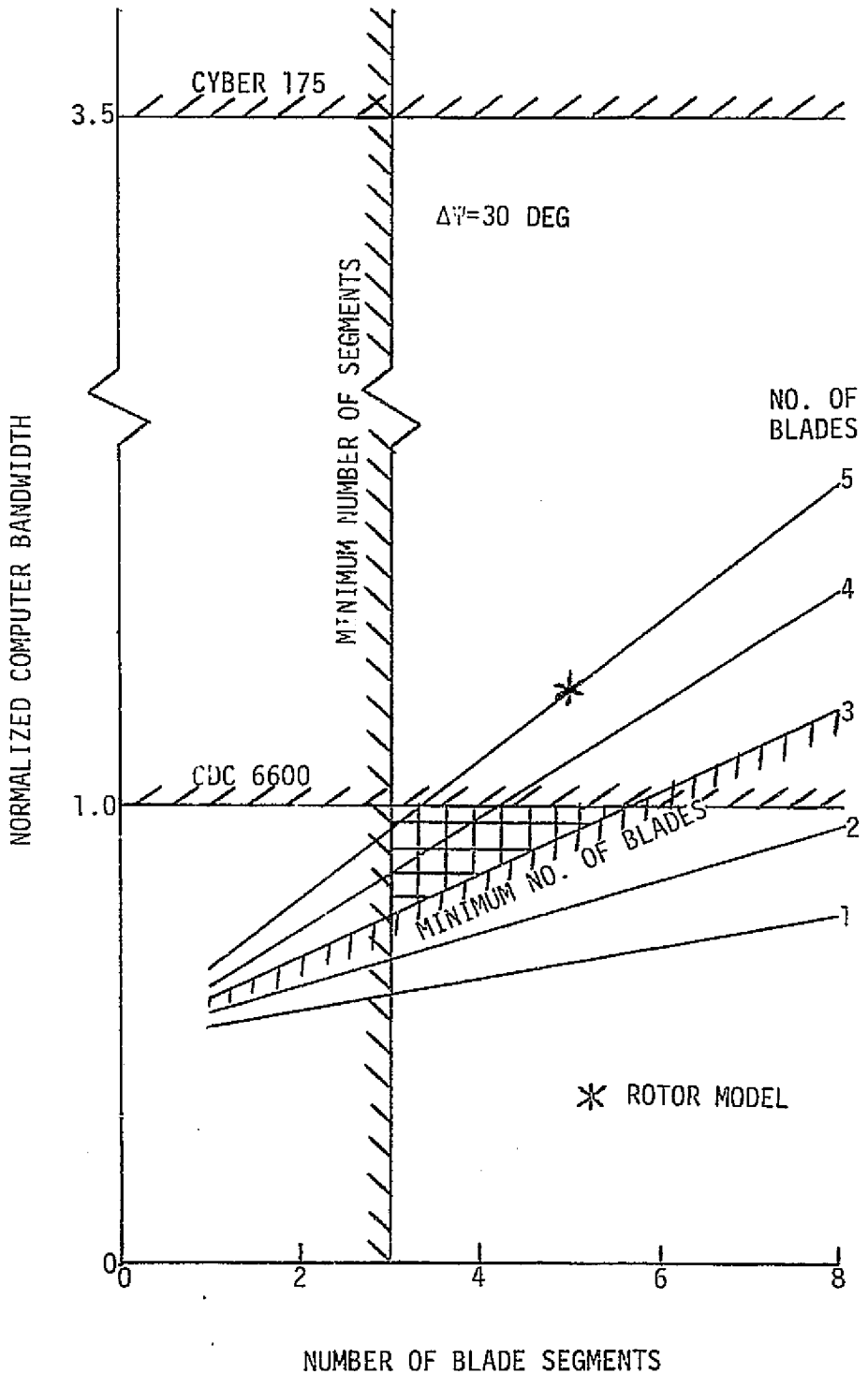

Figure 6.- Comparison of Program Execution Time for a CDC 6600 Computer vs. a CDC CYBER 175 Computer for a 5-Blade, 200 RPM Rotor Model.

the CDC CYBER 175 would be able to handle the representation easily.

Figure 7 presents a case which the CDC CYBER 175 will have trouble handling, that of a Sikorsky Aircraft ABC (advancing blade concept) rotor system, a possible candidate rotor system for the RSRA. This rotor system consists of two 3-bladed coaxial counter rotating systems revolving at 350 RPM. Again an azimuthal advance angle of 30 degrees has been chosen for illustrative purposes, however, this time the Langley Research Center motion/visual software package has also been included. In the case of the ABC rotor system, the number of blades represented cannot be reduced below six since it consists of two 3-bladed systems. From the figure it can be seen that the CDC 6600 cannot represent the rotor system without artifically slowing the rotor and/or opening the azimuthal advance angle. The CDC CYBER 175 can solve several rotor configurations, however, this computer is also limited if expansion in number of blade segments or reduction in azimuthal advance angle is required.

Thus even with the new CDC CYBER 175 computers, cases can arise where degradation of the rotor mathematical model will be required, however at this time the CDC CYBER 175 computers are not yet operational for real-time simulation. Therefore, the problem at hand is that of representing the RSRA vehicle on the CDC 6600 computer with an adequate rotor mathematical model for real-time simulation for both objective and subjective tests knowing that additional computer requirements for visual systems, complete cockpit requirements, landing gear models, electronic flight control computer interfacing, etc. are on the near horizon.

The purpose of this paper is to present a systematic parametric study

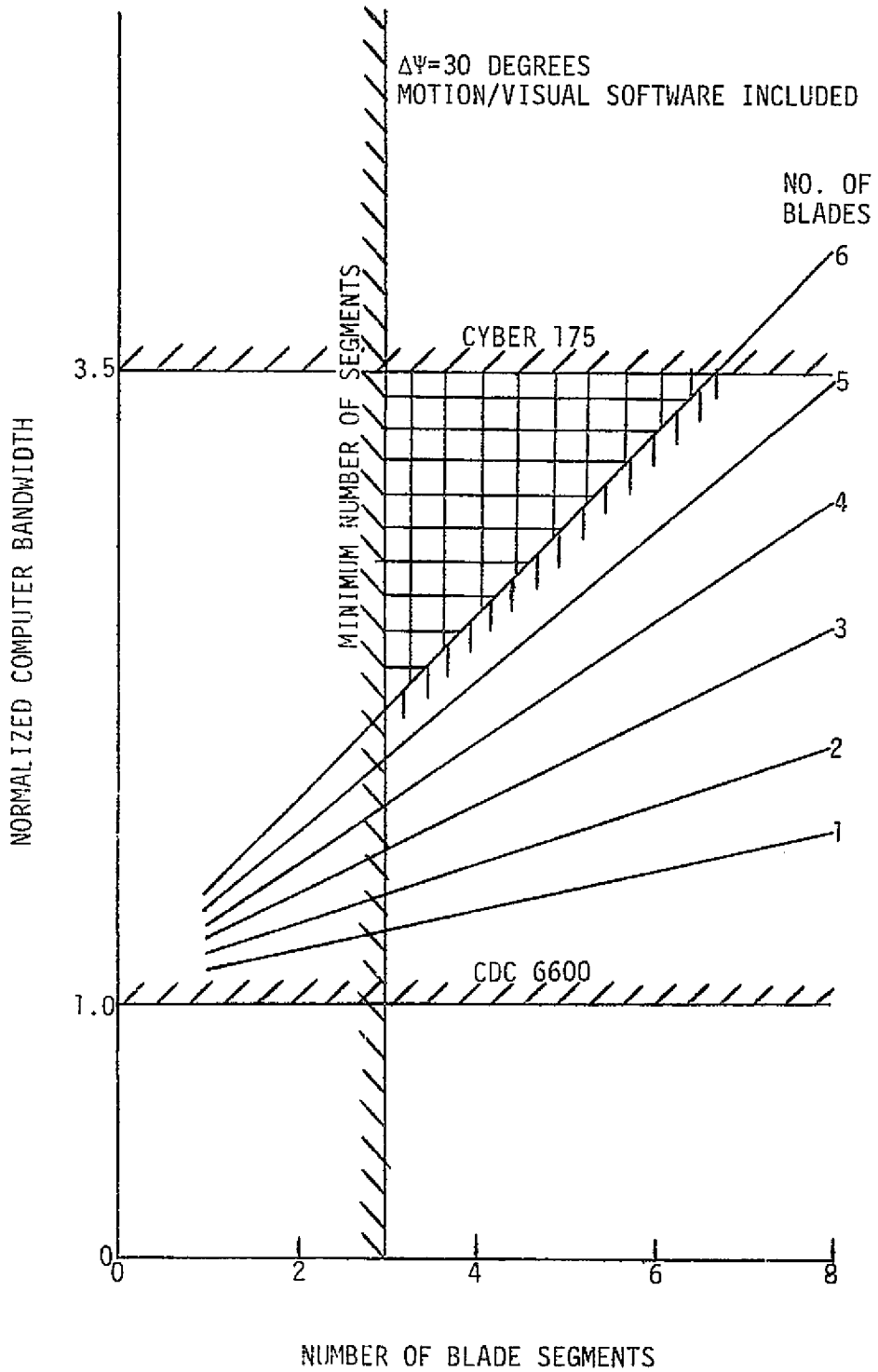

Figure 7.- Comparison of Program Execution Time for a CDC 6600 Computer vs. a CDC CYBER 175 Computer for a 6-Blade, 350 RPM Rotor Model.

consisting of blade reduction, blade segment reduction, integration interval increase (i.e. azimuthal advance angle increase), and combinations of the three methods of degradation. Effects on both static and dynamic solutions will be presented, thus leading to the best method of representing the rotor system under the constraints of real-time computer duty cycle time and accuracy of solution required.

TECHNICAL APPROACH

In order to study the effects of reducing number of blades, number of blade segments, and increasing integration interval size, four types of tests were conducted. They consisted of vehicle static trim comparisons, total rotor force and moment comparisons (mean and standard deviation), blade parameter comparisons for a 360 degree sweep, and dynamic response comparisons for the total vehicle. The vehicle configuration chosen for the study was that of the helicopter.

The rotor mathematical model was set up with 5-blades and 10-blade segments. A rotor speed of 200 RPM (203 RPM - actual RSRA rotor speed) was chosen so that for the integration intervals studied the rotor blades would always assume the same azimuthal locations for each rotation. Finally an integration interval of 1/240 seconds was chosen which in turn caused the blade azimuthal advance angle to be 5 degrees. The above description constitutes the "truth" configuration and was used as a base to which all other configurations could be compared.

The rotor mathematical model was degraded systematically. The number of blade segments was held constant at 5 and integration interval constant at 1/240 seconds as the number of blades was reduced. The number of blades was then held constant at 5 as the number of blade segments was reduced. A separate configuration was studied which consisted of 3-blades and 3-blade segments to study combination effects. In order to study the effect of integration interval size, two rotor mathematical configurations - 5-blades 5-blade segments and 3-blades 3-blade segments; and three interval sizes - 1/240 seconds, 1/30 seconds, and 1/20 seconds were chosen. These intervals

were chosen for the following reasons: 1/30 seconds is approximately the integration interval used at the LaRC for the RSRA simulation and 1/20 seconds is approximately the integration interval utilized by another user of the mathematical model for the same simulation. Appendix B describes the methods used in degrading the rotor model. Table 1 details all configurations used in this study.

The static trim tests were set up in the following manner. The RSRA vehicle was initialized at 500 feet of altitude with the rotor mathematical model set for the desired configuration. The RSRA vehicle was then trimmed at various airspeeds over the airspeed range. Three airspeeds were utilized for this comparison, that of 0 knots (hover), 60 knots (transition), and 120 knots (forward velocity cruise). While the vehicle was stabilized at each trim airspeed, all control positions and aircraft attitudes were recorded. These consisted of collective position, longitudinal and lateral cyclic positions, pedal position, vehicle pitch and roll attitudes, and vehicle angle of attack.

The total rotor force and moment tests were set up by initializing the RSRA vehicle to the trim conditions determined in the static trim tests. The computer program was then allowed to reside in the reset (initial condition) mode for 30 seconds to allow any disturbances caused by the initialization process to settle out. The vehicle was flown in straight and level trimmed flight for 5 seconds during which all forces and moments from the rotor were recorded to determine their mean steady state value.

$$\left(\mu = \frac{1}{n} \sum_{i=1}^{n} x_i \right).$$

ROTOR SPEED (RPM)	NUMBER OF BLADES	NUMBER OF BLADE SEGMENTS	INTEGRATION INTERVAL (SEC)	AZIMUTHAL ADVANCE ANGLE (DEG)
200*	5	10	$\frac{1}{240}$	5
200	5	5	$\frac{1}{240}$	5
200	4	5	$\frac{1}{240}$	5
200	3	5	$\frac{1}{240}$	5
200	5	4	$\frac{1}{240}$	5
200	5	3	$\frac{1}{240}$	5
200	3	3	$\frac{1}{240}$	5
200	5	5	$\frac{1}{30}$	40
200	3	3	$\frac{1}{30}$	40
200	5	5	$\frac{1}{20}$	60
200	3	3	$\frac{1}{20}$	60

* This is the true solution configuration ("truth" rotor).

TABLE 1. - Rotor Mathematical Model Configurations Utilized in this Study.

The standard deviation

$$\left(\sigma = \sqrt{\frac{\sum_{i=1}^{n} \left(x_i - \mu \right)^2}{n - 1}} \right)$$

of each was also computed to give some insight into how steady the forces and moments were for the trim condition. A run of 5 seconds was chosen so that enough data would be available for the calculations, while the inherent total vehicle instabilities would not have had enough time to contaminate the results.

The 360 degree blade sweep test was set up by once again initializing the RSRA vehicle to the previously determined trim conditions. Again the computer program resided in the reset mode for 30 seconds. The vehicle was then flown in straight and level trimmed flight long enough, approximately .3 seconds, for the index blade to make one complete revolution. During the 360 degree revolution, data was taken at each azimuthal position achieved by the blade. Data recorded consisted of the index blade forces and moments and flapping and lagging motions.

The total vehicle dynamic response tests were set up by again initializing the RSRA vehicle to the trim conditions determined previously in the static trim tests. The computer program resided in reset for 30 seconds again to allow any disturbances due to the initialization procedure to settle out. The RSRA vehicle was then flown in straight and level trimmed flight. At one second into the flight, a 5 percent lateral cyclic (100 percent stick travel equals full left stick to full right stick) pulse was applied for one second and then the stick was returned to the trim position.

The run continued until either 20 seconds had elapsed or the vehicle flew into the ground, pitched up to exactly 90 degrees (this causes the computer program to sustain a fatal error due to how the Euler angles are computed), or the rotor blade flapping went unstable (this also causes a fatal error in the computer program). During the 20 seconds of the test run all pertinent vehicle states were recorded. These consisted of the total vehicle body linear and angular accelerations, linear and angular velocities, body attitudes, and blade flapping and lagging motions.

The total rotor force and moment tests, the 360 degree blade sweep tests, and the total vehicle dynamic response tests were conducted for the hover and 120 knot cases only. The 60 knot case, transition, was not tested due to the vehicle stability problems which arise in this region of flight. Since the actual vehicle would not try to fly in this region for any length of time, this was considered to be an unrealistic case for the tests being conducted in this study.

RESULTS AND DISCUSSION

Static Trim Comparisons

The RSRA vehicle was initialized at 500 feet of altitude and was trimmed over the speed range for the various rotor configurations. The 5-blade 10-blade segment "truth" model is presented as the base for comparison in all cases. The 5-blade 5-blade segment configuration presented in each case is the standard LaRC rotor configuration. Table 2 presents the effect of blade reduction on static trim. For all airspeeds considered, the largest errors occur in collective position (XC) and roll attitude (ϕ). Approximately the same magnitude of error exists for both the 5-blade configuration comparison and the 3-blade configuration.

Table 3 presents the effect of blade segment reduction on static trim. As was the case with blade reduction, the largest errors occur in collective position and roll attitude. When comparing the errors obtained from blade segment reduction to those of blade reduction, the blade segment errors are two to three times as large and a definite difference exists between the 5-blade 5-blade segment comparison and the 5-blade 3-blade segment comparison which was not apparent in the blade reduction cases.

Table 4 presents the effect of combination blade and blade segment reduction on static trim for fixed integration interval of 1/240 seconds. The two cases chosen were the configuration used for the LaRC man-in-the-loop simulation and a worst possible case. As with the previous cases, the largest errors occur in collective position and roll attitude. Comparing these results with Tables 2 and 3 exhibits that the overwhelming error in the combination reduction case comes from the blade segment reduction effect. While these errors would not be noticed by a pilot flying the simulation, they could have an

ROTOR CONFIGURATION	XC (%)	XB (%)	XA (%)	XP (%)	θ (DEG)	φ (DEG)	α (DEG)
			HOVER				
5b x 10s	53.04699	58.41983	54.45756	55.90087	6.764940	-4.136830	-89.96700
5b x 5s	52.46661	58.42831	54.40668	55.75633	6.763598	-4.086040	-89.96701
3b x 5s	52.46610	58.42818	54.40633	55.75616	6.763569	-4.086060	-89.96700
			60 KNOTS				
5b x 10s	29.51111	73.84943	47.44258	69.46115	6.337858	-1.368949	4.470616
5b x 5s	28.92961	73.76982	47.43329	69.41892	6.342854	-1.411199	4.475236
3b x 5s	28.92930	73.77001	47.43313	69.41901	6.342919	-1.411176	4.495846
			120 KNOTS				
5b x 10s	45.03538	81.09580	48.58129	75.61161	1.658597	-2.039050	1.318606
5b x 5s	44.46544	80.89494	48.59390	75.49239	1.656651	-1.991862	1.316005
3b x 5s	44.46537	80.89530	48.59775	75.49306	1.656688	-1.991759	1.343623

TABLE 2.- Effect of Blade Reduction on Static Trim.
(Integration Interval of 1/240 Seconds).

ROTOR CONFIGURATION	XC (%)	XB (%)	XA (%)	XP (%)	θ (DEG)	ϕ (DEG)	α (DEG)
			HOVER				
5b x 10s	53.04699	58.41983	54.45756	55.90087	6.764940	-4.136830	-89.96700
5b x 5s	52.46661	58.42831	54.40668	55.75633	6.763598	-4.086040	-89.96701
5b x 3s	51.30444	58.44290	54.28289	55.39254	6.771419	-4.073162	-89.96700
			60 KNOTS				
5b x 10s	29.51111	73.84943	47.44258	69.46115	6.337858	-1.368949	4.470616
5b x 5s	28.92961	73.76982	47.43329	69.41892	6.342854	-1.411199	4.475236
5b x 3s	27.78420	73.55880	47.22502	69.15835	6.365632	-1.447041	4.503353
			120 KNOTS				
5b x 10s	45.03538	81.09580	48.58129	75.61161	1.658527	-2.039050	1.318606
5b x 5s	44.46544	80.89494	48.59390	75.49239	1.656651	-1.991862	1.316005
5b x 3s	43.27490	80.57574	48.44242	75.29523	1.677412	-1.939358	1.337667

TABLE 3.- Effect of Blade Segment Reduction on Static Trim.
(Integration Interval of 1/240 Seconds).

ROTOR CONFIGURATION	XC (%)	XB (%)	XA (%)	XP (%)	θ (DEG)	ϕ (DEG)	α (DEG)
			HOVER				
5b x 10s	53.04699	58.41983	54.45756	55.90087	6.764940	-4.136830	-89.96700
5b x 5s	52.46661	58.42831	54.40668	55.75633	6.763598	-4.086040	-89.96701
3b x 3s	51.30376	58.44268	54.28260	55.39237	6.771403	-4.073179	-89.96700
			60 KNOTS				
5b x 10s	29.51111	73.84943	47.44258	69.46115	6.337858	-1.368949	4.470616
5b x 5s	28.92961	73.76982	47.43329	69.41892	6.342854	-1.411199	4.475236
3b x 3s	27.78441	73.55918	47.22311	69.15825	6.365660	-1.447091	4.469474
			120 KNOTS				
5b x 10s	45.03538	81.09580	48.58129	75.61161	1.658597	-2.039050	1.318606
5b x 5s	44.46544	80.89494	48.59390	75.49239	1.656651	-1.991862	1.316005
3b x 3s	43.27574	80.57614	48.43808	75.29504	1.677440	-1.939436	1.310593

TABLE 4.- Effect of Combination Blade and Blade Segment Reduction on Static Trim. (Integration Interval of 1/240 Seconds).

effect on analytical studies (new rotors, stability augmentation systems, etc.) run with no pilot in-the-loop.

Table 5 presents the effect of increasing integration interval, and therefore blade azimuthal advance angle, from 1/240 seconds to 1/30 seconds ($\Delta\Psi = 5^{o}$ to $\Delta\Psi = 40^{o}$) on static trim for several rotor configurations. Again, the largest errors in control position appear in the collective position. The worst errors in vehicle attitude occur in roll angle for the lower velocities and in pitch angle for the higher velocities.

Table 6 presents the effect of increasing integration interval from 1/240 seconds to 1/20 seconds ($\Delta\Psi = 5^{o}$ to $\Delta\Psi = 60^{o}$) on static trim for the same rotor configurations as in Tables 4 and 5. As in the previous cases, collective position has the largest control position error and roll angle has the largest attitude error. However, the rotor model has deteriorated to such an extent that obvious errors are appearing in each parameter.

To summarize, reduction of the number of blades appears to have little effect on the trim results which indicates that the method[1] utilized by the rotor mathematical model in scaling the rotor forces and moments to the correct number of blades is accomplishing the desired effects. While the errors encountered in reducing the number of blade segments are slightly larger than those of reducing the number of blades, the method[1] utilized in determining the positions and lengths of the blade segments appears to be accomplishing the desired effect of representing the blade with a minimum number of segments. The largest errors in static trim occur as the integration interval, and therefore, the azimuthal advance angle, is increased. This has the effect of causing the blades to miss areas on the rotor tip path plane needed to

[1] Appendix B.

ROTOR CONFIGURATION	XC (%)	XB (%)	XA (%)	XP (%)	θ (DEG)	φ (DEG)	α (DEG)
			HOVER				
5b x 10s, 1/240	53.04699	58.41983	54.45756	55.90087	6.764940	-4.136830	-89.96700
5b x 5s, 1/30	52.65046	58.47476	54.46184	55.76493	6.801064	-4.587175	-89.96702
3b x 3s, 1/30	51.41746	58.48106	54.36350	55.35631	6.788709	-4.582146	-89.96700
			60 KNOTS				
5b x 10s, 1/240	29.51111	73.84943	47.44258	69.46115	6.337858	-1.368949	4.470616
5b x 5s, 1/30	29.25455	73.74465	47.96587	70.20912	6.274201	-1.687877	4.373877
3b x 3s, 1/30	28.22293	73.51772	47.63262	69.81966	6.278102	-1.666196	4.334077
			120 KNOTS				
5b x 10s, 1/240	45.03538	81.09580	48.58129	75.61161	1.658597	-2.039050	1.318606
5b x 5s, 1/30	42.27594	79.66078	49.11662	76.03675	1.852863	-2.162515	1.527534
3b x 3s, 1/30	41.02345	79.34420	48.99291	76.10195	1.855325	-2.078395	1.500810

TABLE 5.- Effect of Increasing Integration Interval from 1/240 Seconds to 1/30 Seconds on Static Trim for Several Rotor Configurations.

ROTOR CONFIGURATION	XC (%)	XB (%)	XA (%)	XP (%)	θ (DEG)	ϕ (DEG)	α (DEG)
			HOVER				
5b x 10s, 1/240	53.04699	58.41983	54.45756	55.90087	6.764940	-4.136830	-89.96700
5b x 5s, 1/20	52.73945	58.53902	54.49965	55.79664	6.787256	-4.621847	-89.96700
3b x 3s, 1/20	51.54731	58.56285	54.36806	55.41915	6.794836	-4.585965	-89.96598
			60 KNOTS				
5b x 10s, 1/240	29.51111	73.84943	47.44258	[illegible]6115	6.337858	-1.368949	4.470616
5b x 5s, 1/20	28.98774	73.35731	48.94406	7[illegible]5405	6.311381	-1.467257	4.428835
3b x 3s, 1/20	27.93671	73.26891	48.86043	69.95404	6.266589	-1.490066	4.400220
			120 KNOTS				
5b x 10s, 1/240	45.03538	81.09580	48.58129	75.61161	1.658597	-2.039050	1.318606
5b x 5s, 1/20	28.30536	70.21162	49.14399	80.96419	2.817083	-.745959	2.645589
3b x 3s, 1/20	35.76099	76.34667	45.57589	78.60525	2.279696	-2.006857	2.066883

TABLE 6.- Effect of Increasing Integration Interval from 1/240 Seconds to 1/20 Seconds on Static Trim for Several Rotor Configurations.

adequately define the rotor forces and moments.

Total Rotor Force and Moment Comparison

The total rotor force and moment tests were set up by initializing the RSRA vehicle to the trim conditions determined in the static trim tests. The vehicle was then flown in straight and level flight for five seconds during which the rotor forces and moments were recorded so that a mean value and standard deviation could be determined for each, thus providing a performance measure to compare the rotor configurations. Figures 8 and 9 present the effect of blade reduction on total rotor forces and moments for the hover and 120 knot cases respectively. The figures show the rotor thrust, horizontal force, side force, pitching moment, rolling moment, and torque plotted against number of blades. Reducing the number of blades has relatively little effect on the mean values, however differences in the standard deviations can be noticed. For the hover case, the number of blades must be reduced to three to see a significant difference, while for the 120 knot case, significant differences appear when the number of blades is reduced to four. In general as forward velocity increases and the number of blades is decreased, the standard deviation increases indicating larger internal oscillations are occuring in the rotor.

Figures 10 and 11 present the effect of blade segment reduction on total rotor forces and moments for the hover and 120 knot cases respectively. The figures show the forces and moments plotted against number of blade segments. For both velocities, small differences occur in the mean values as the number of blade segments is reduced with the largest difference occuring in torque, while the differences in standard deviation are very slight. Thus the major

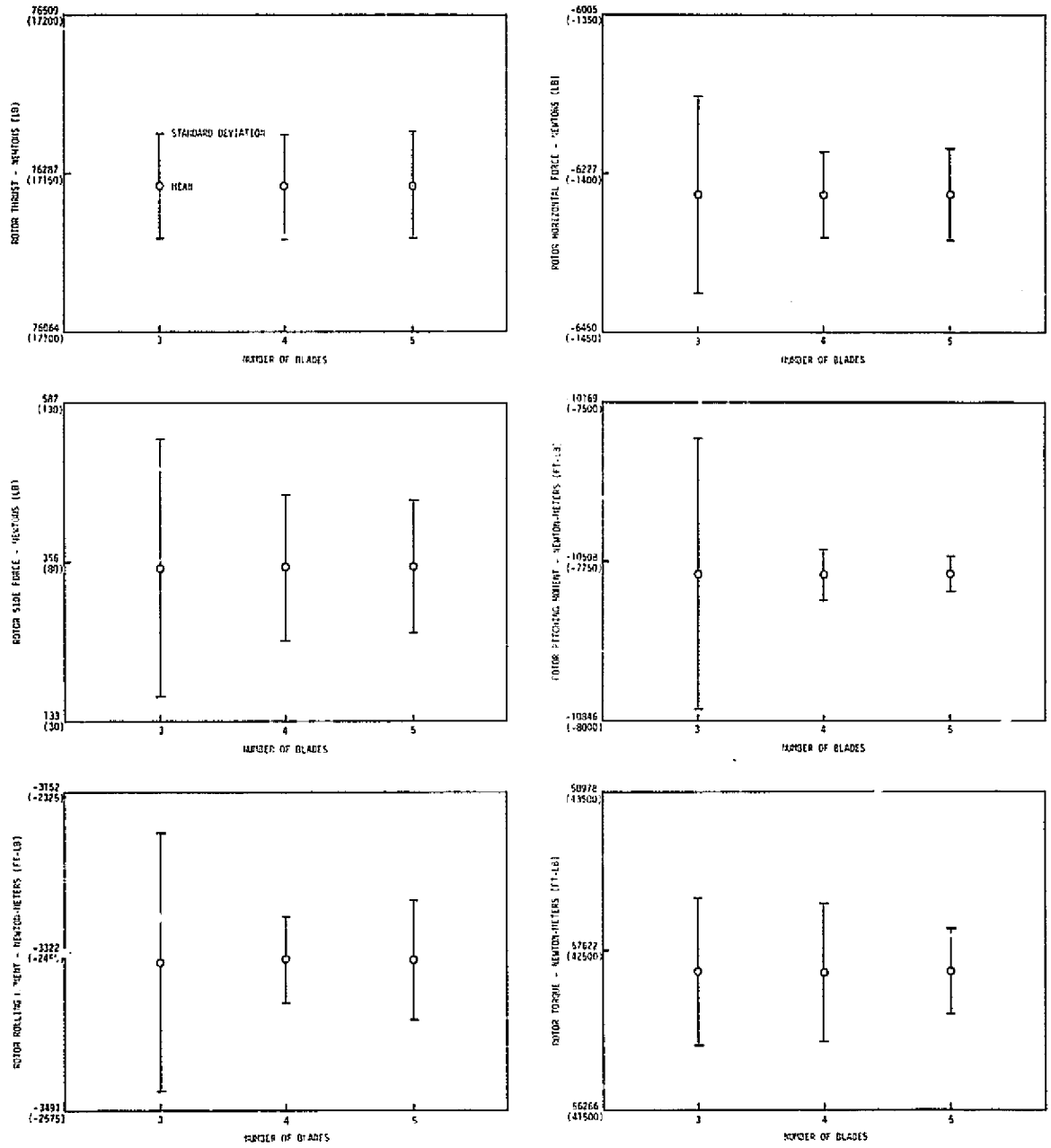

Figure 8.- Effect of Blade Reduction on Total Rotor Forces and Moments at Hover. (Integration Interval of 1/240 Seconds, 5 Blade Segments).

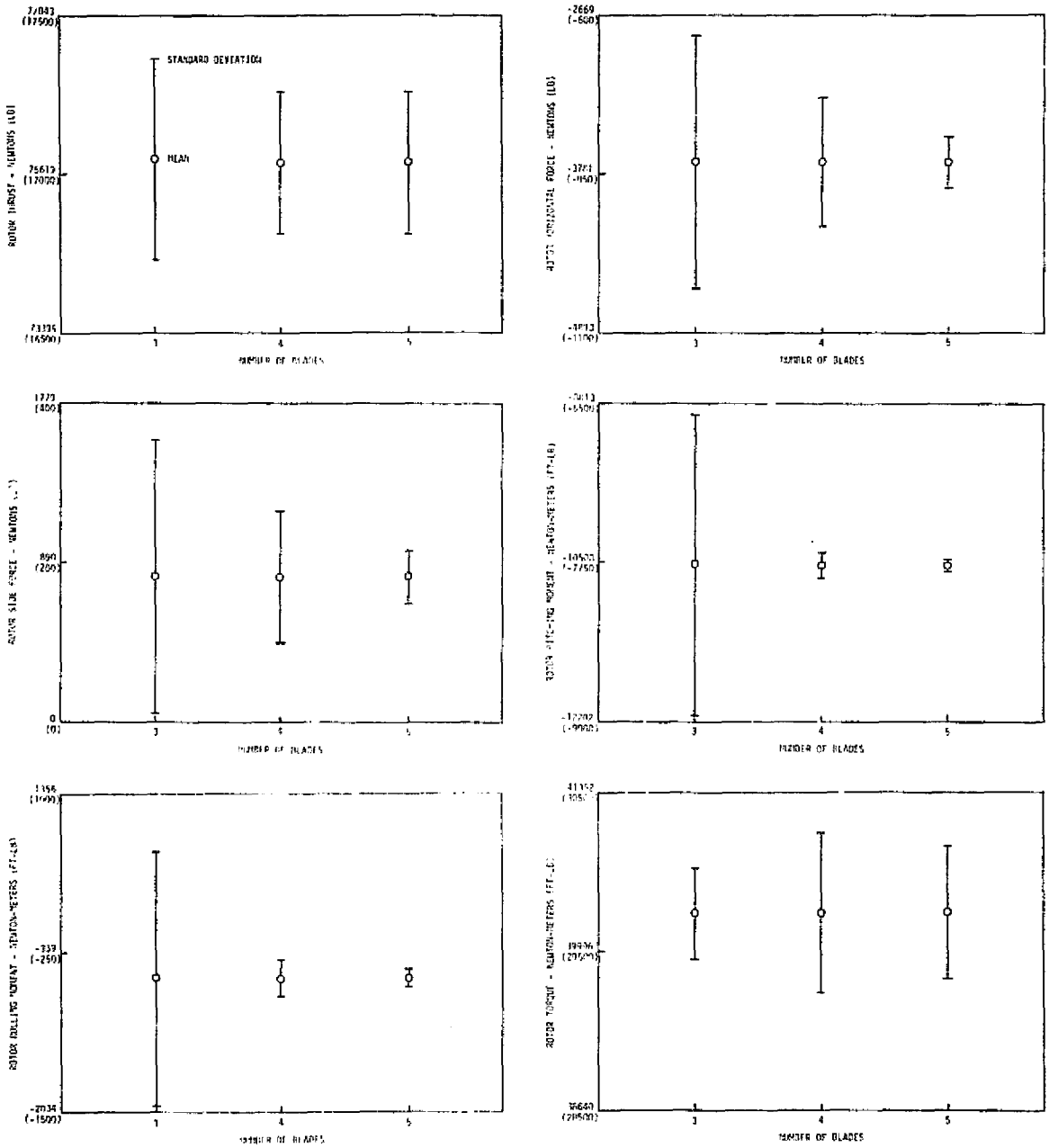

Figure 9.- Effect of Blade Reduction on Total Rotor Forces and Moments at 120 Knots. (Integration Interval of 1/240 Seconds, 5 Blade Segments).

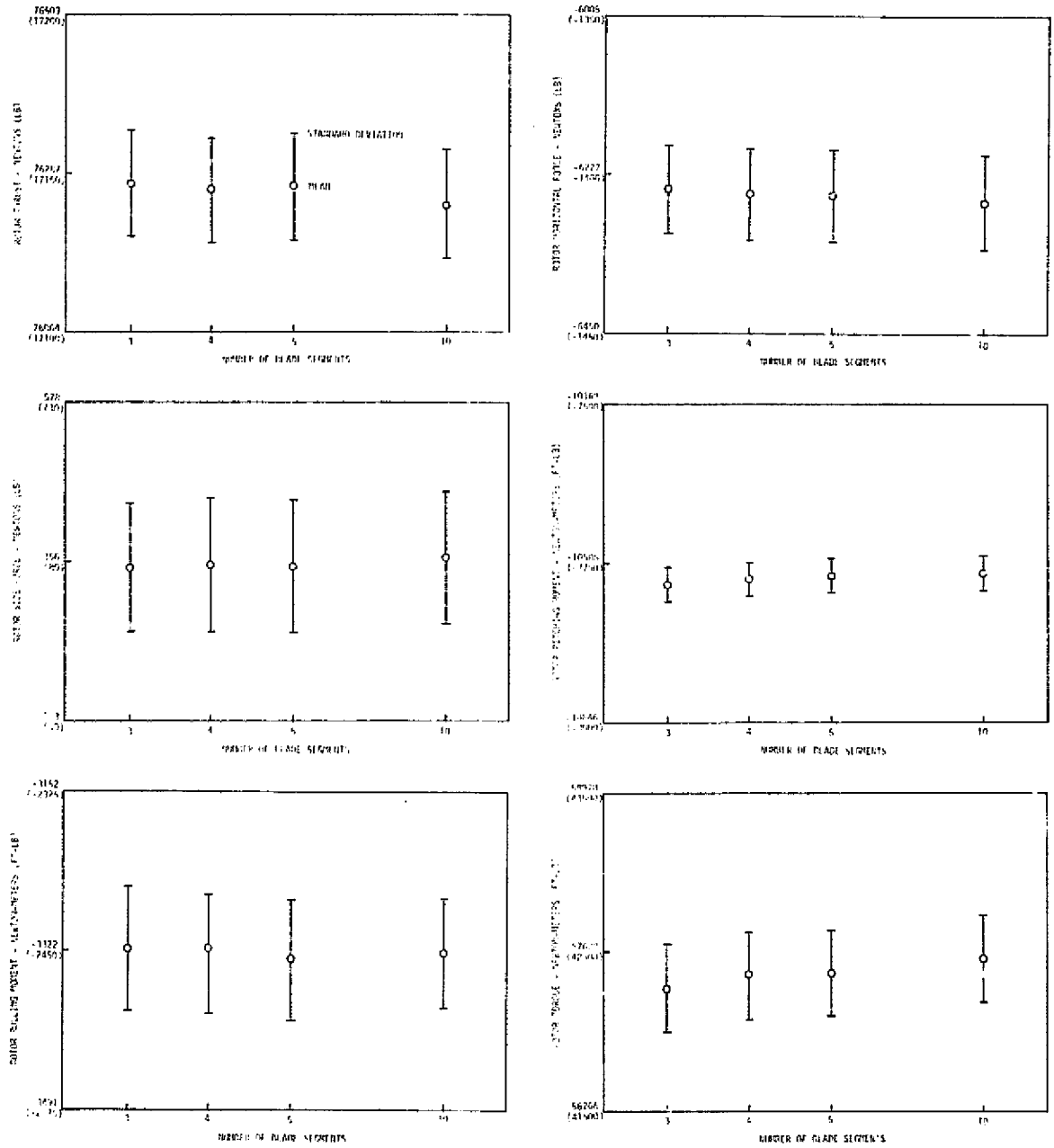

Figure 10.- Effect of Blade Segment Reduction on Total Rotor Forces and Moments at Hover. (Integration Interval of 1/240 Seconds, 5 Blades).

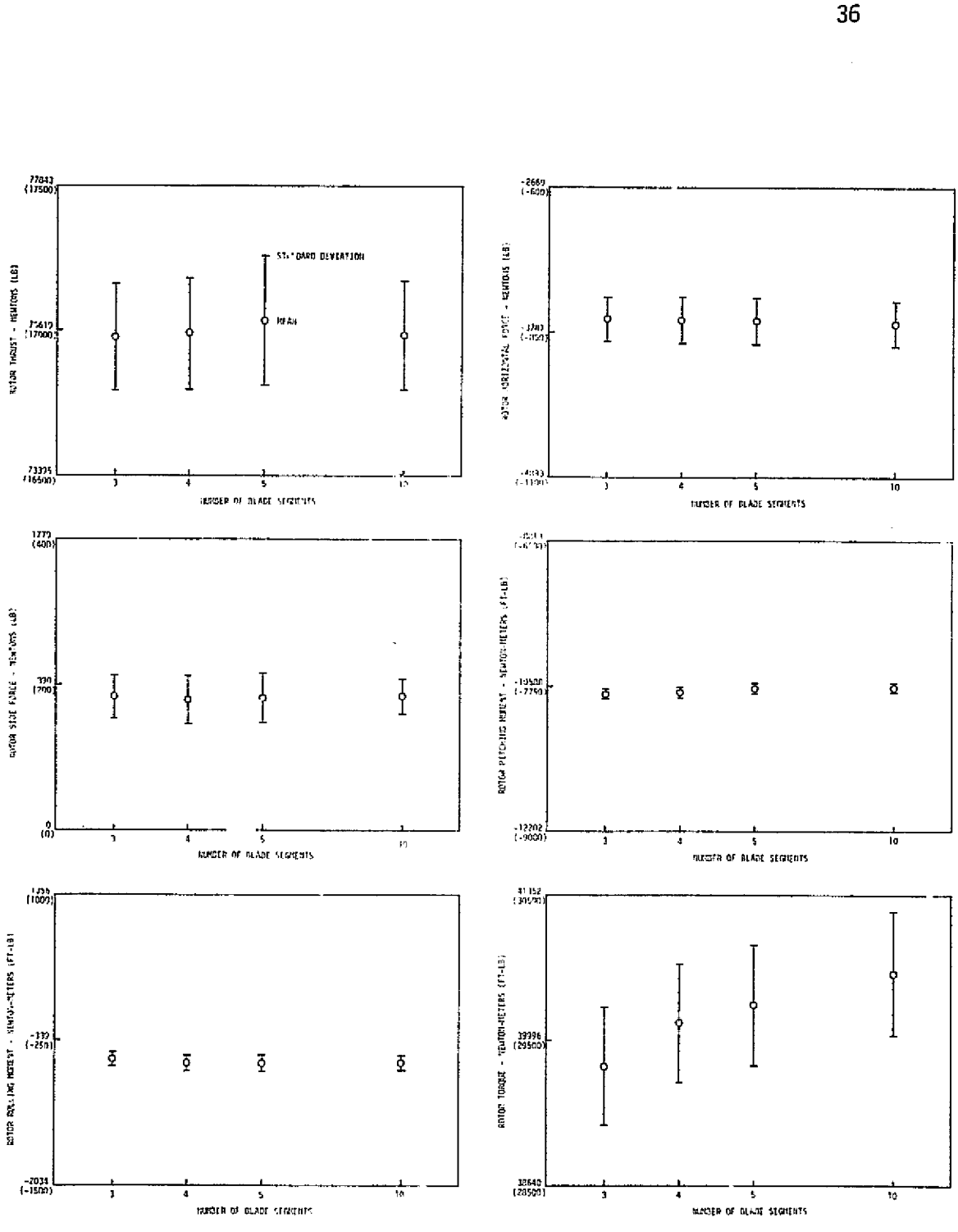

Figure 11.- Effect of Blade Segment Reduction on Total Rotor Forces and Moments at 120 Knots. (Integration Interval of 1/240 Seconds, 5 Blades).

effect of reduction of blade segments on the total rotor forces and moments is a corresponding reduction in rotor torque which is accentuated as forward velocity increases.

Figures 12 and 13 present the effect of increasing integration interval, and therefore azimuthal advance angle, on total rotor forces and moments for the hover and 120 knot cases respectively. Two rotor configurations are plotted, 5-blades 5-blade segments (LaRC configuration) and 3-blades 3-blade segments (previous user's configuration). For both velocity cases, only slight differences occur in the mean values of the rotor forces and moments for the 5-blade 5-blade segment configuration when increasing the integration interval from 1/240 seconds to 1/30 seconds with the largest difference being in the rotor torque. While there are noticeable differences in the standard deviations, their magnitude is relatively small. When increasing to an integration interval of 1/20 seconds, obvious errors occur in the mean values with extremely large errors occuring in the rotor moments, especially for 120 knots. Correspondingly, extremely large increases in the standard deviations occur. The 3-blade 3-blade segment configuration tends to follow the same trends, however in general, this configuration shows larger differences in the mean and standard deviation values, these larger differences being due to the additional combined effects of reducing the number of blades and blade segments.

To summarize, reducing the number of blades appears to have relatively little effect on the total rotor force and moment mean values indicating, as in the static trim results that the method used to scale the forces and moments to the correct number of blades is achieving the desired

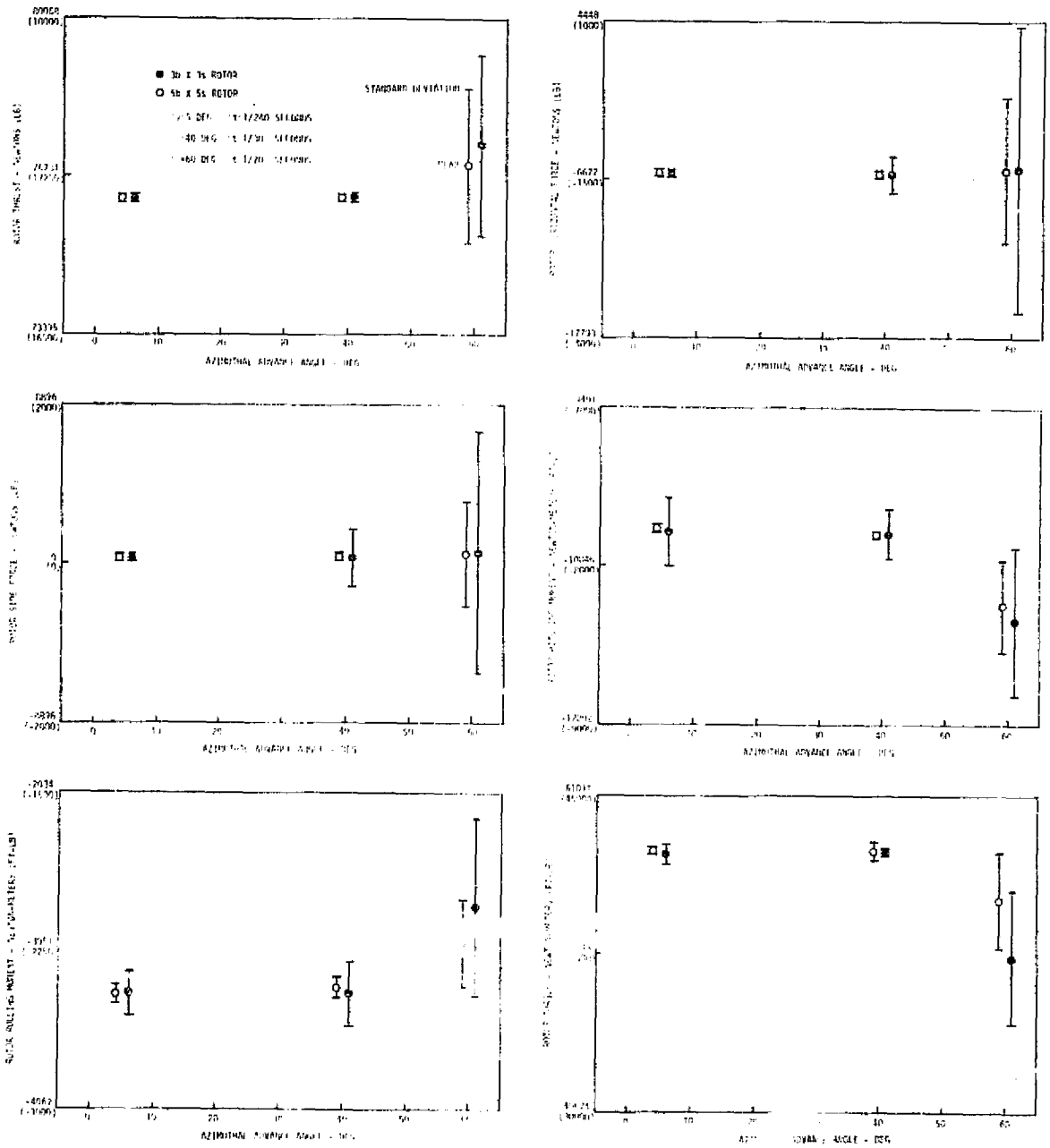

Figure 12.- Effect of Increasing Integration Interval on Total Rotor Forces and Moments at Hover.

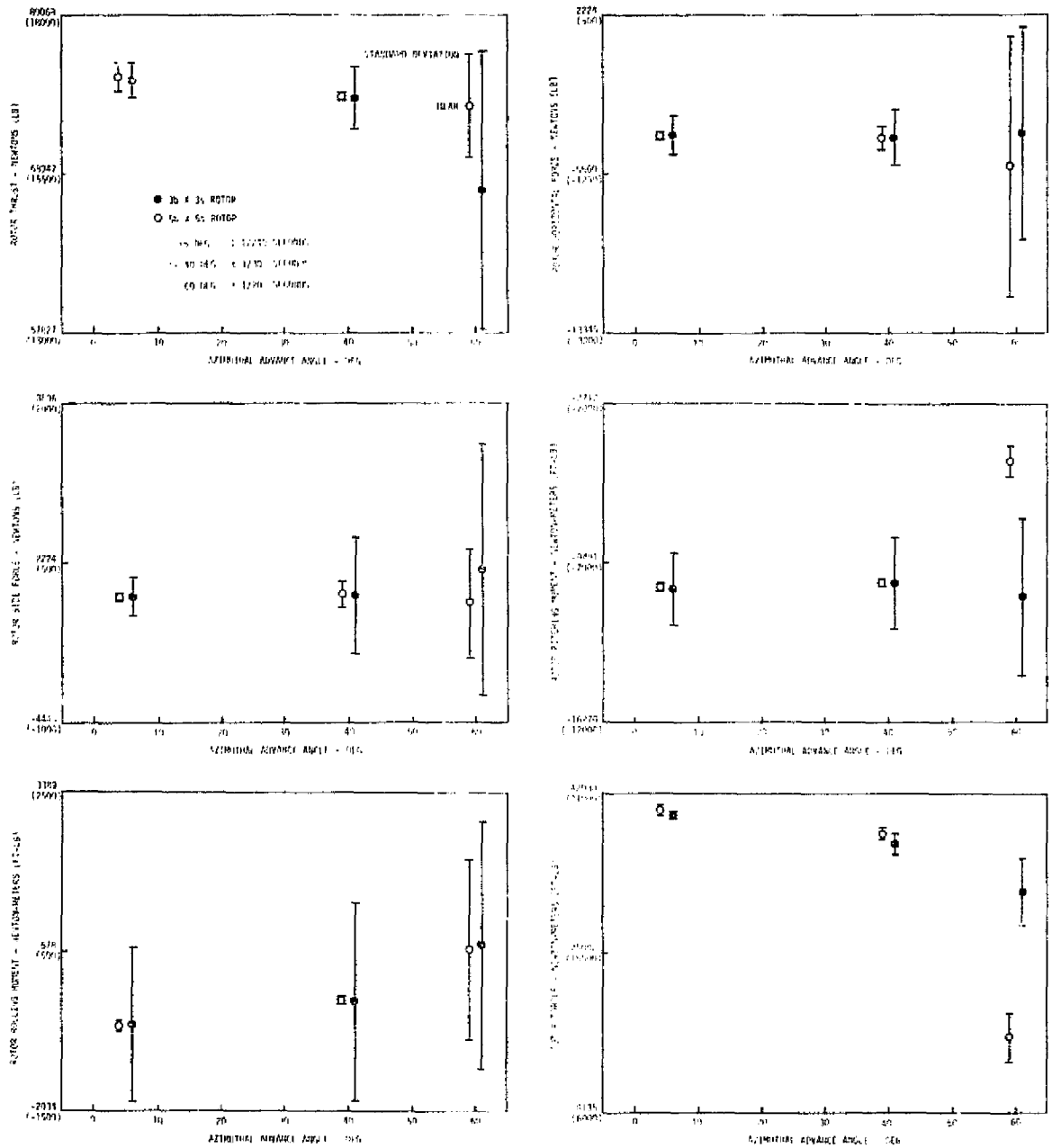

Figure 13.- Effect of Increasing Integration Interval on Total Rotor Forces and Moments at 120 Knots.

results. However, the large increase in standard deviations as the number of blades is decreased tends to indicate that some large internal oscillations are occuring which may not be desirable from a dynamic point of view. As was the case with the static trim results, reducing the number of blade segments appears to have relatively little effect on either the mean values (with the exception of torque) or the standard deviations indicating once again that the method used for positioning the segments and determining their lengths is accomplishing the desired effect of representing the blade with a minimum number of segments. The largest errors from a total rotor force and moment point of view occur when the integration interval, and therefore the azimuthal advance angle, is increased, once again indicating that the blades are missing areas on the rotor tip path plane needed to adequately define the individual blade forces and moments and thus define the total rotor forces and moments.

360 Degree Blade Sweep Comparison

The 360 degree blade sweep test was set up by initializing the RSRA vehicle to the previously determined trim conditions. The index blade was allowed to make one complete revolution. During this revolution, data were taken at each azimuthal position achieved by the blade. Data recorded consisted of blade forces and moments and blade flapping and lagging motions. Since reducing the number of blades has no meaning in this test, no data will be presented except for a sample case to indicate how the remaining blades must increase their effective forces and moments to compensate for the missing blades.

Figure 14 presents a comparison of the 5-blade 5-blade segment rotor with the "truth" rotor for a one revolution blade sweep at 120 knots. The only noticeable difference in any of the parameters is a slight reduction in torque.

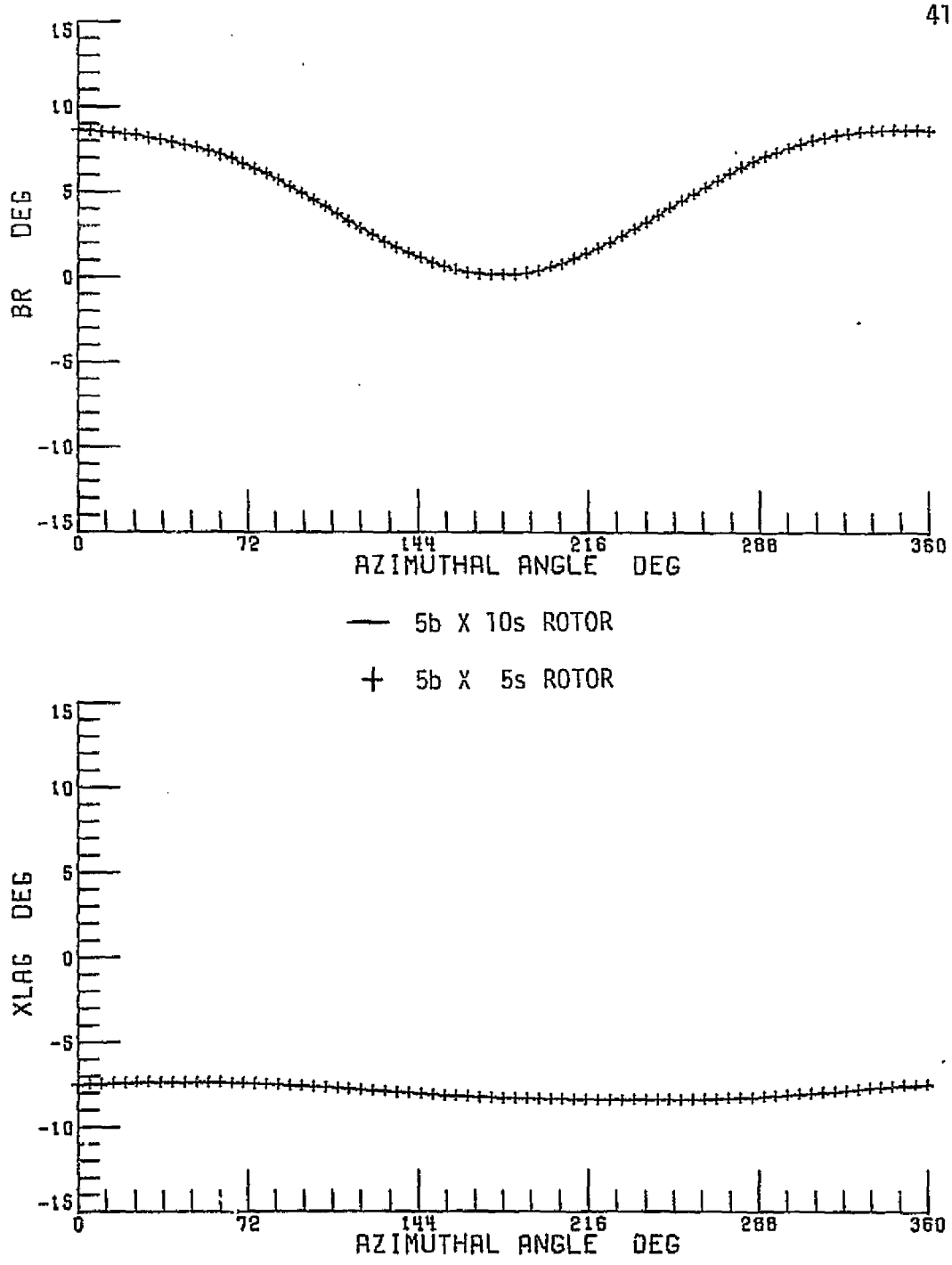

Figure 14.- Comparison of a 5-Blade 5-Blade Segment Rotor Model with the "Truth" Rotor Model at 120 Knots for One Blade Revolution. (Integration Interval of 1/240 Seconds).

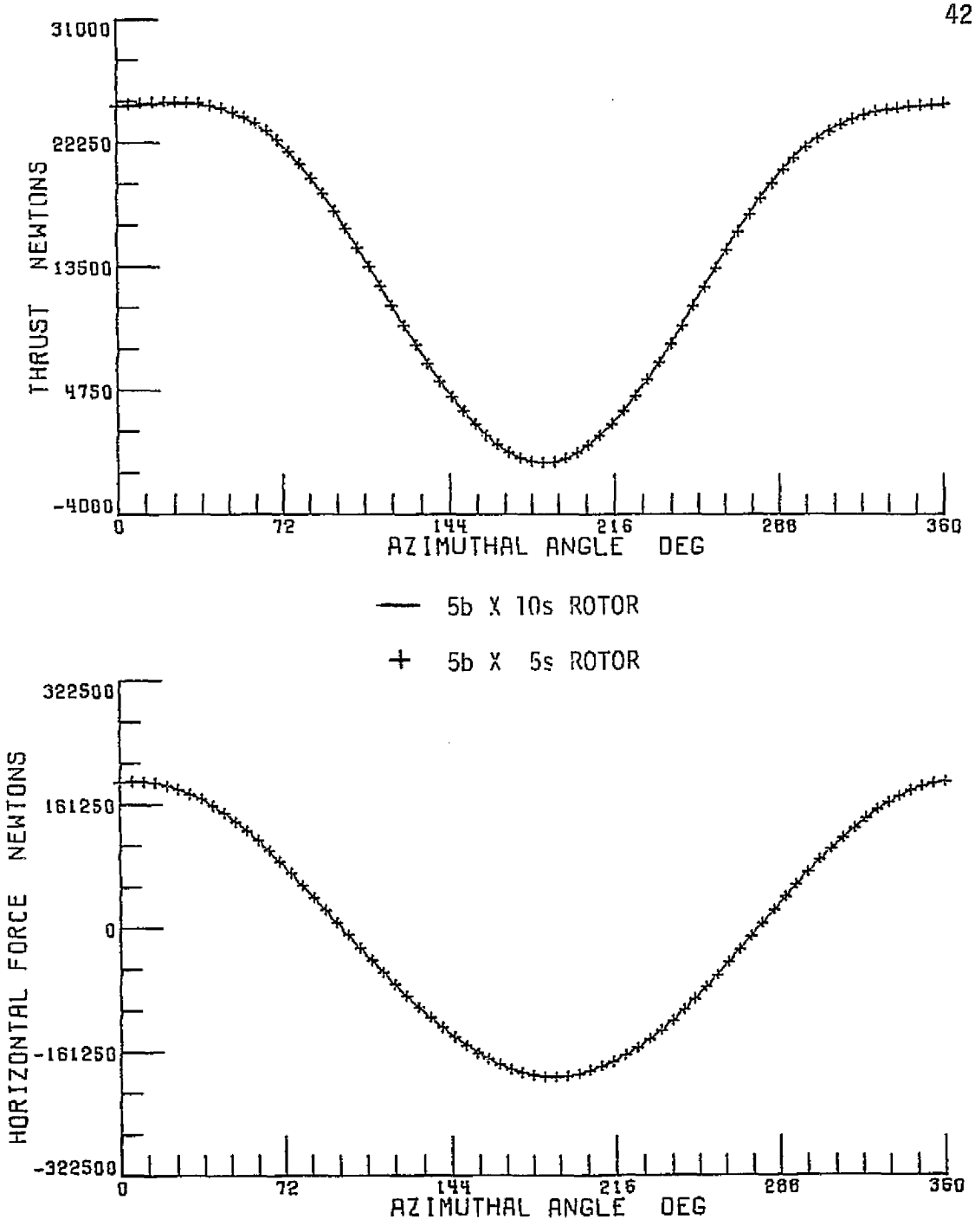

Figure 14.- Continued.

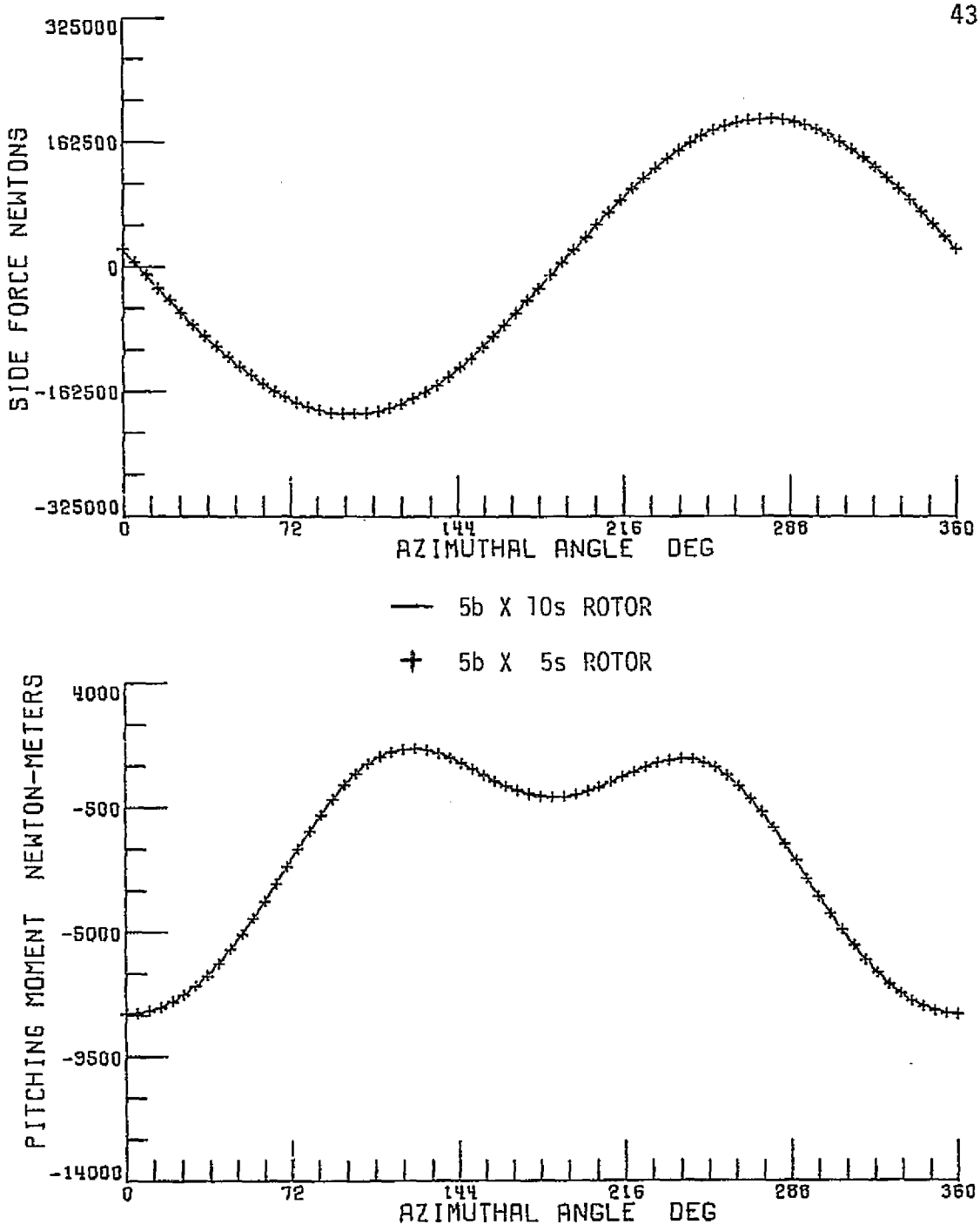

Figure 14.- Continued.

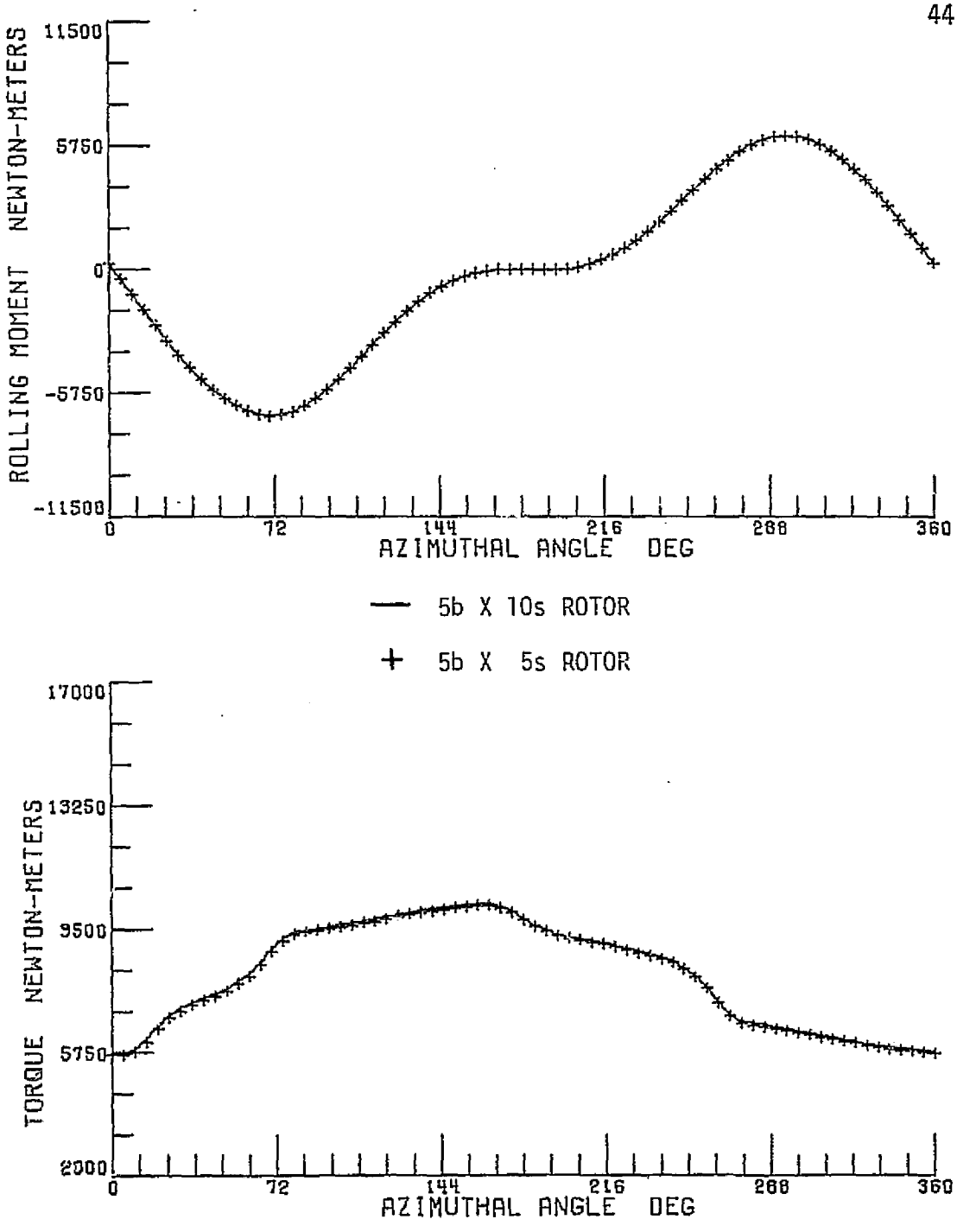

Figure 14.- Concluded.

The data gathered for the hover case show no difference in any of the parameters.

Figure 15 presents the effect of blade segment reduction on blade parameters for one revolution at 120 knots. Very slight differences are apparent in lagging angle (XLAG), thrust, and pitching moment. The most prominent difference is a fairly constant reduction in torque over the entire 360 degree revolution. The data gathered for the hover case show no difference in any of the parameters except for a slight change in torque in the retreating section of the blade sweep.

Figure 16 presents the effect of increasing integration interval to 1/30 seconds and 1/20 seconds on blade parameters for one revolution at 120 knots. For the case of integration interval of 1/30 seconds, slight differences exist in flapping angle (BR), thrust, pitching moment, and rolling moment. A constant bias exists in lagging angle of approximately 0.5 degrees. The largest error exists in torque which shows a relatively constant lower value except for a very small portion of the sweep where it assumes a higher value. For the hover case, only a slight difference in torque was apparent.

For the case of integration interval of 1/20 seconds, errors are apparent in all of the parameters with only side force and horizontal force representing the correct solution. The largest errors exist in lagging angle which is showing a relatively constant four degree bias, and torque which shows an extremely lower value than the correct solution. For the hover case, slight differences appear in all parameters except for lagging angle which shows a bias of one degree, and torque which in general is below the correct solution.

Figure 17 presents an example of how the forces and moments change for one blade when a 3-blade rotor system must compensate for the loss of 2 blades in

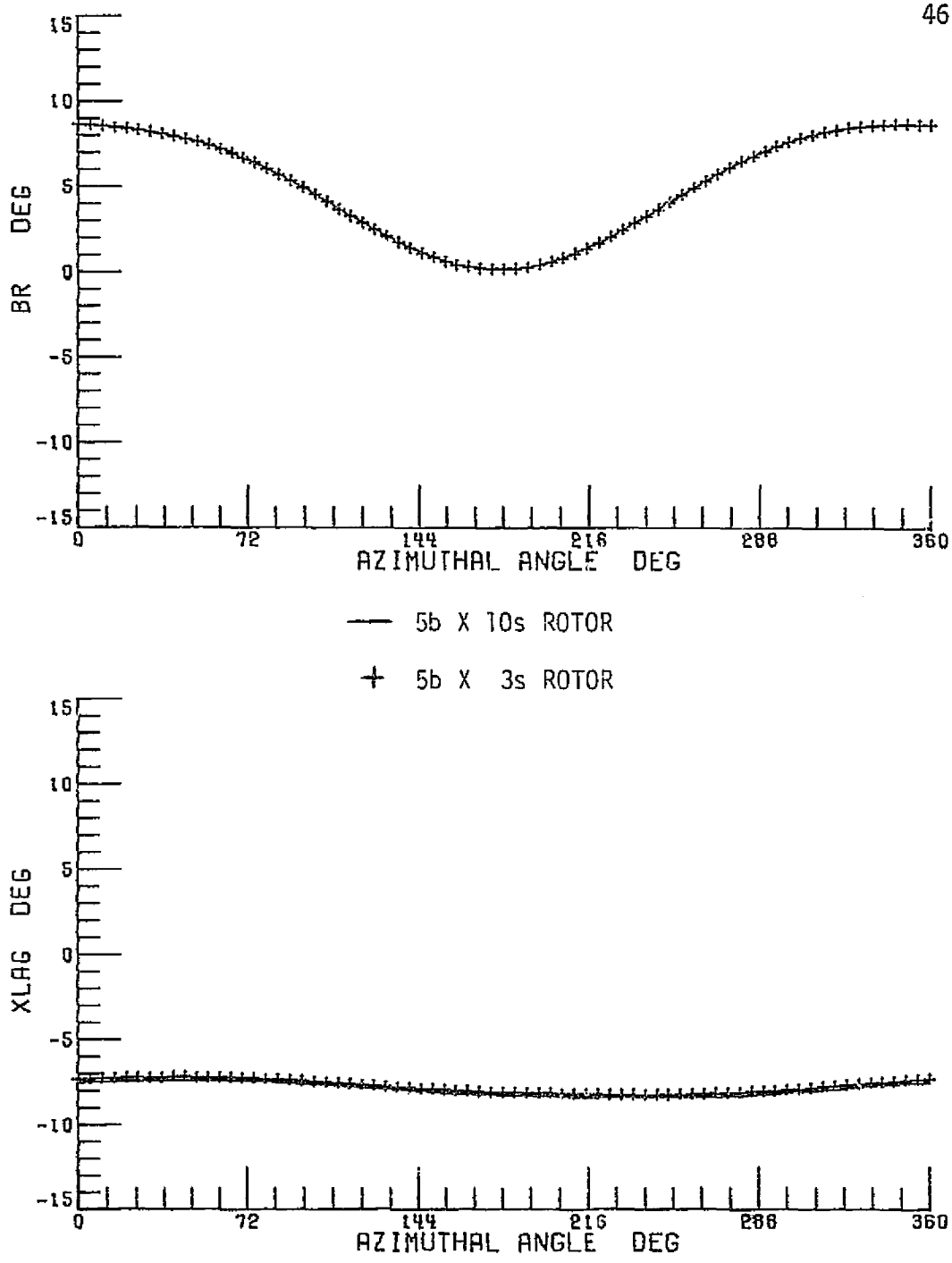

Figure 15.- Effect of Blade Segment Reduction on One Blade Revolution Data at 120 Knots. (Integration Interval of 1/240 Seconds).

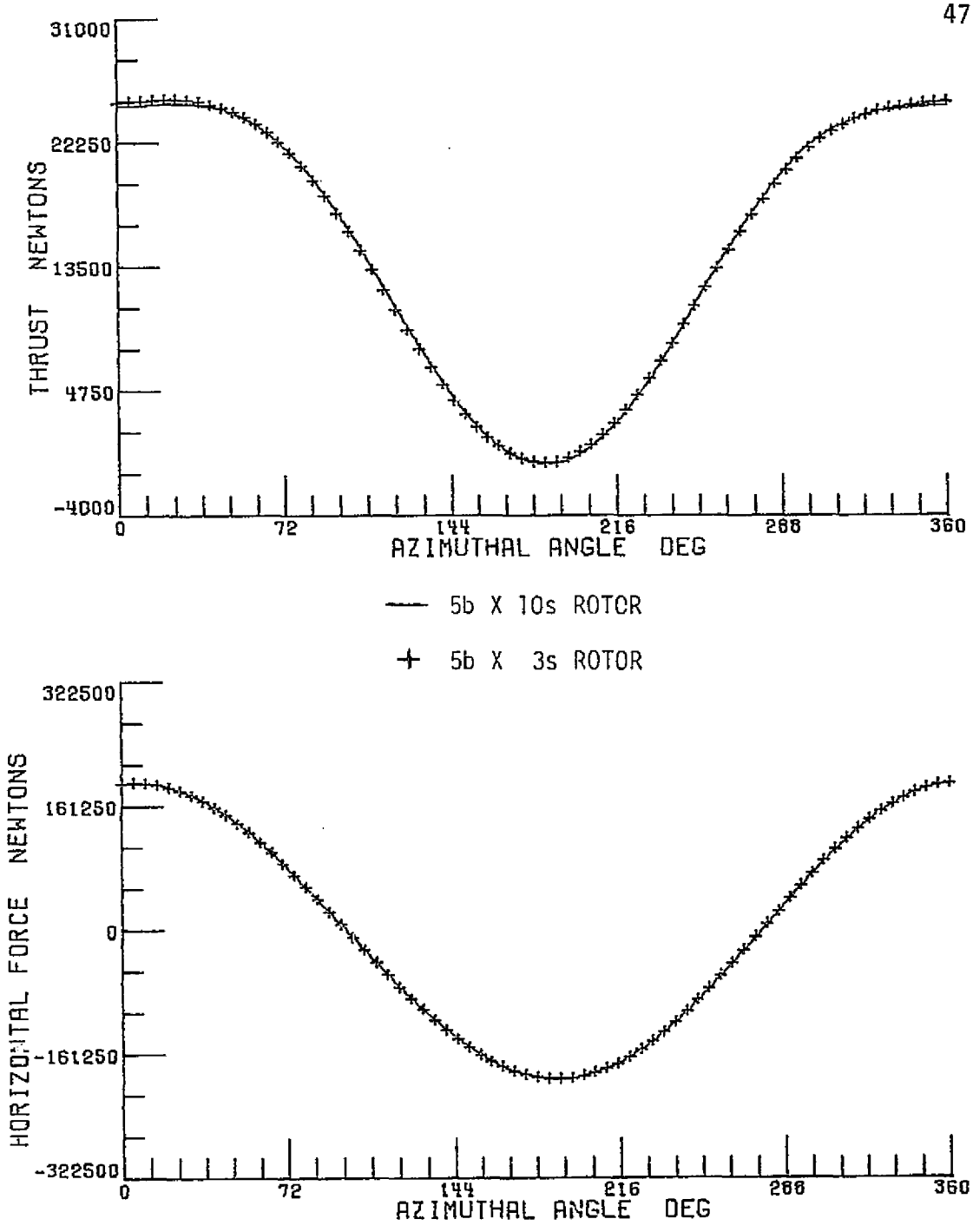

Figure 15.- Continued.

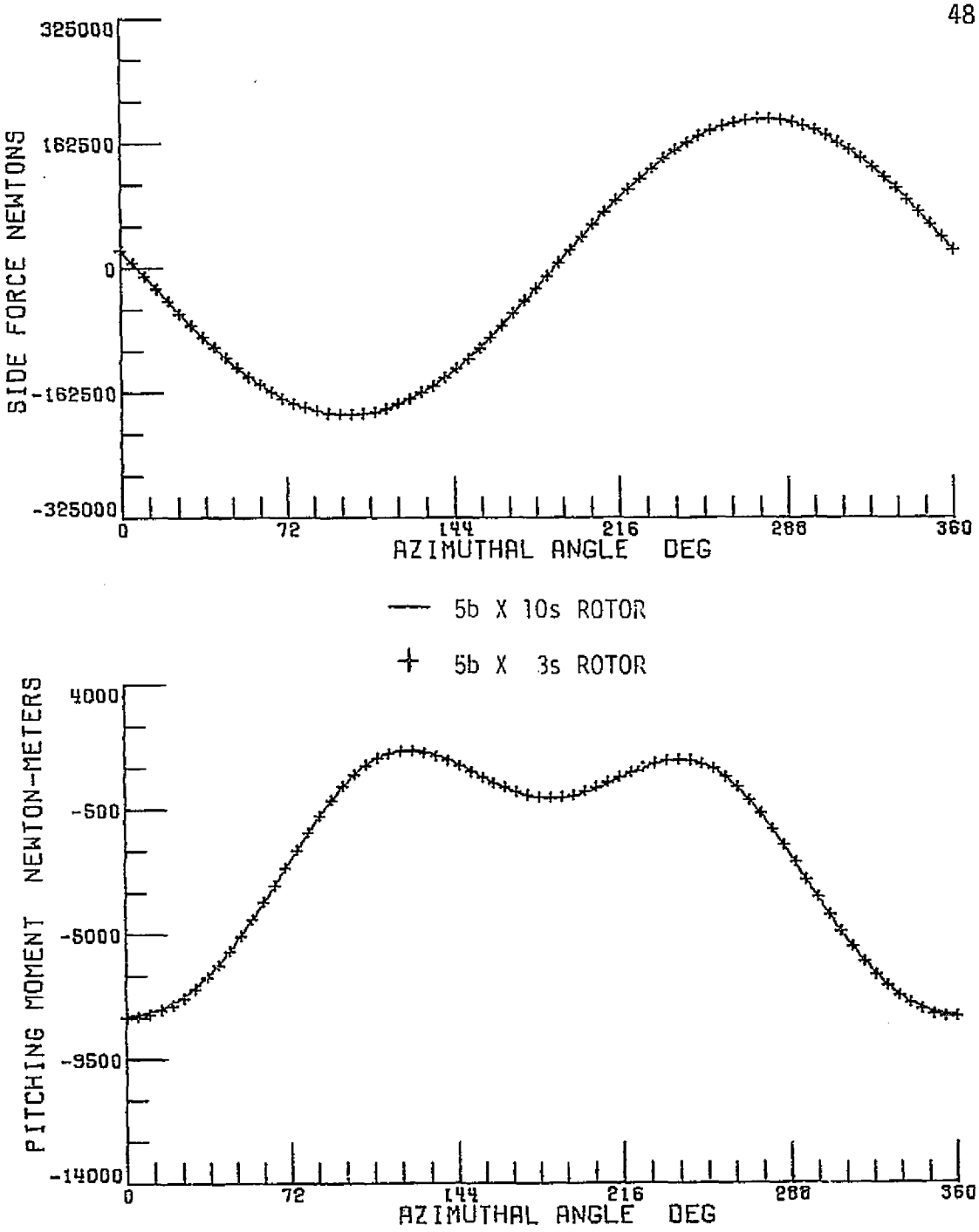

Figure 15.- Continued.

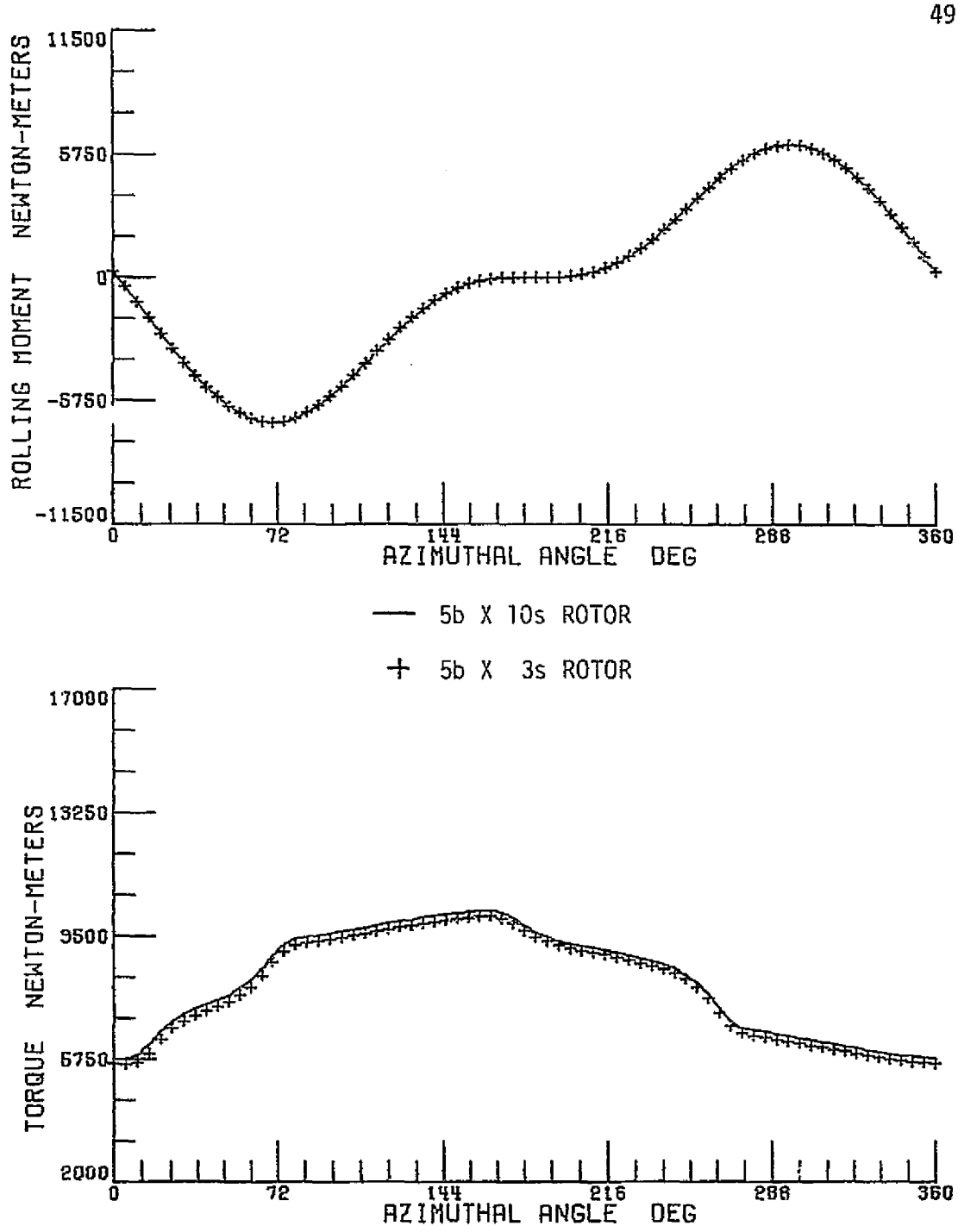

Figure 15.- Concluded.

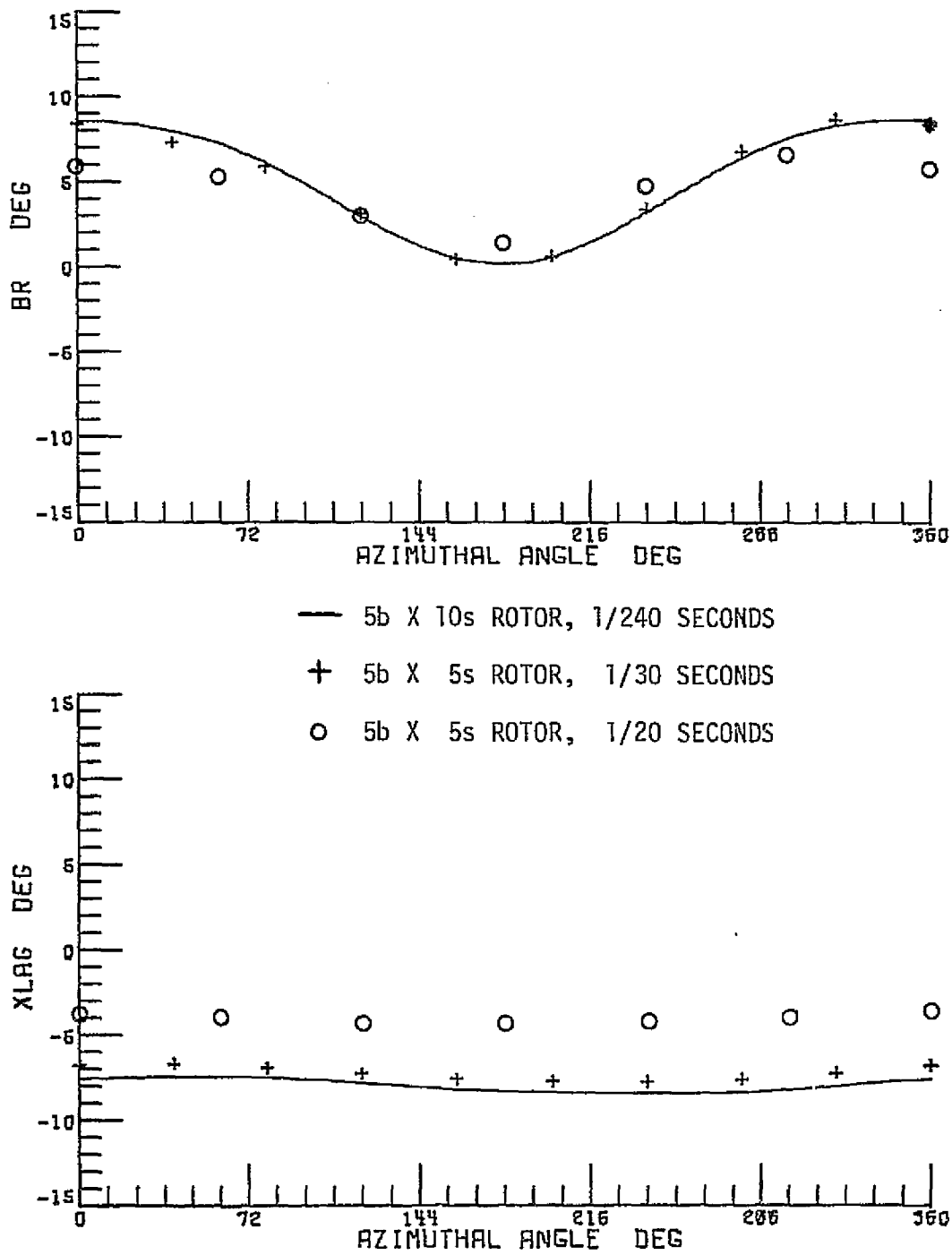

Figure 16.- Effect of Increasing Integration Interval to 1/30 Seconds and 1/20 Seconds on One Blade Revolution Data at 120 Knots.

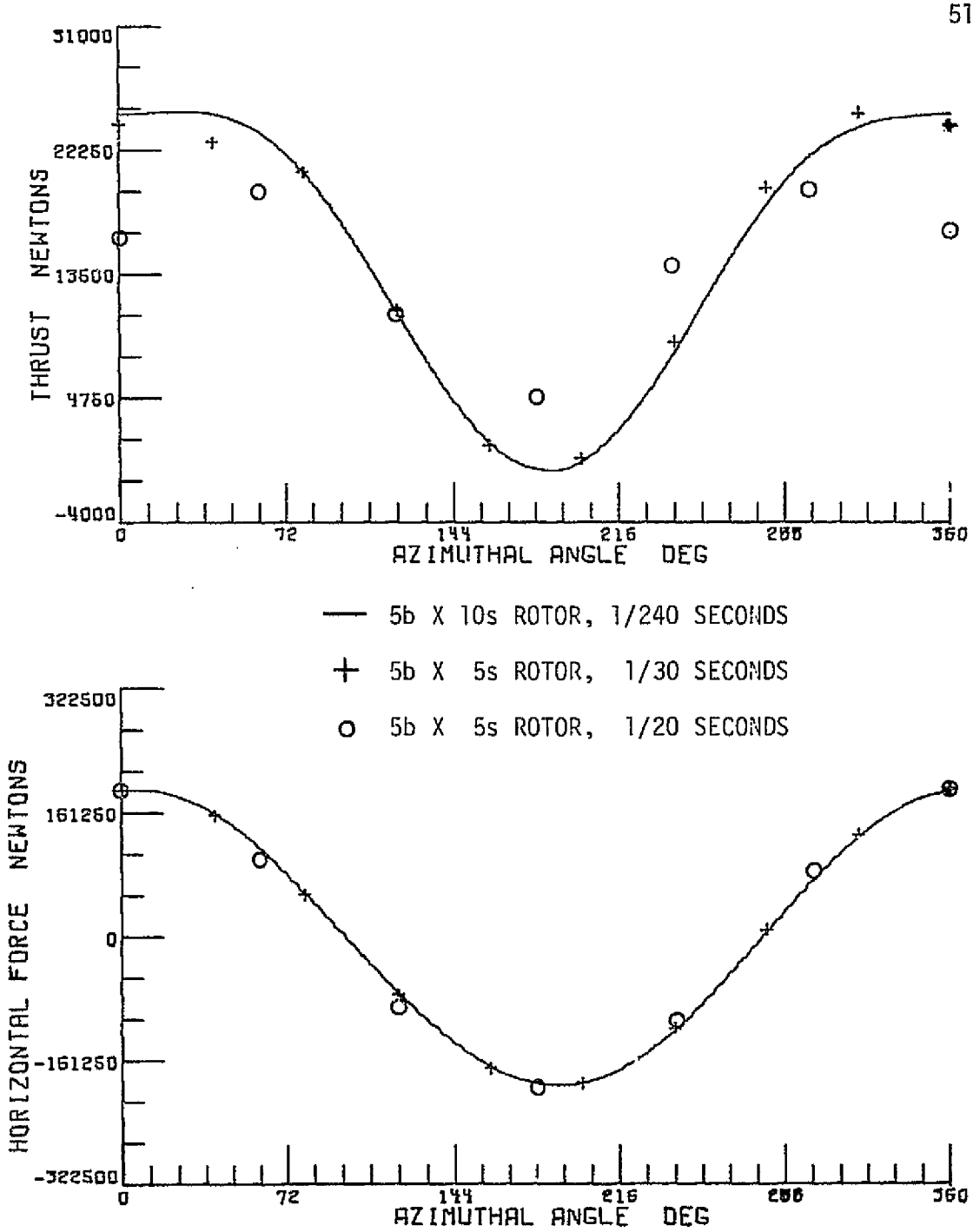

Figure 16.- Continued.

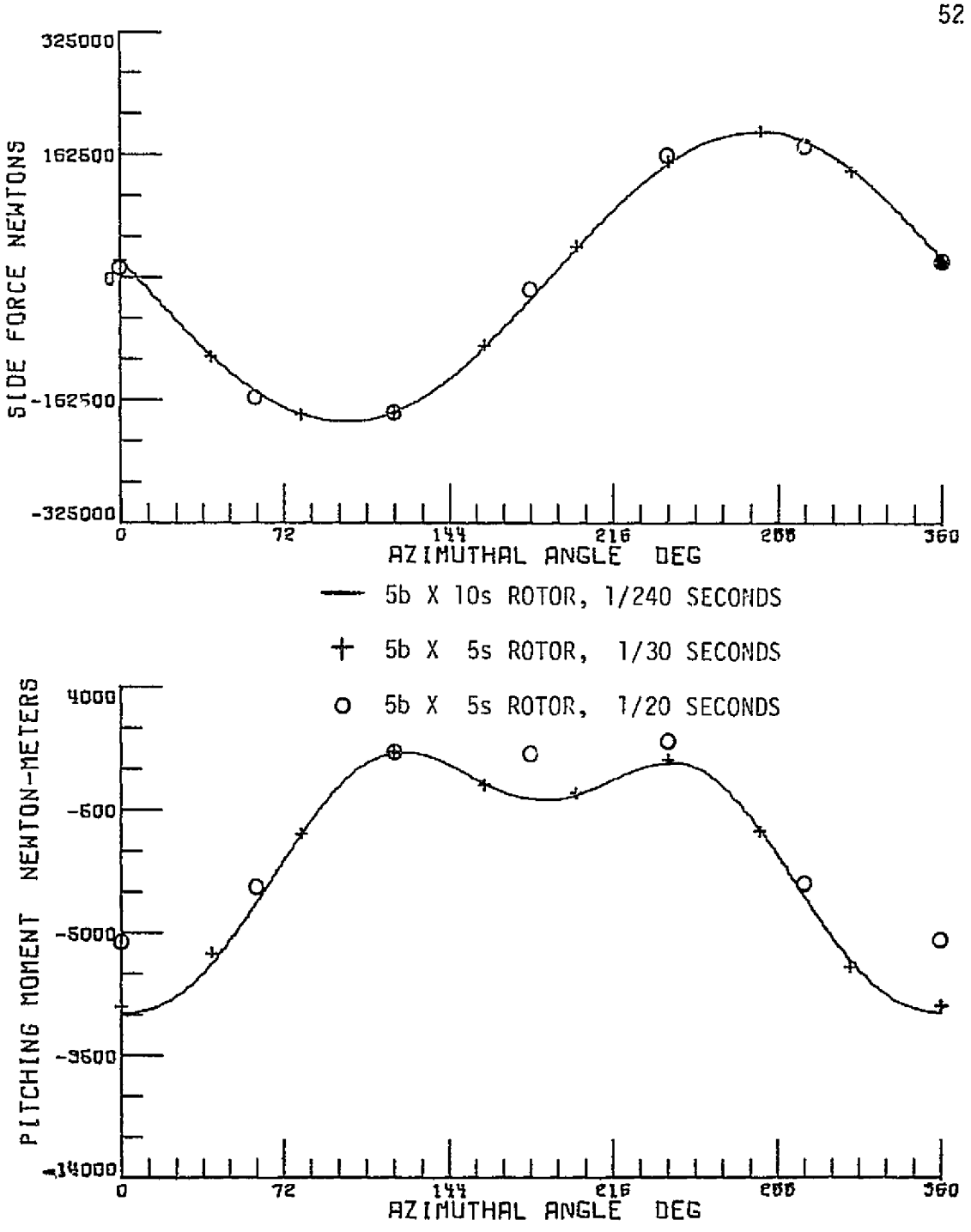

Figure 16.- Continued.

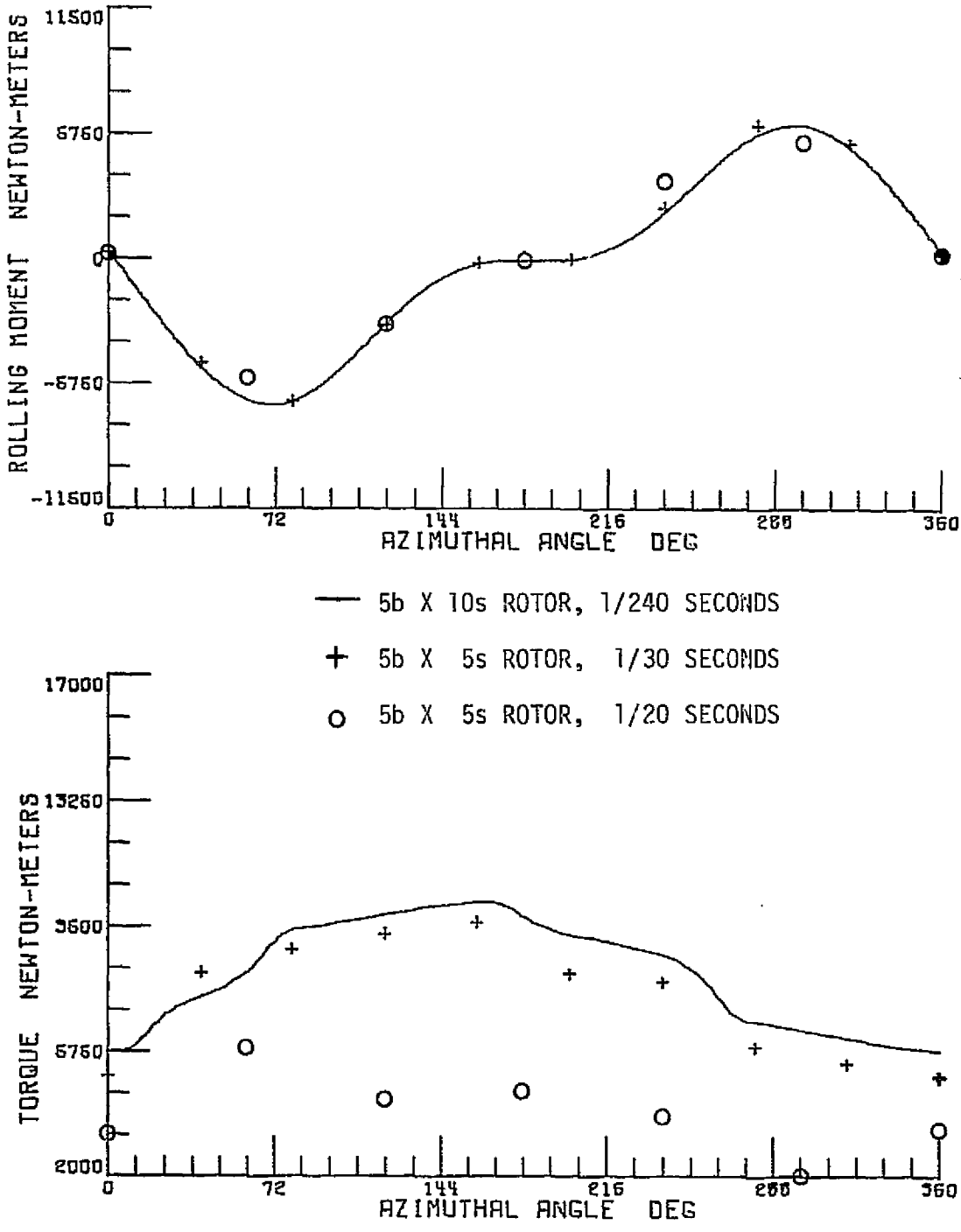

Figure 16.- Concluded.

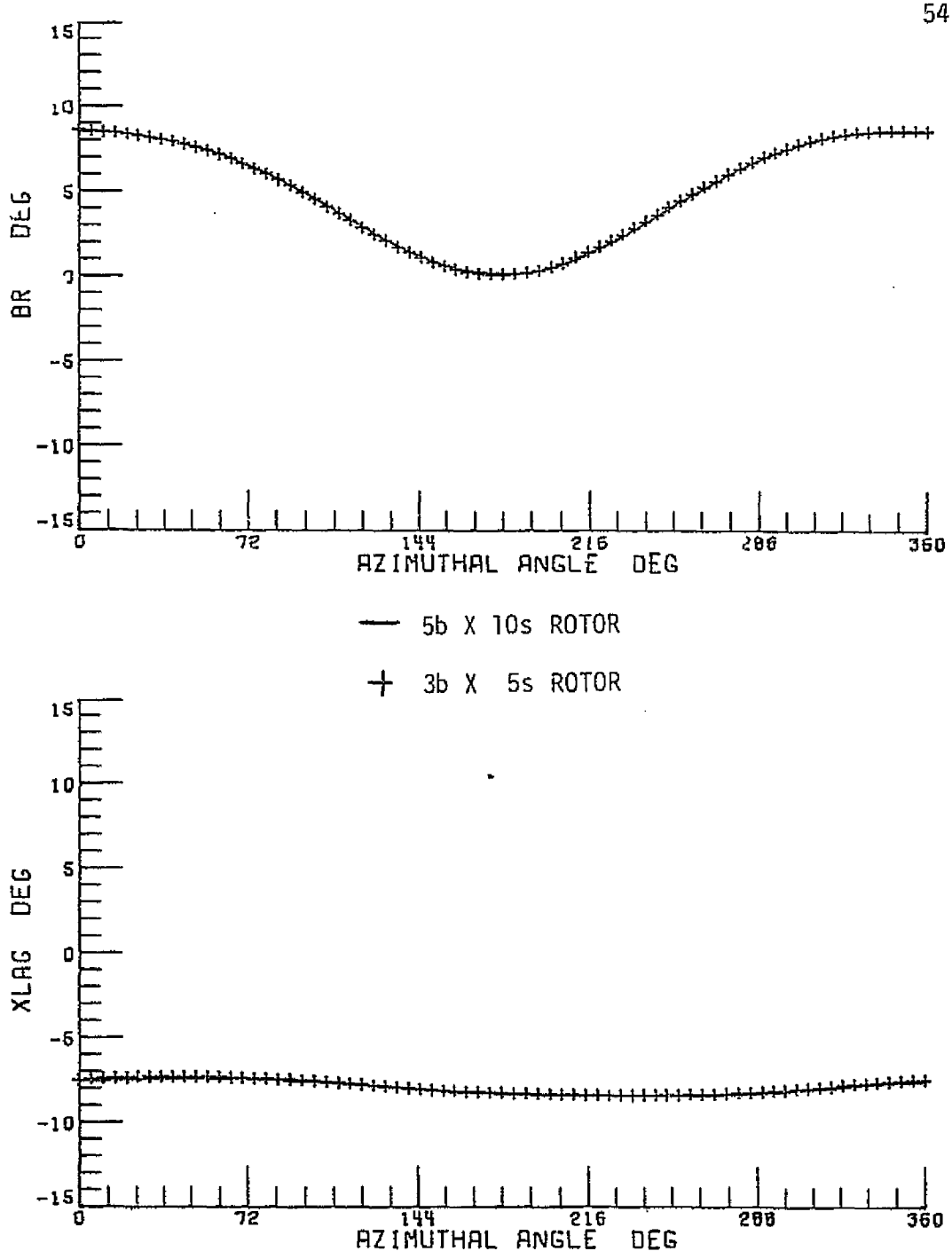

Figure 17.- Example of Increased Load on Remaining Blades After Blade Reduction. (Integration Interval of 1/240 Seconds).

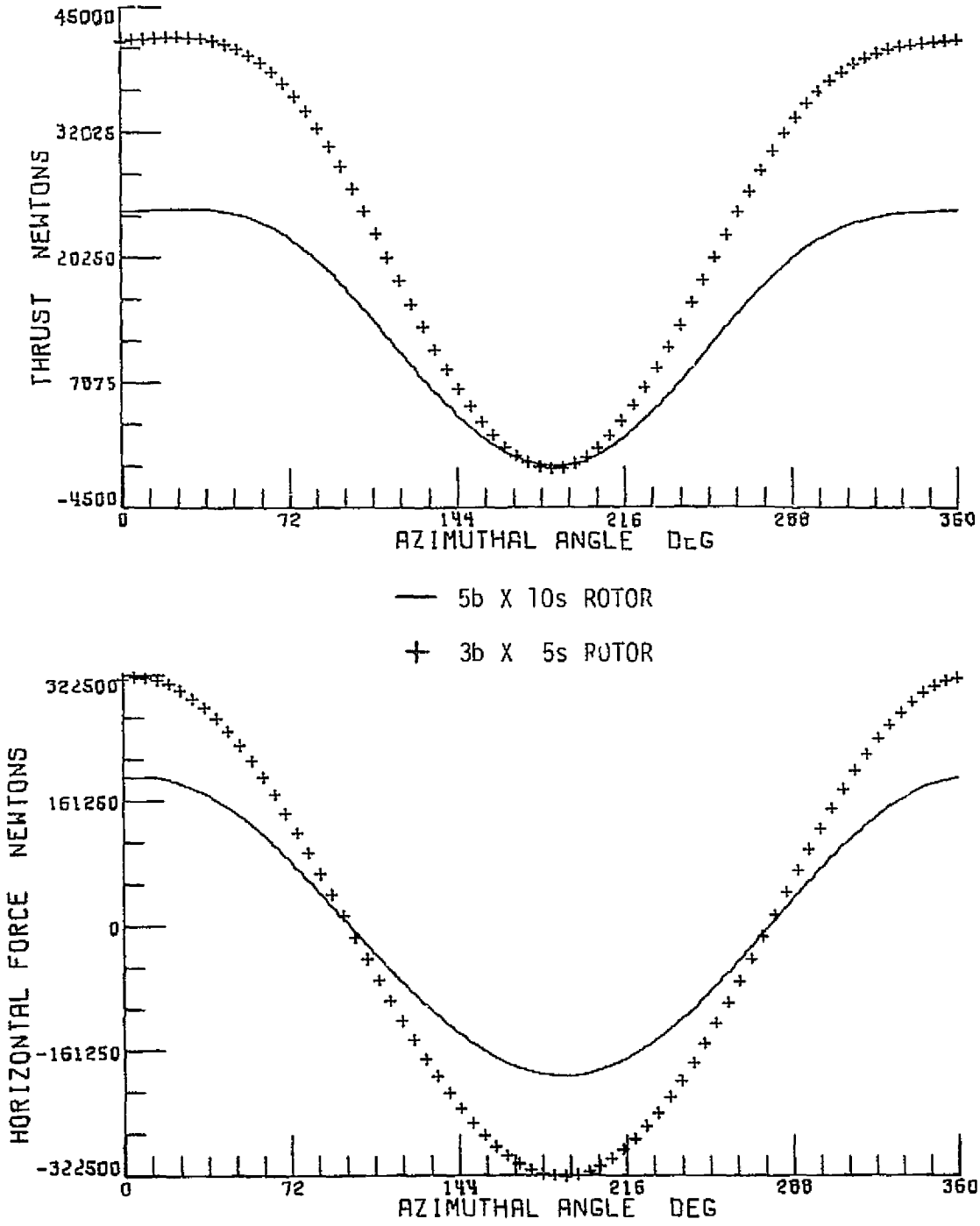

Figure 17.- Continued.

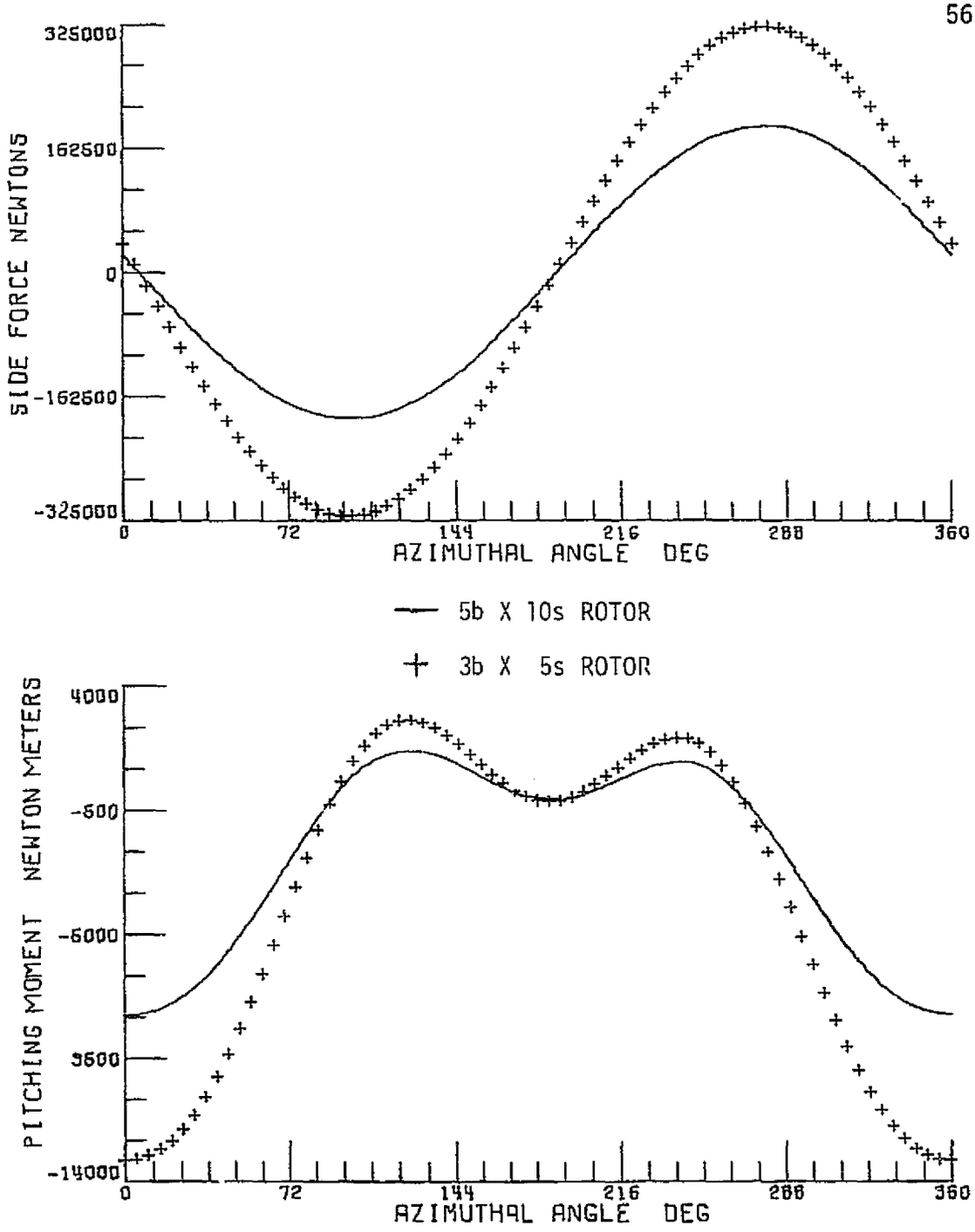

Figure 17.- Continued.

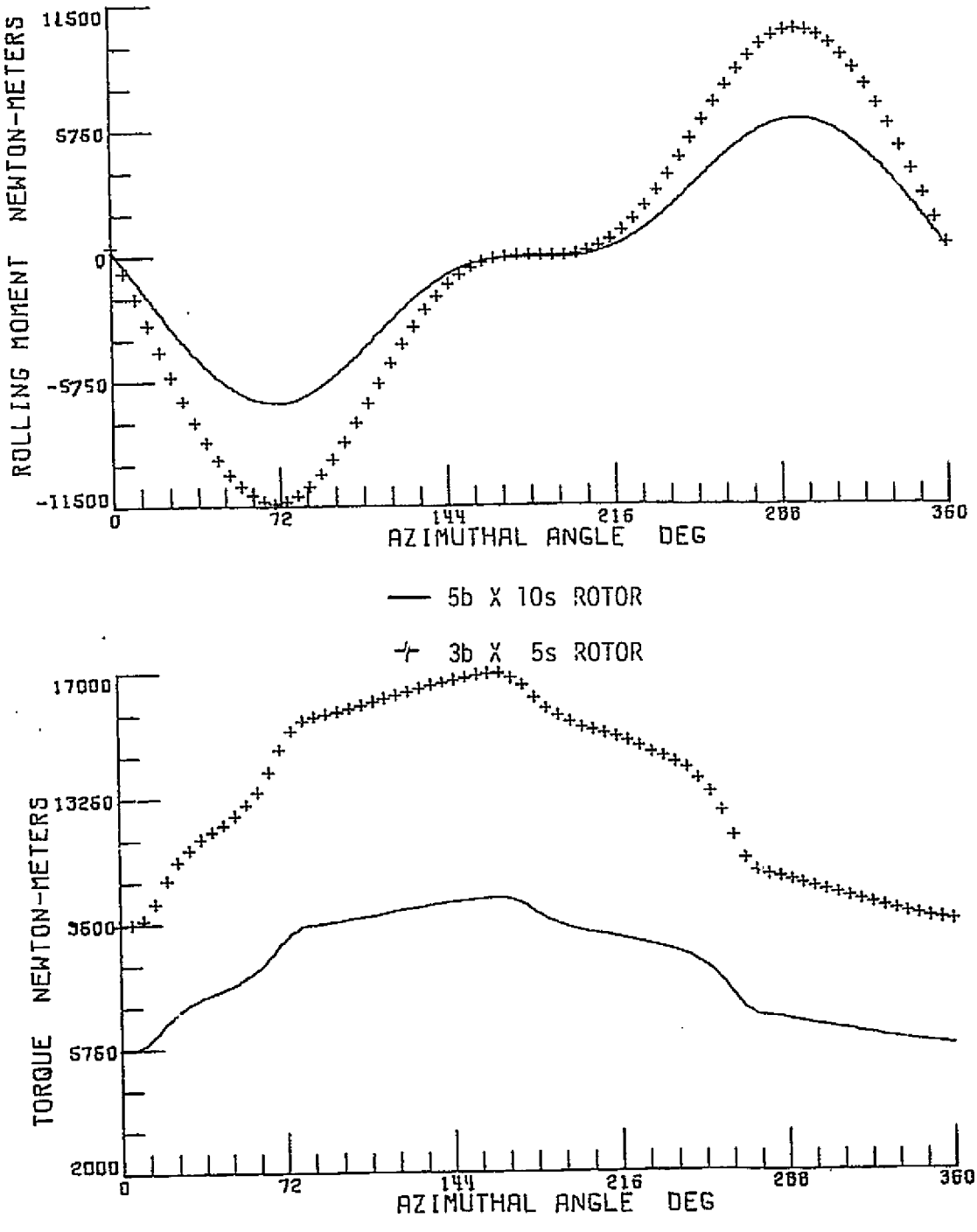

Figure 17.- Concluded.

simulating a 5-blade rotor system. The example presented is that of a 3-blade 5-blade segment rotor compared to the "truth" rotor, both at an integration interval of 1/240 seconds and at a forward velocity of 120 knots. The flapping and lagging motions show no noticeable difference, however, the compensating effect is very apparent in all of the forces and moments, with the maximum amplitudes being much higher for the 3-blade rotor.

To summarize, reducing the number of blade segments appears to have relatively little effect on the blade parameters as the blade makes an entire 360 degree revolution. This backs up the results obtained in the static trim tests and the total rotor force and moment tests. Once again, as was the case with the two previous tests, the largest errors occur when the integration interval, and therefore the azimuthal advance angle, is increased. One final point is brought forth by this test, that is, if the number of blades is reduced, the individual blade data are no longer representative of how an actual blade would be performing in a rotor system. This is due to the compensating effect which occurs when less than the actual number of blades are simulated.

Dynamic Response Comparison

The total vehicle dynamic response tests were set up by initializing the RSRA vehicle to the trim conditions determined previously in the static trim tests. At one second into the flight, a 5 percent lateral cyclic pulse was applied for one second and then the stick was returned to the trim position. During the test run all pertinent vehicle states, such as linear and angular accelerations and velocities, body attitudes, and blade flapping and lagging motions, were recorded. Of these states, body roll acceleration (PBD), body roll rate (PB), roll angle (PHI), pitch angle (THET), and blade

flapping angle (BR) are presented for illustration of the effects of the various mathematical model degradations. Each case presented is compared to the "truth" rotor to illustrate these effects.

Figure 18 presents a time-history comparison of a 5-blade 5-blade segment rotor (LaRC rotor configuration) with the 5-blade 10-blade segment "truth" rotor at the 120 knot condition. A slightly larger amplitude is seen in the high frequency content of the roll acceleration which in turn causes a slightly different roll rate and roll attitude. Very slight differences also occur in pitch attitude and flapping angle. In general these differences are well within the bounds of acceptance. The results of the hover case are, in general, slightly better than the 120 knot case.

Figure 19 presents the effect of blade reduction on vehicle dynamic response at 120 knots. The case represented is that of a 3-blade 5-blade segment rotor compared to the "truth" rotor. The effect of the reduction of number of blades is very apparent in the roll acceleration and roll rate curves. The mathematical model is over-amplifying the rotor response when it scales the rotor forces and moments for the correct number of blades in the rotor system. The high frequency oscillation in roll acceleration and roll rate is affecting roll attitude, however the effect is relatively small Pitch angle and flapping angle also have small differences. The hover case shows the same effects, however, to a smaller degree.

Figure 20 presents the effect of blade segment reduction on vehicle dynamic response at 120 knots. The case presented is that of a 5-blade 3-blade segment rotor with an integration interval of 1/240 seconds. Relatively little difference is seen in any of the states when compared with the "truth" rotor, with the most noticeable difference being in blade flapping angle. The hover case

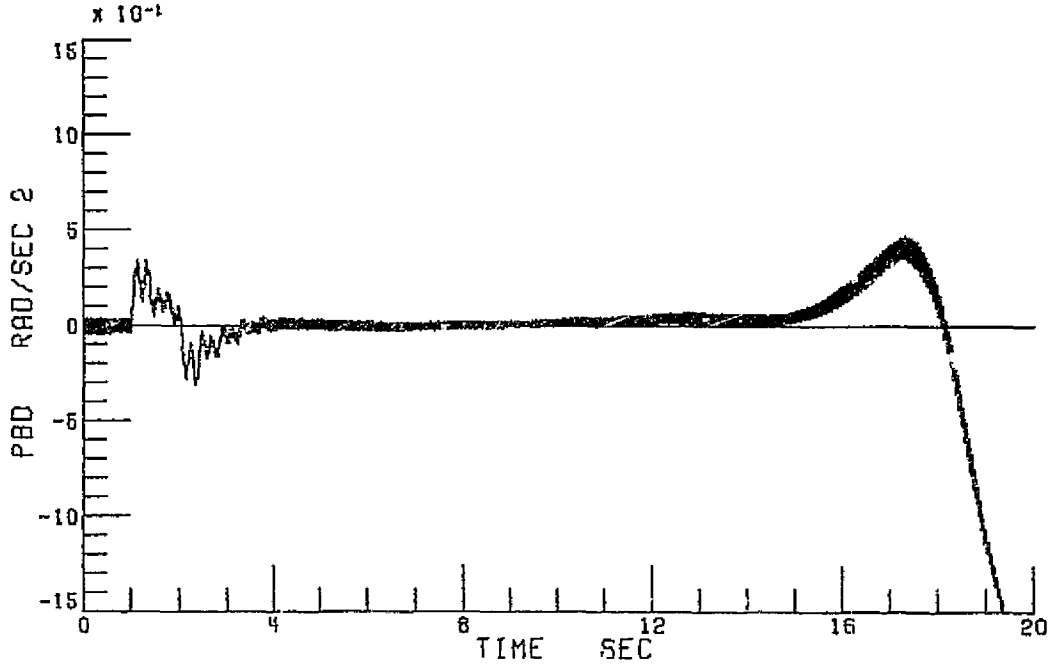

5b X 5s ROTOR

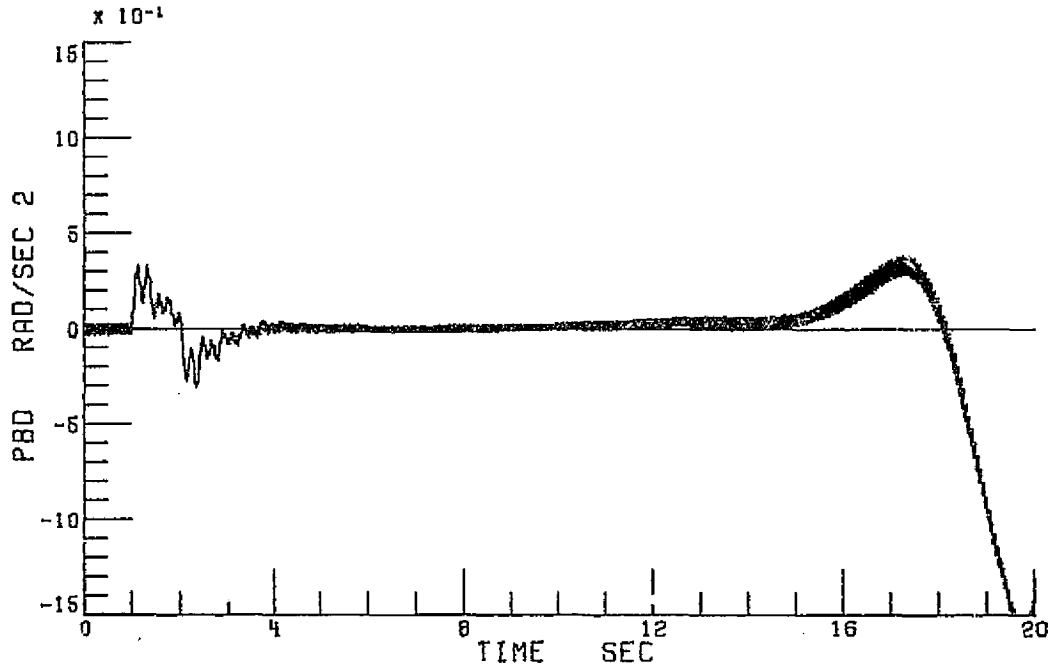

5b X 10s ROTOR

Figure 18.- Dynamic Response Comparison of 5-Blade 5-Blade Segment Rotor Model with "Truth" Rotor Model at 120 Knots. (Integration Interval of 1/240 Seconds).

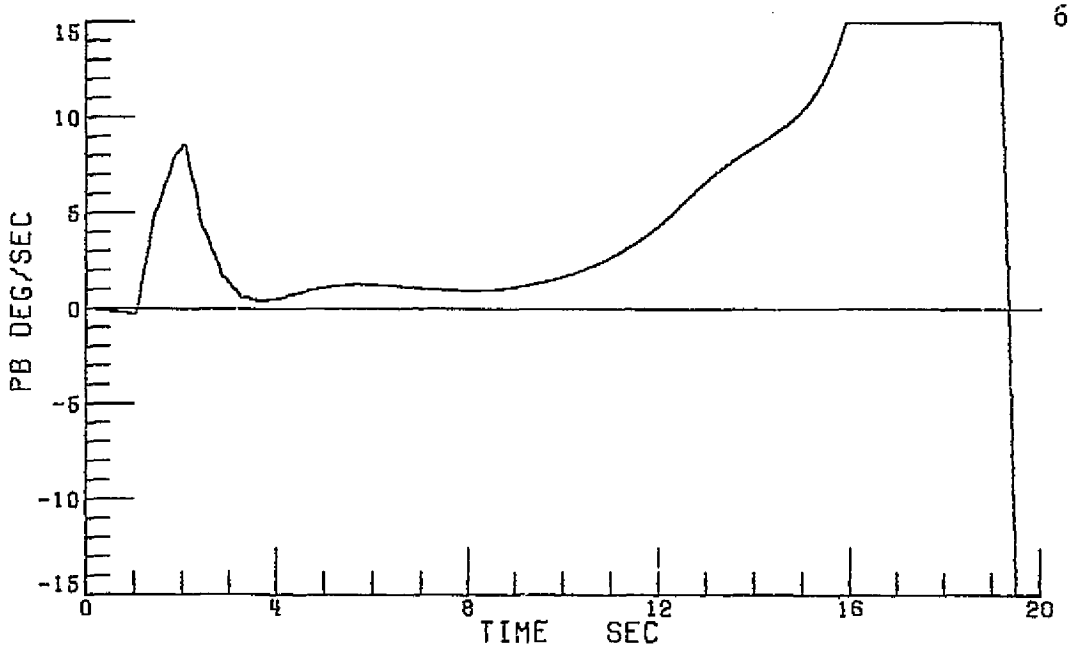

5b X 5s ROTOR

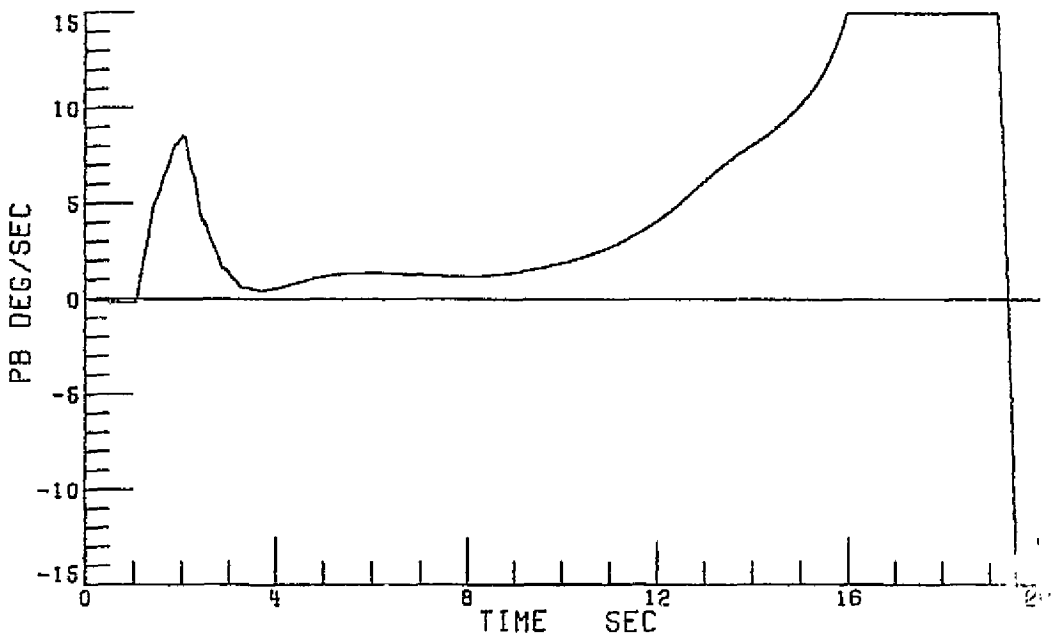

5b X 10s ROTOR

Figure 18.- Continued.

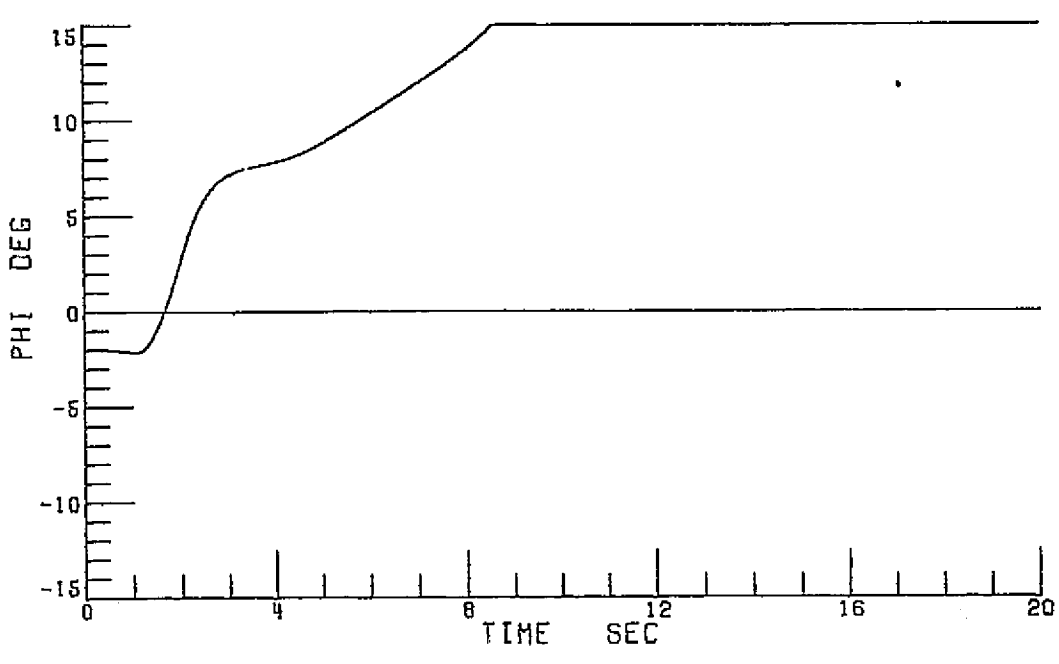

5b X 5s ROTOR

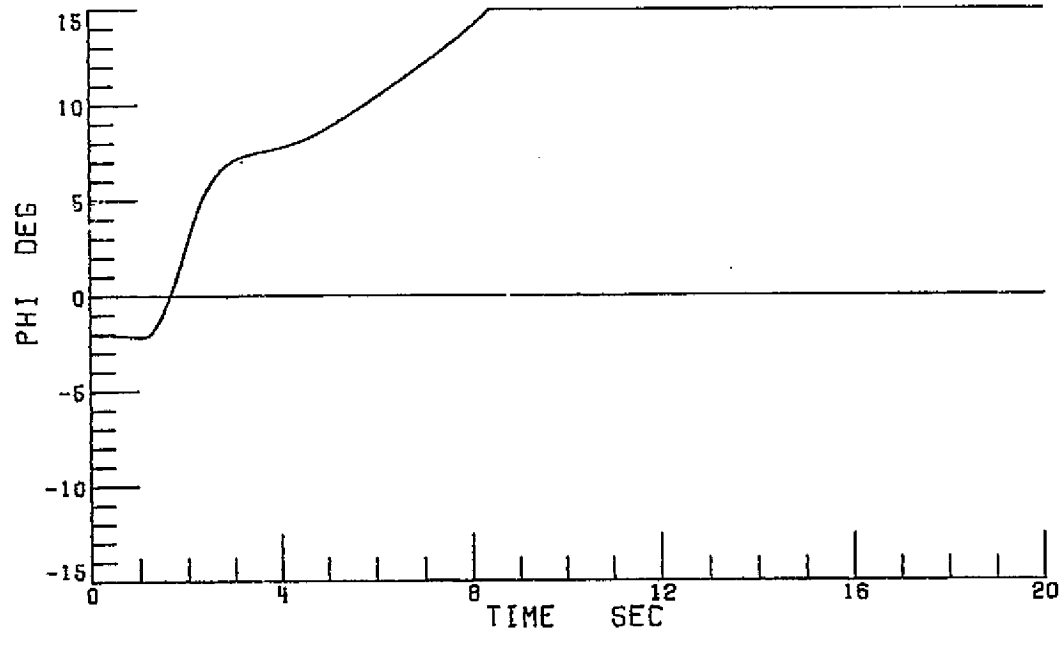

5b X 10s ROTOR

Figure 18.- Continued.

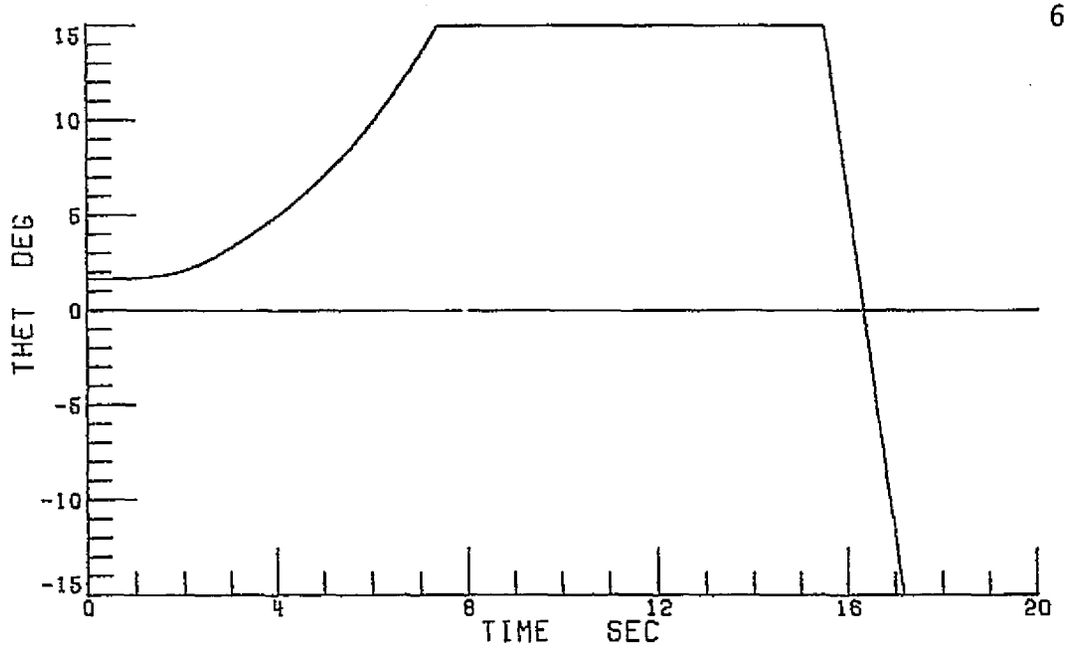

5b X 5s ROTOR

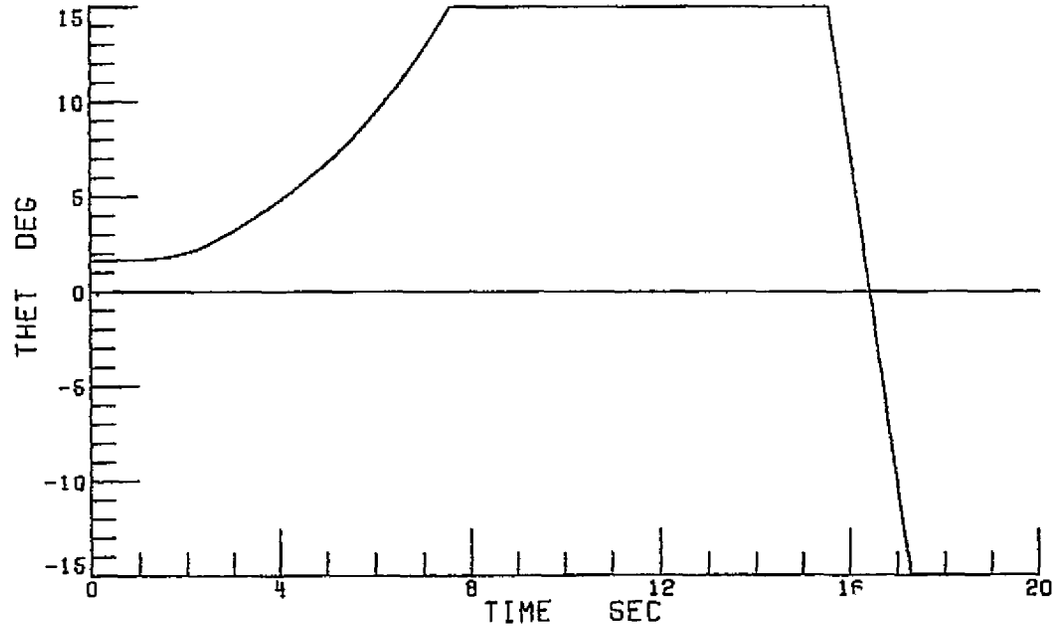

5b X 10s ROTOR

Figure 18.- Continued.

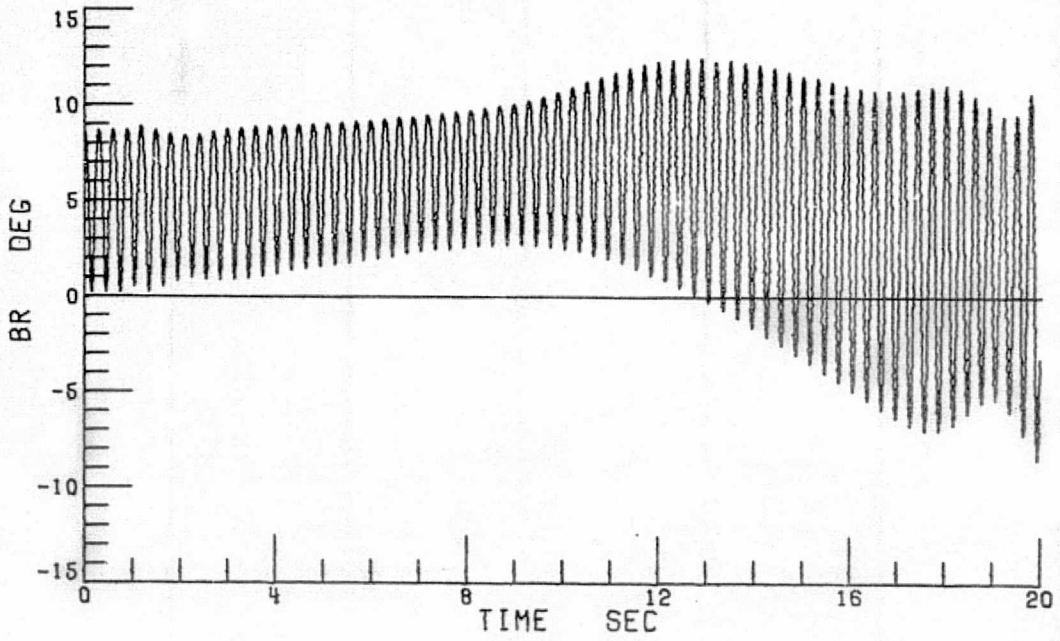

5b X 5s ROTOR

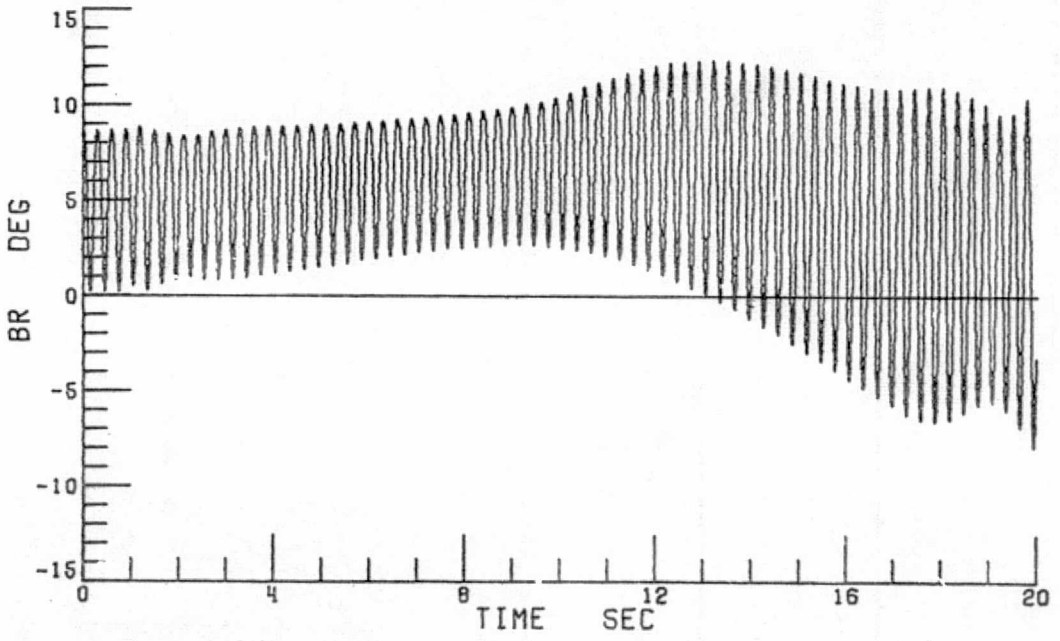

5b X 10s ROTOR

Figure 18.- Concluded.

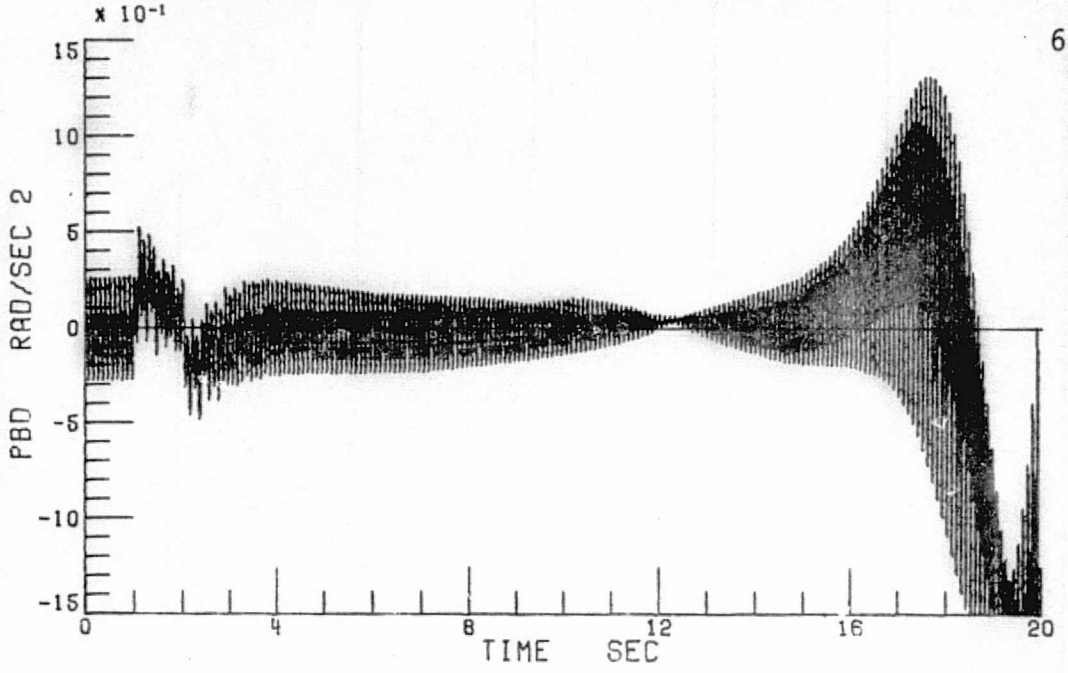

3b X 5s ROTOR

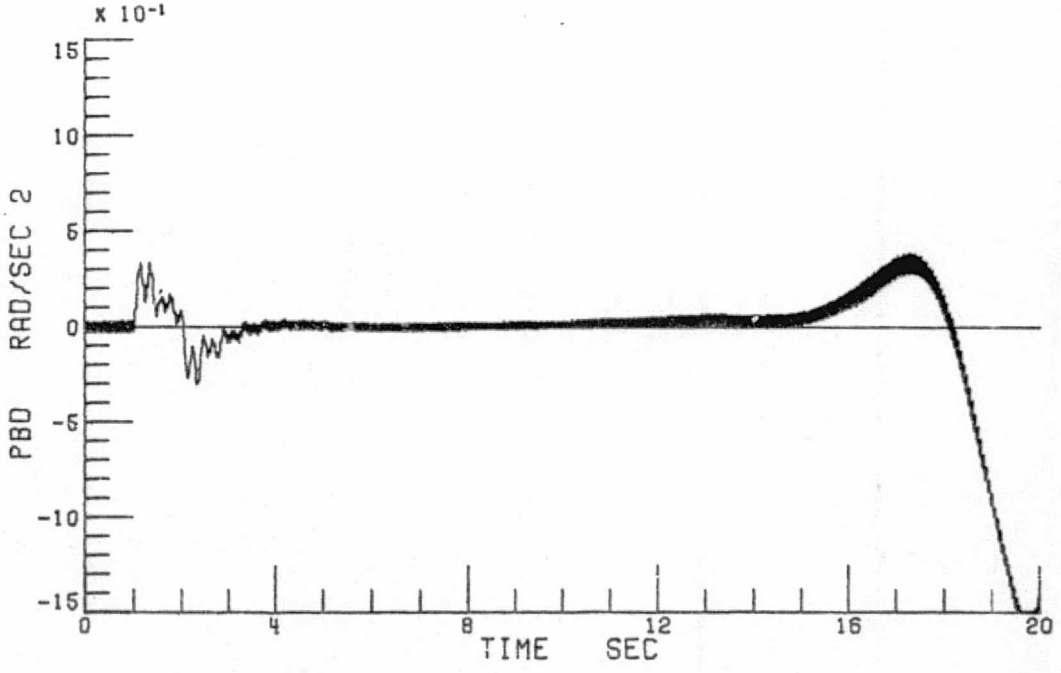

5b X 10s ROTOR

Figure 19.- Effect of Blade Reduction on Vehicle Dynamic Response at 120 Knots. (Integration Interval of 1/240 Seconds).

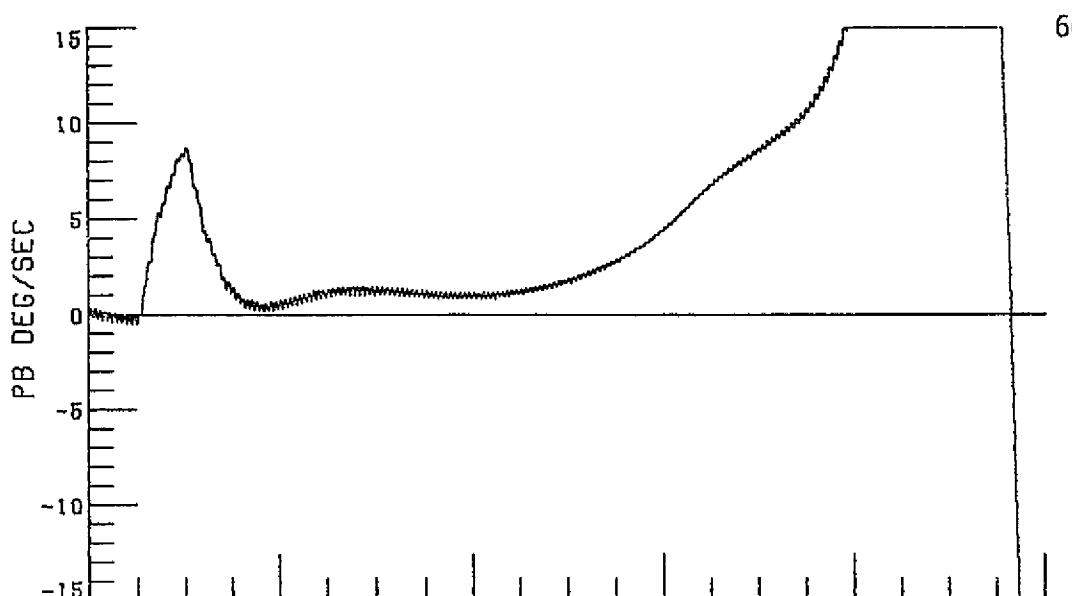

3b X 5s ROTOR

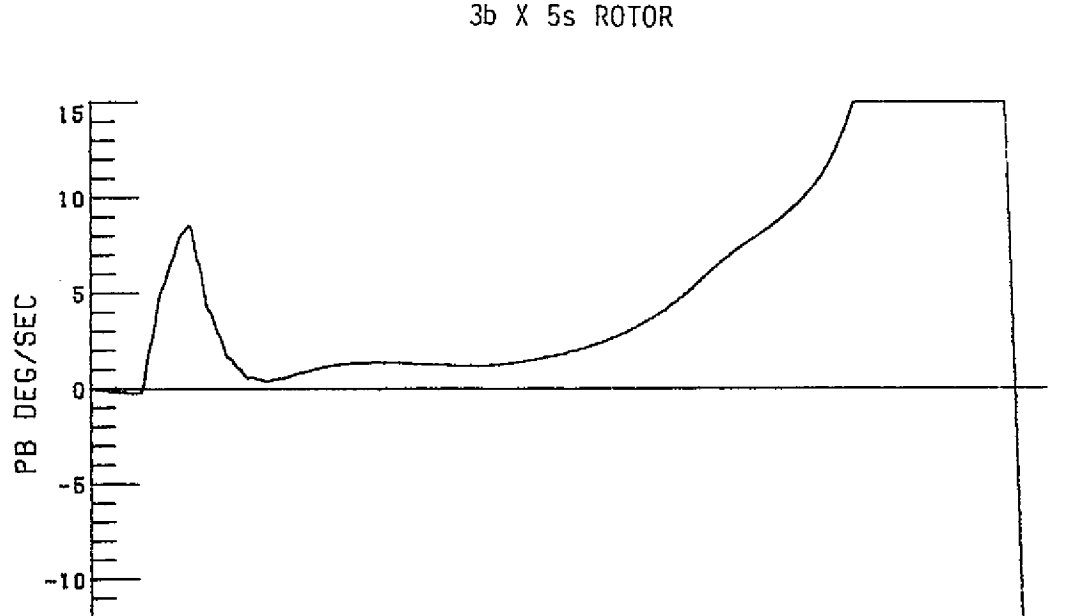

5b X 10s ROTOR

Figure 19.- Continued.

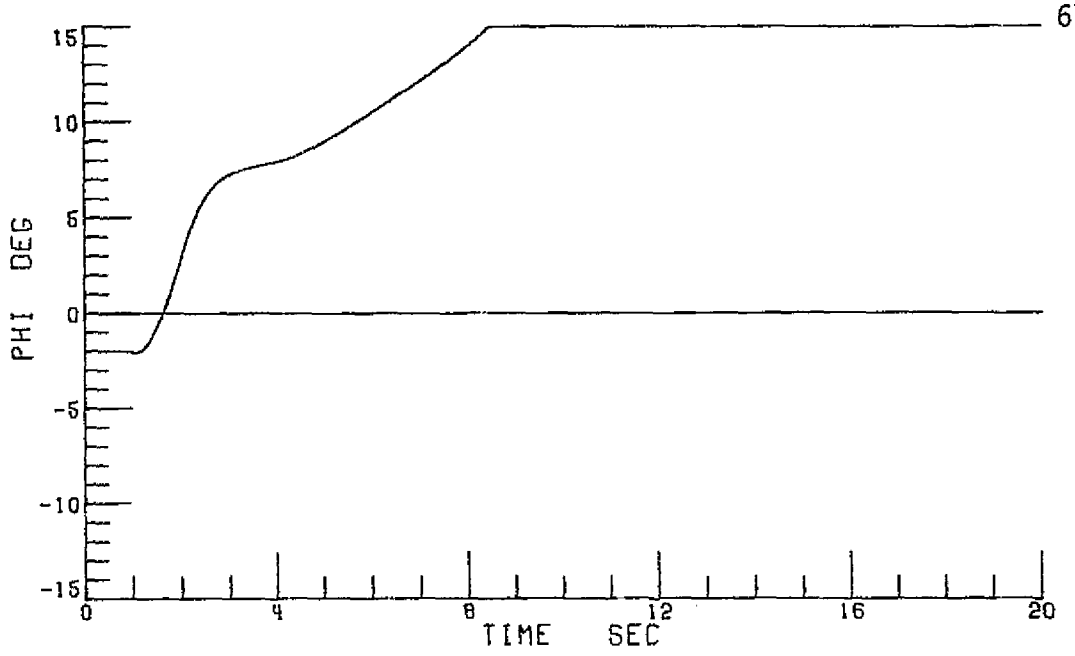

3b X 5s ROTOR

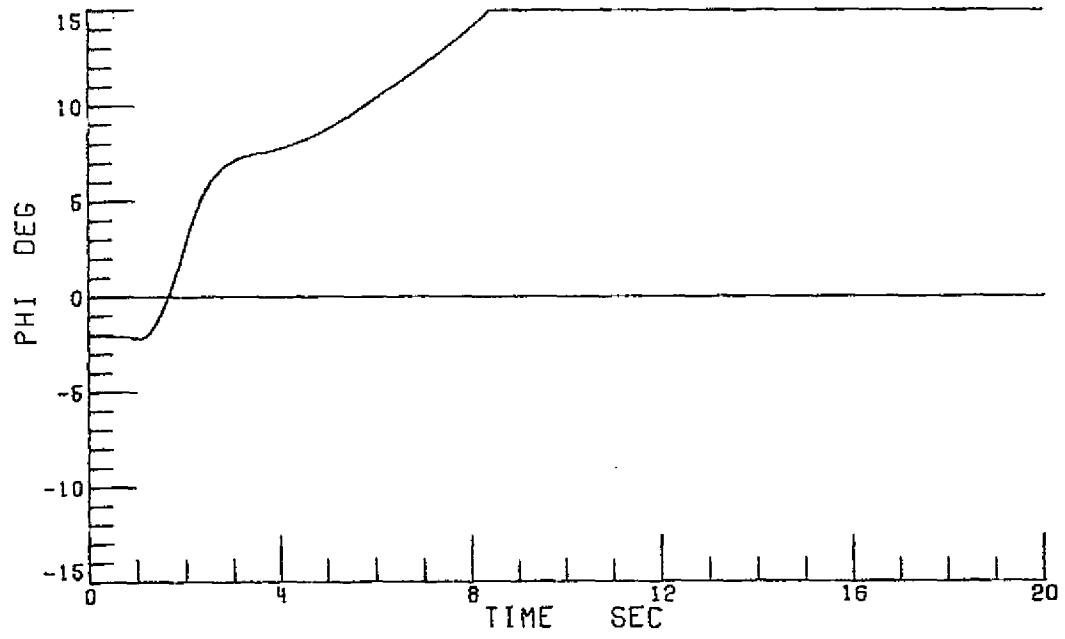

5b X 10s ROTOR

Figure 19.- Continued.

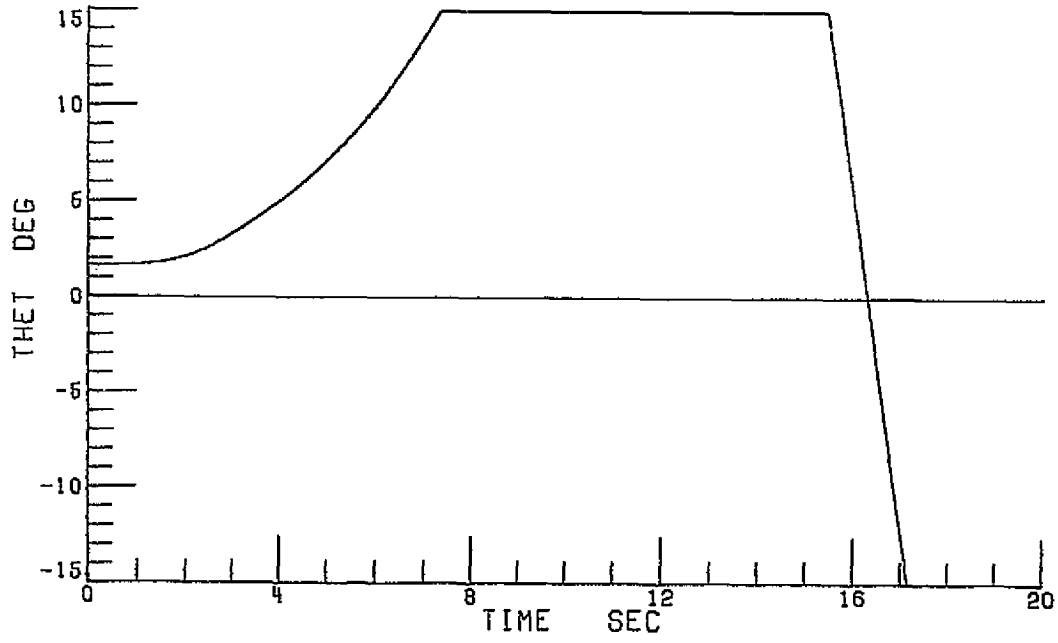

3b X 5s ROTOR

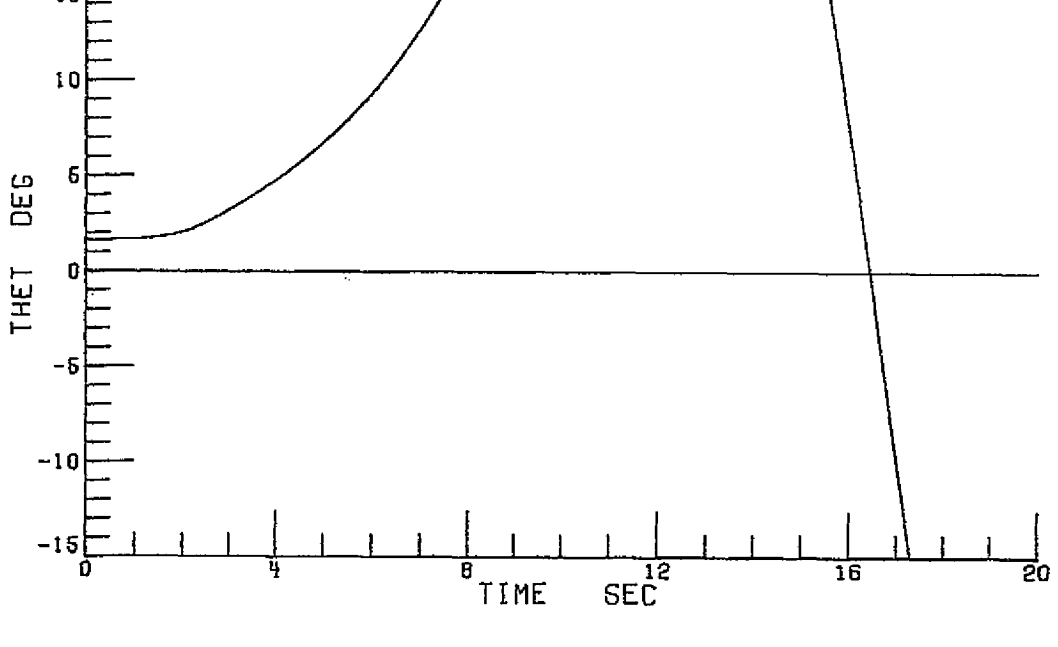

5b X 10s ROTOR

Figure 19.- Continued.

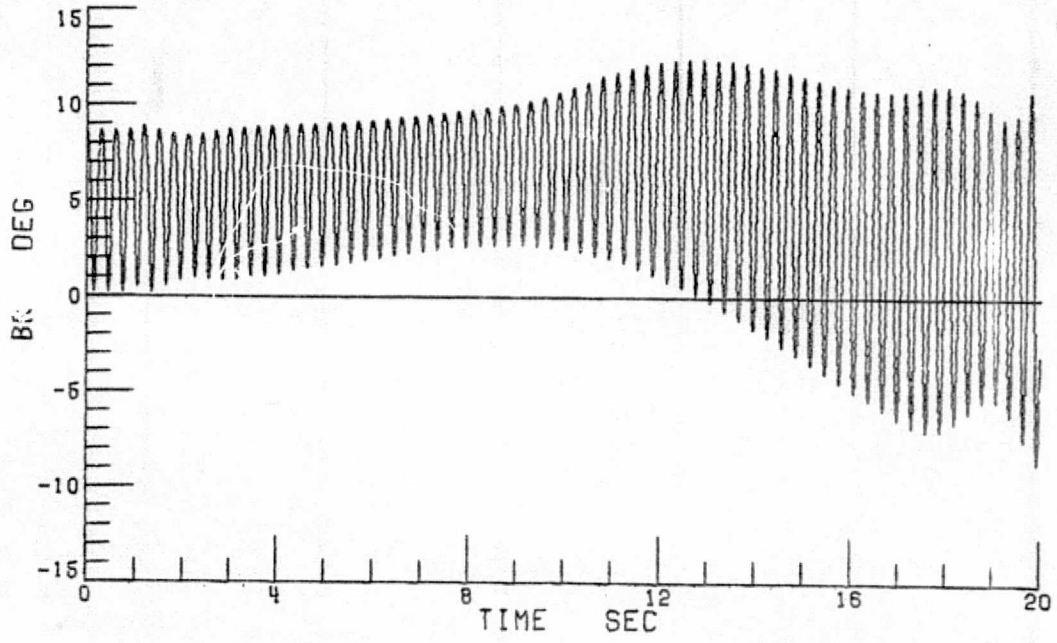

3b X 5s ROTOR

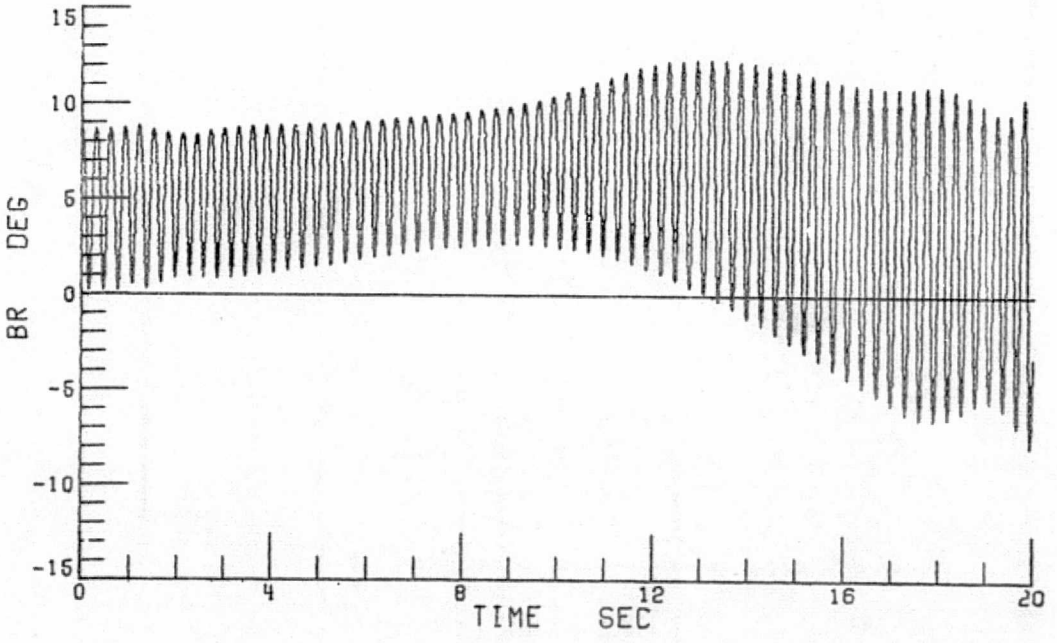

5b X 10s ROTOR

Figure 19.- Concluded.

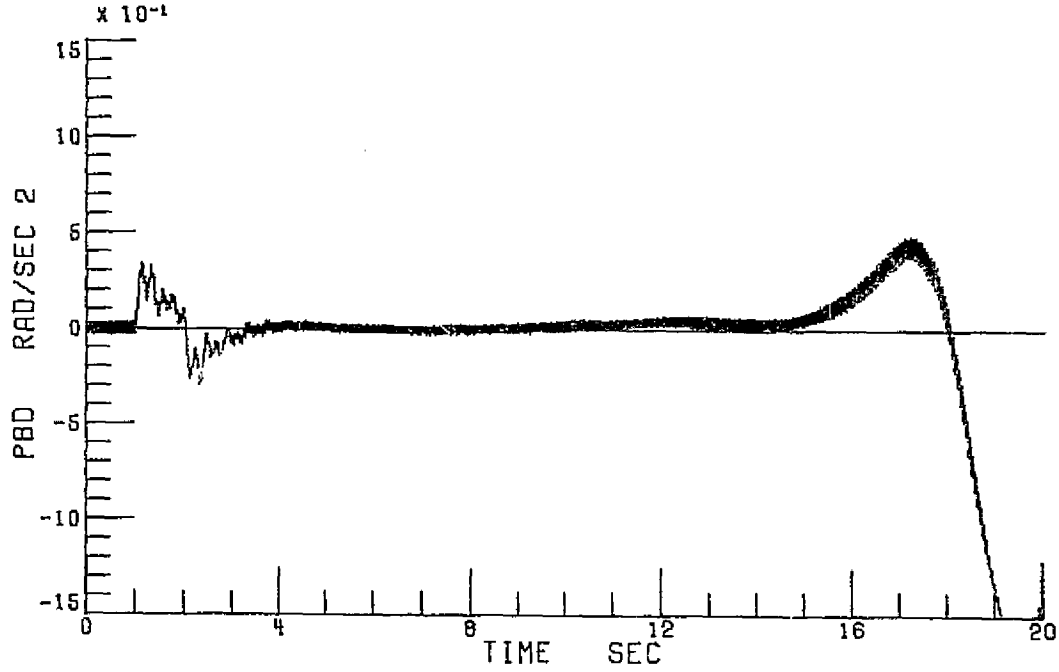

5b X 3s ROTOR

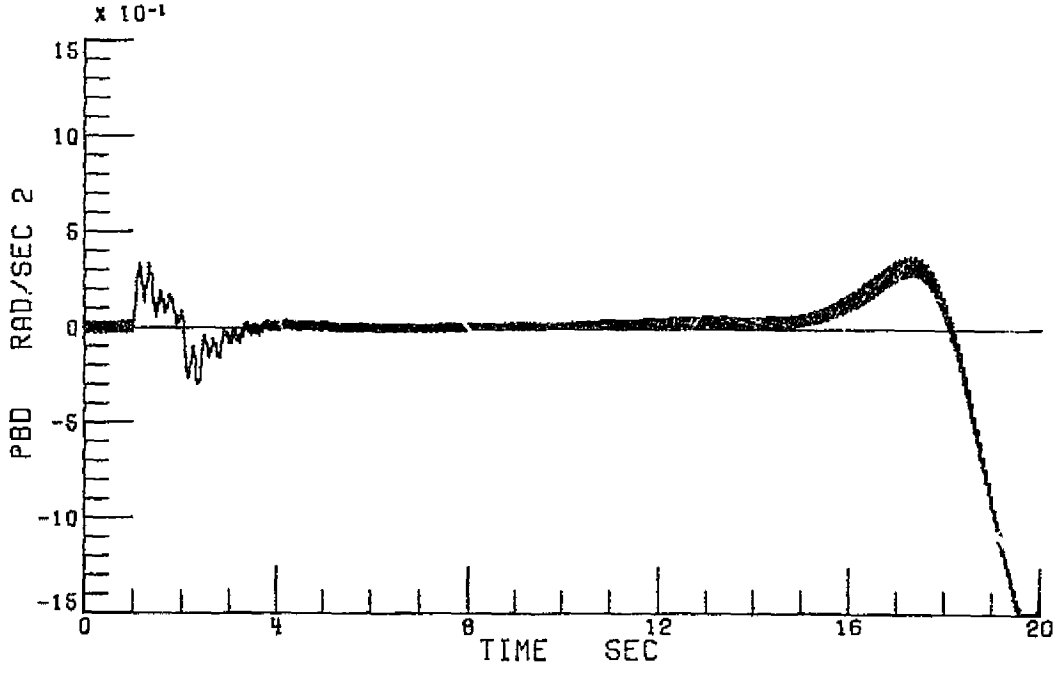

5b X 10s ROTOR

Figure 20.- Effect of Blade Segment Reduction on Vehicle Dynamic Response at 120 Knots. (Integration Interval of 1/240 Seconds).

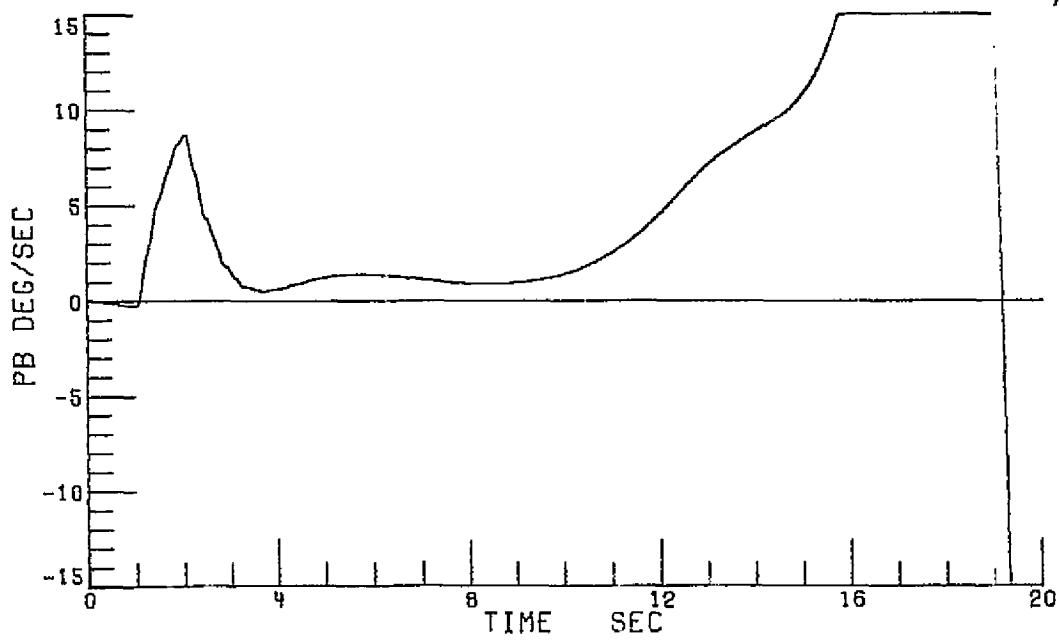

5b X 3s ROTOR

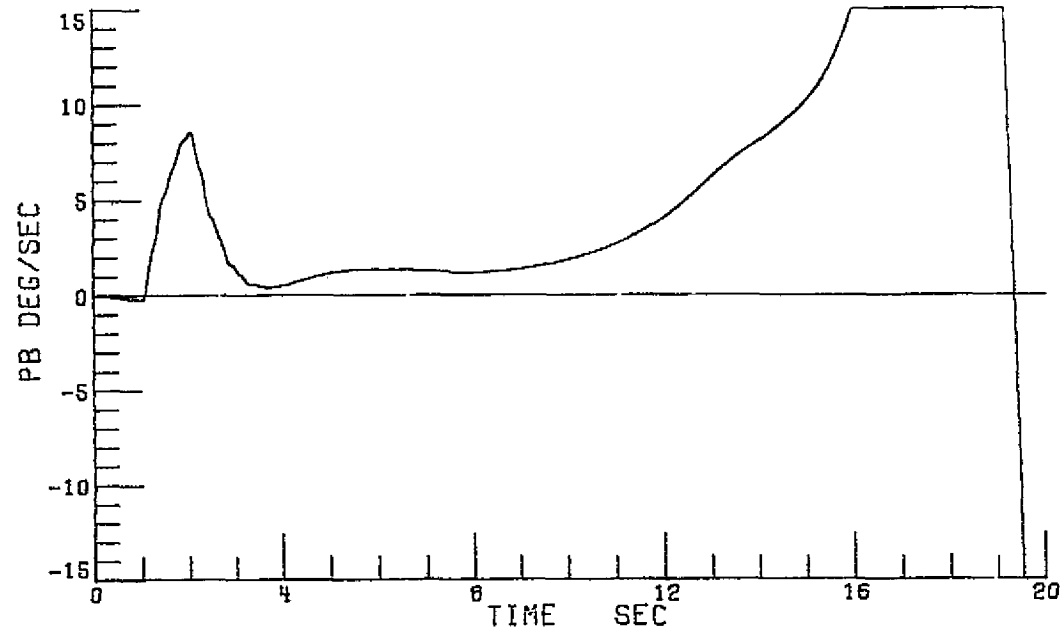

5b X 10s ROTOR

Figure 20.- Continued.

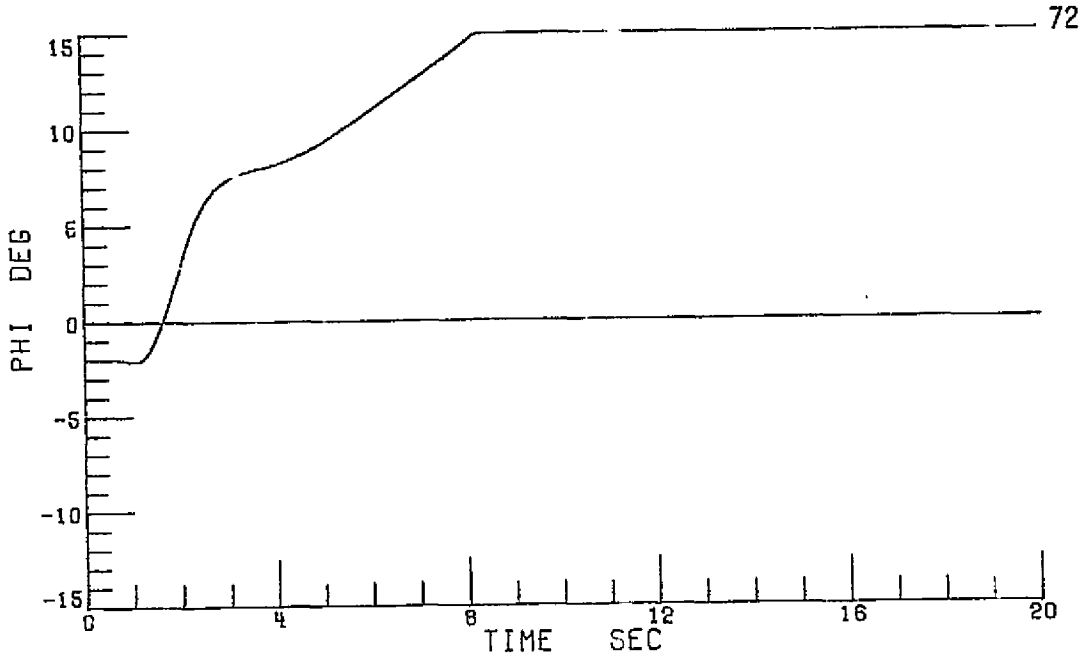

5b X 3s ROTOR

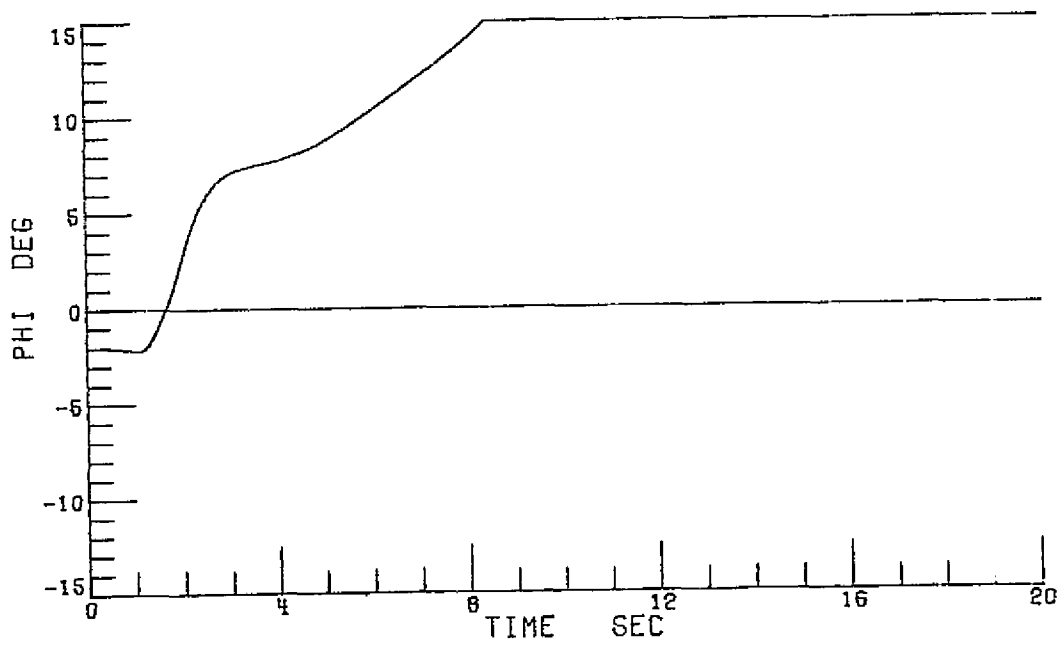

5b X 10s ROTOR

Figure 20.- Continued.

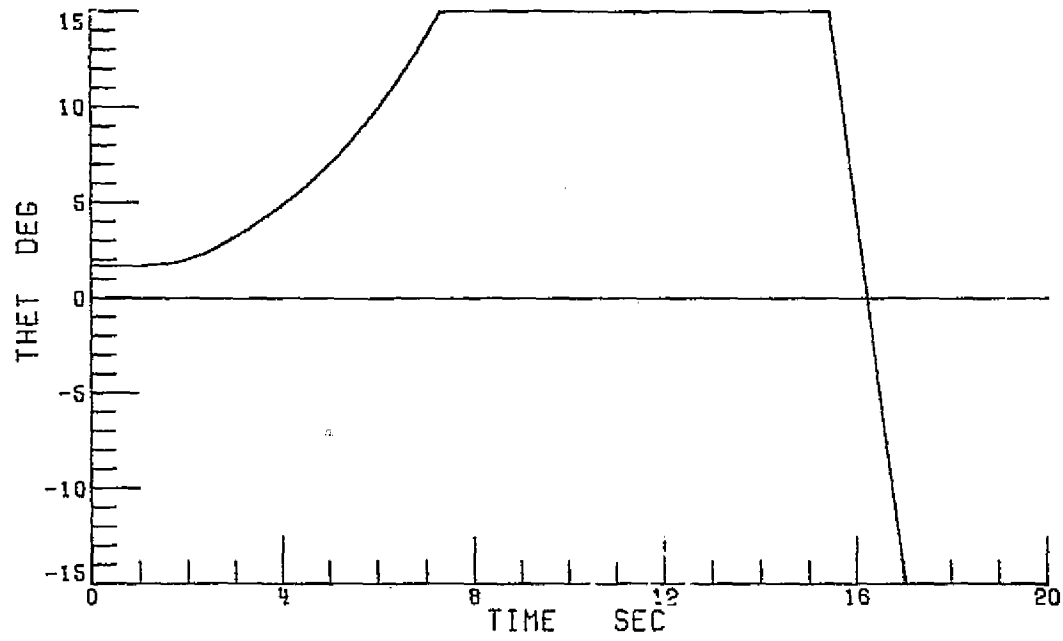

5b X 3s ROTOR

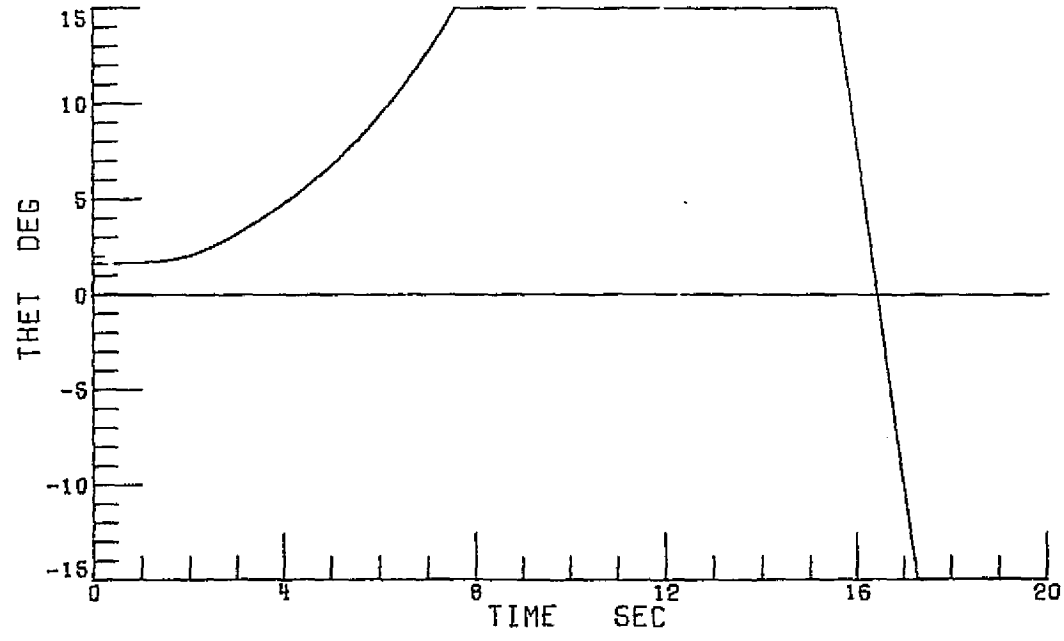

5b X 10s ROTOR

Figure 20.- Continued.

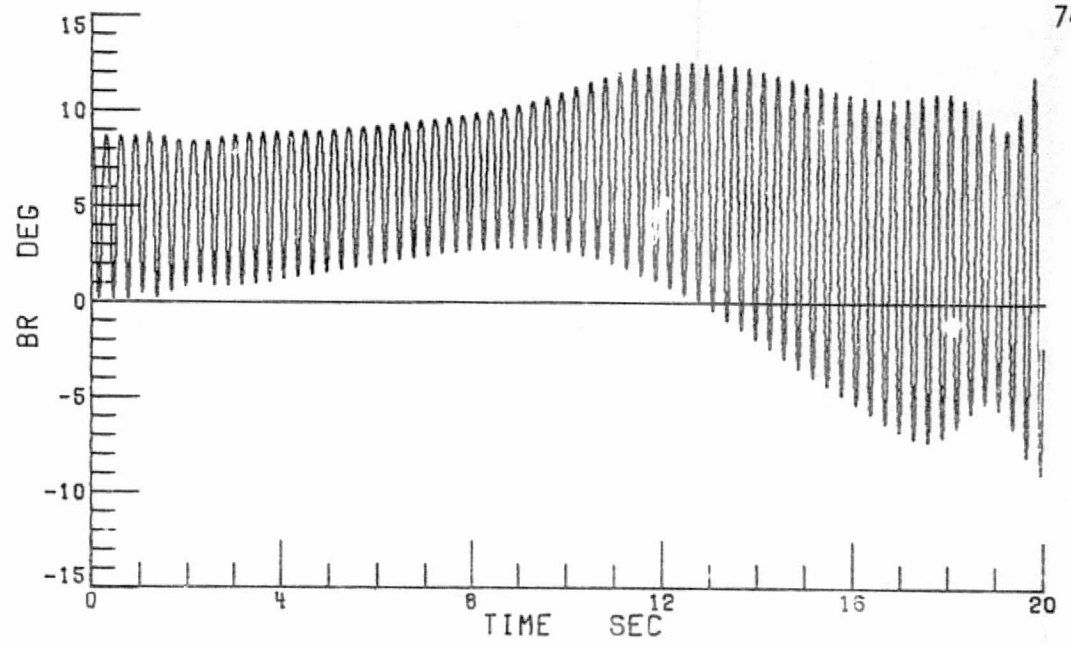

5b X 3s ROTOR

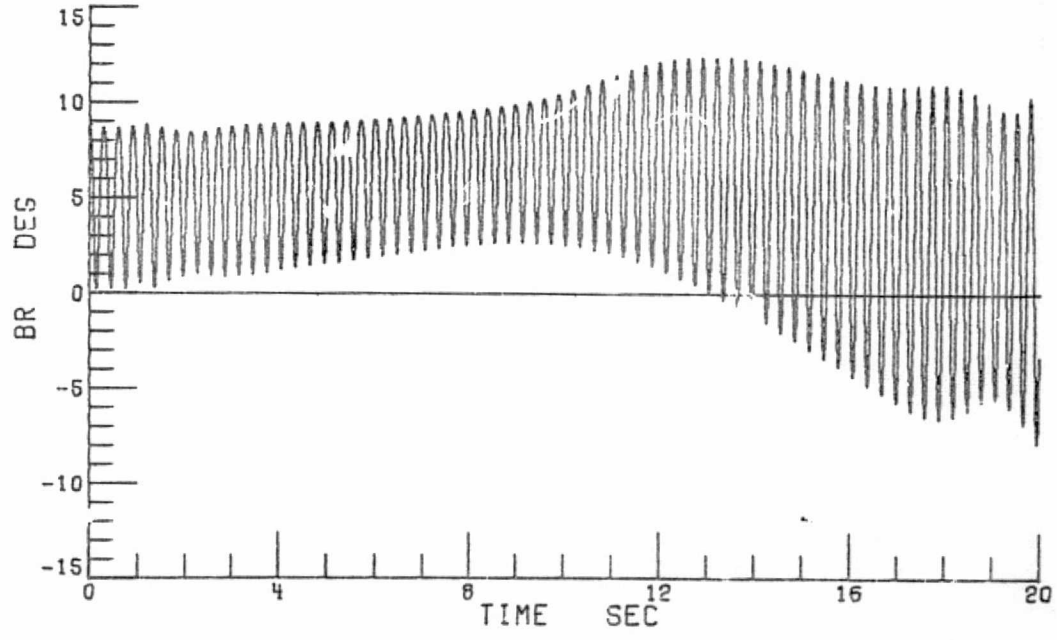

5b X 10s ROTOR

Figure 20.- Concluded.

shows the same effects, but again, to a smaller degree.

Figure 21 presents the effect of combination blade and blade segment reduction on vehicle dynamic response for 120 knots. It can be seen by comparing this figure to Figure 19, that the overwhelming majority of difference between the 3-blade 3-blade segment rotor and the "truth" rotor comes from the reduction in number of blades, and that blade segment reduction has relatively no effect.

Figure 22 presents the effect of increasing integration interval from 1/240 seconds to 1/30 seconds on vehicle dynamic response at 120 knots. The rotor configuration considered is the 5-blade 5-blade segment rotor and again, it is compared to the "truth" rotor. There is now an oscillation in roll acceleration which approaches .3 rad/sec^2. As the vehicle goes to higher forward velocities and the rotor starts to load, the amplitude of this oscillation will increase, and more of its' effect will filter through the body numerical integrators to roll rate and roll angle. The increased amplitude of the oscillation is very apparent now in roll rate, and it has also made its' appearance in roll angle. The average amplitude of roll rate has been affected, and the vehicle has rolled over to 15 degrees some two seconds faster. The effect of vehicle dynamic coupling is also apparent in pitch angle. It now takes the vehicle one second longer to reach 15 degrees of pitch angle, and for the first time the blade flapping angle is being affected. The blade flapping is tending to smooth itself out in amplitude instead of following the correct response as depicted by the "truth" rotor. For the hover case, the same trends are apparent, but to a smaller extent.

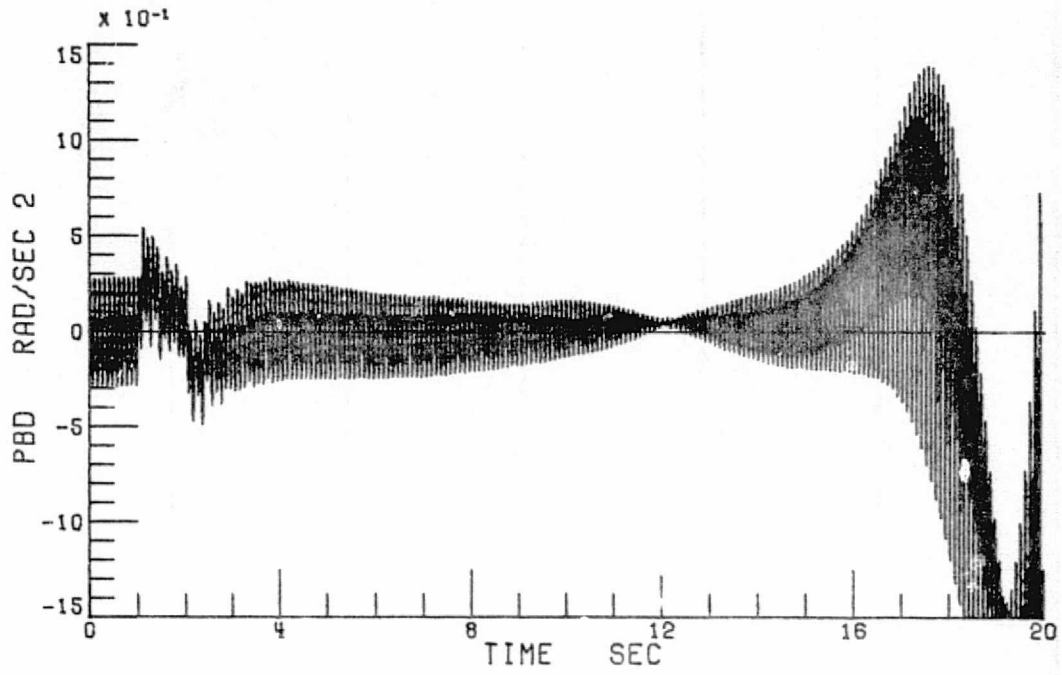

3b X 3s ROTOR

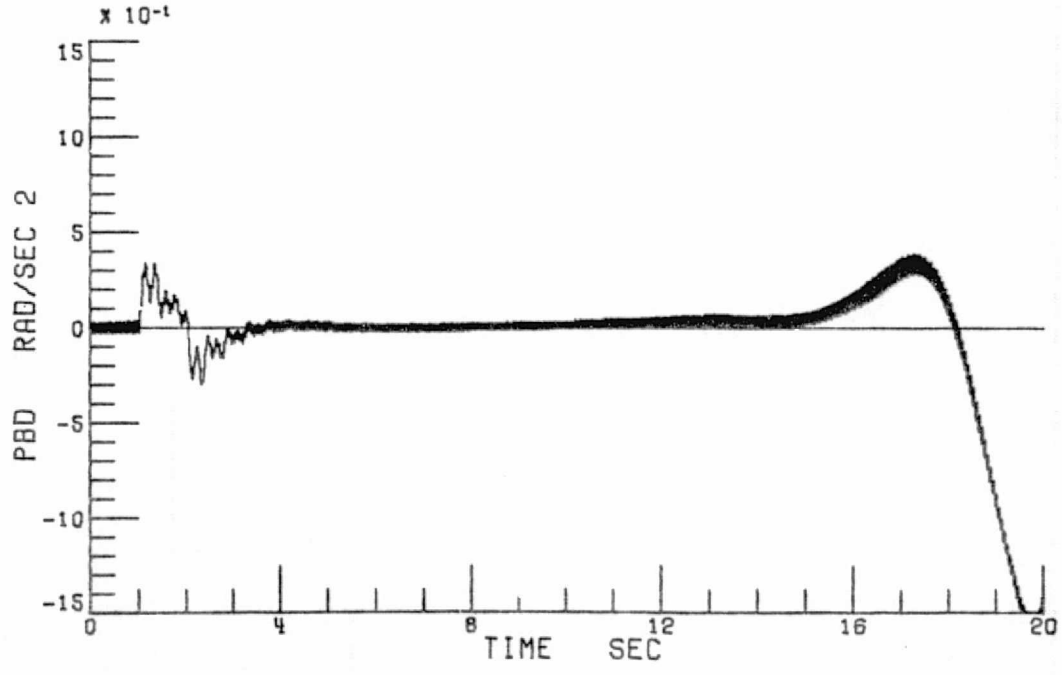

5b X 10s ROTOR

Figure 21.- Effect of Combination Blade and Blade Segment Reduction on Vehicle Dynamic Response at 120 Knots. (Integration Interval of 1/240 Seconds).

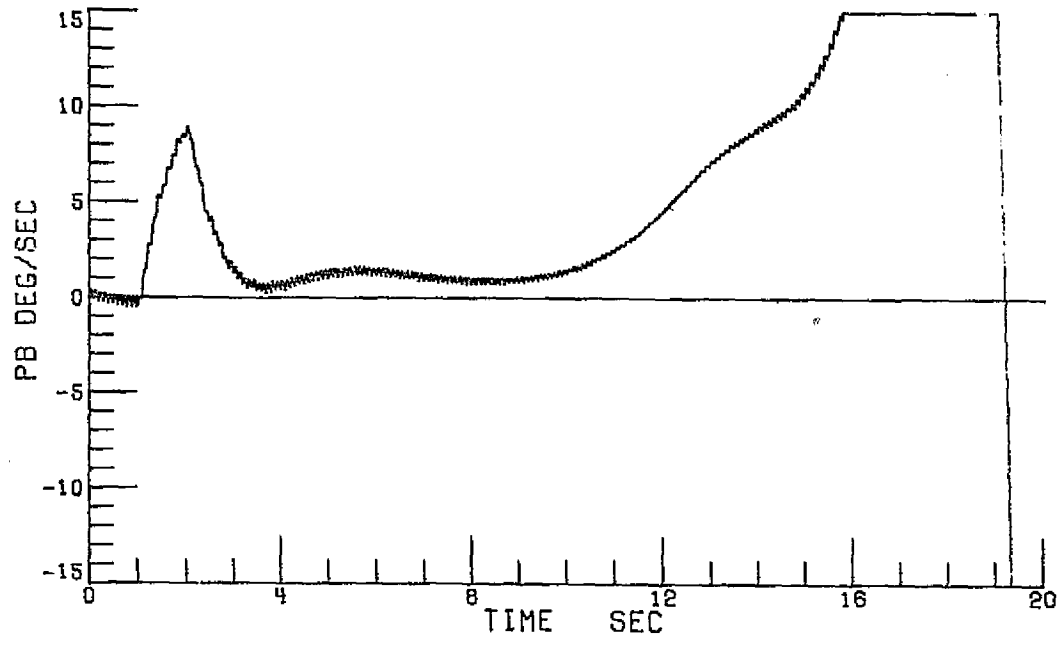

3b X 3s ROTOR

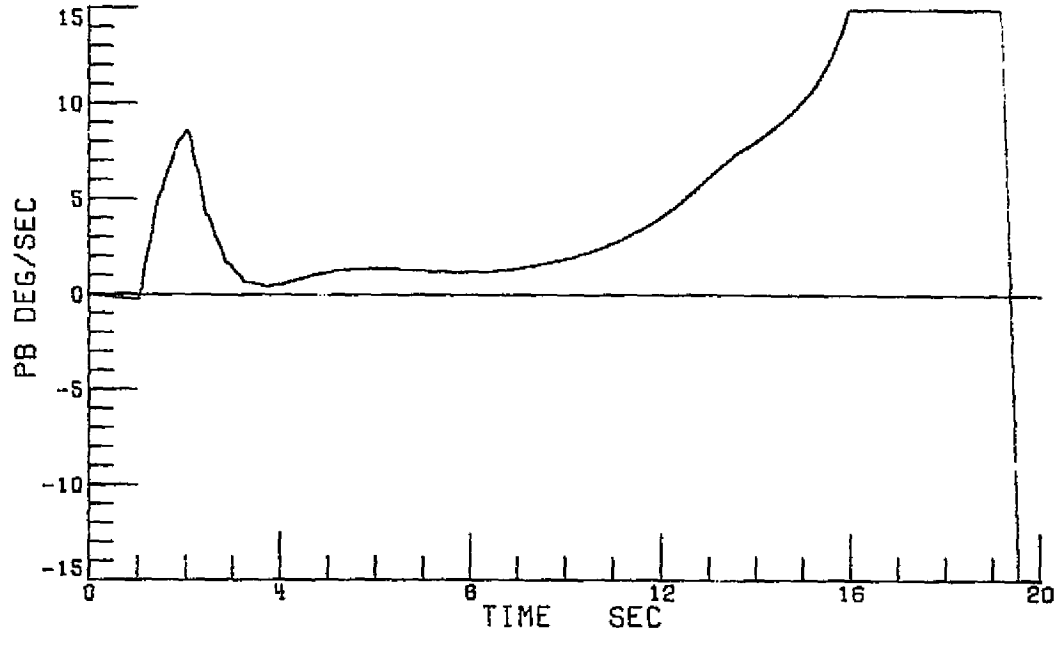

5b X 10s ROTOR

Figure 21.- Continued.

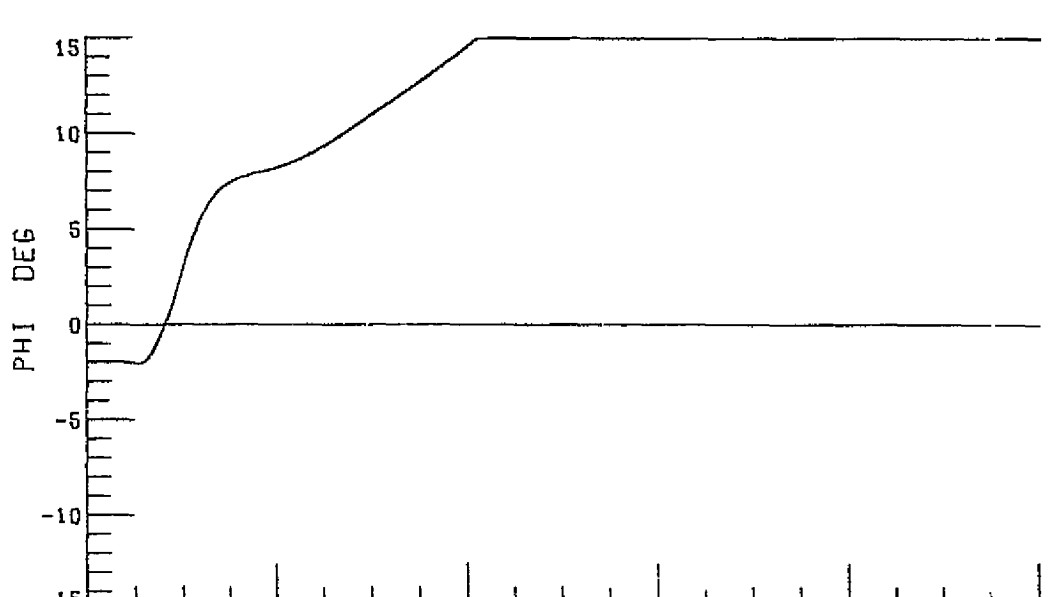

3b X 3s ROTOR

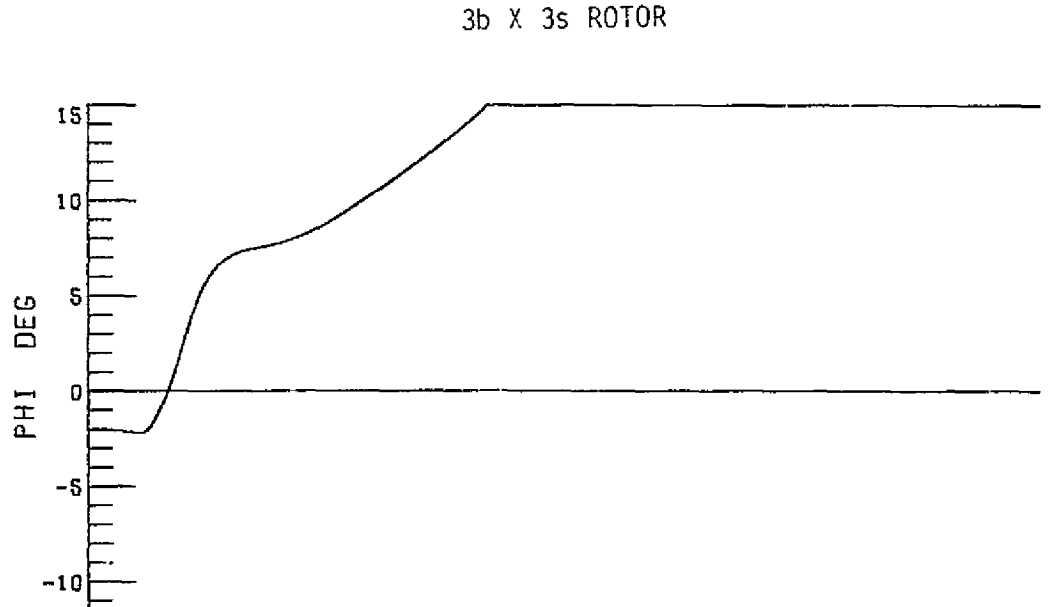

5b X 10s ROTOR

Figure 21.- Continued.

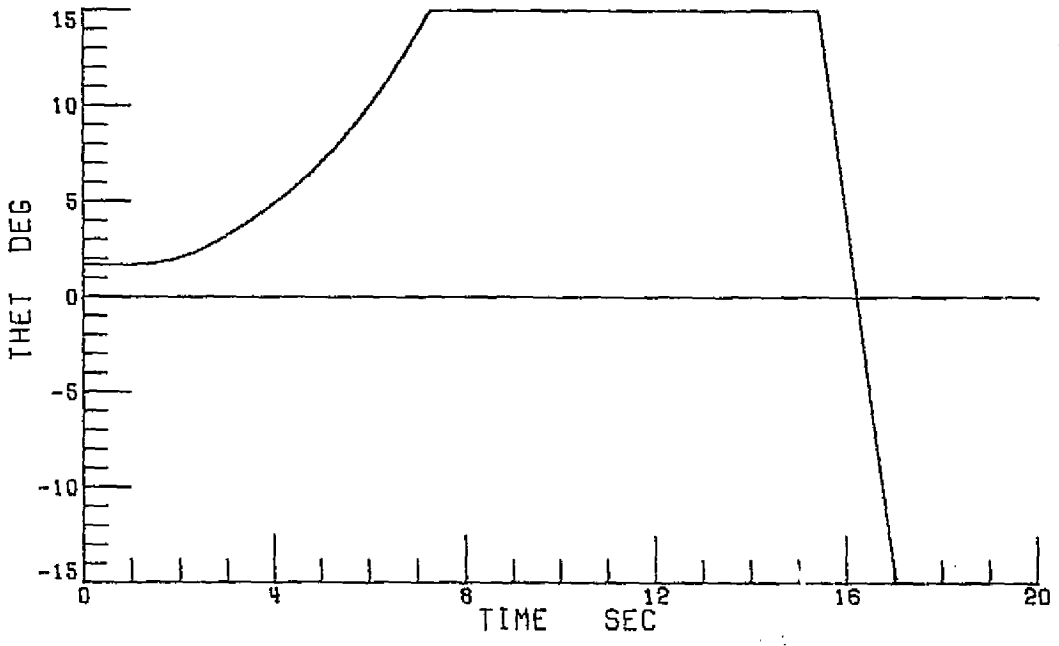

3b X 3s ROTOR

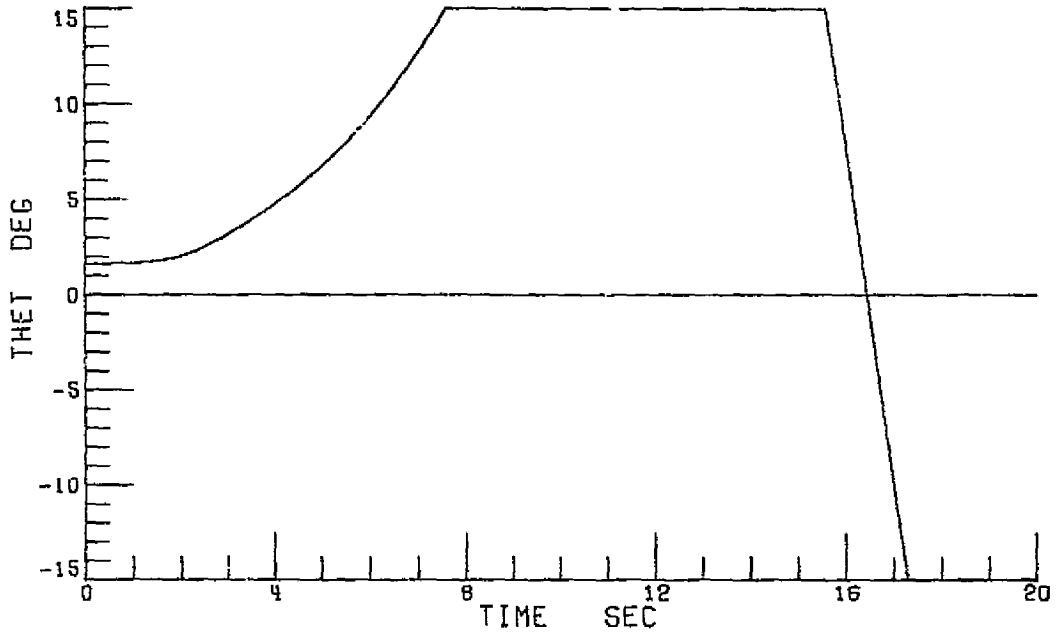

5b X 10s ROTOR

Figure 21.- Continued.

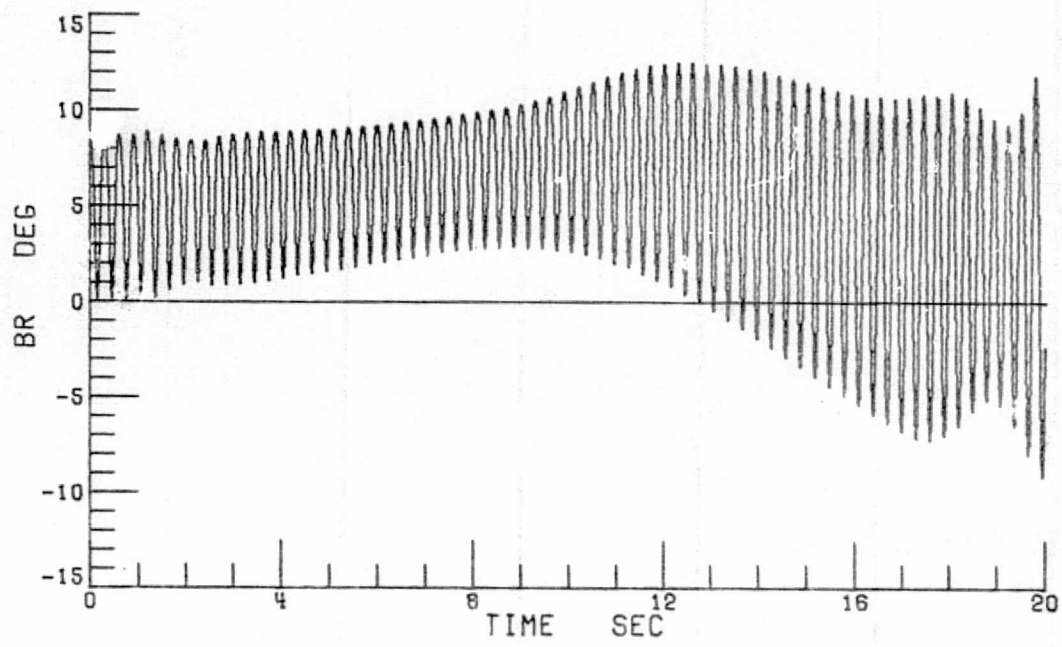

3b X 3s ROTOR

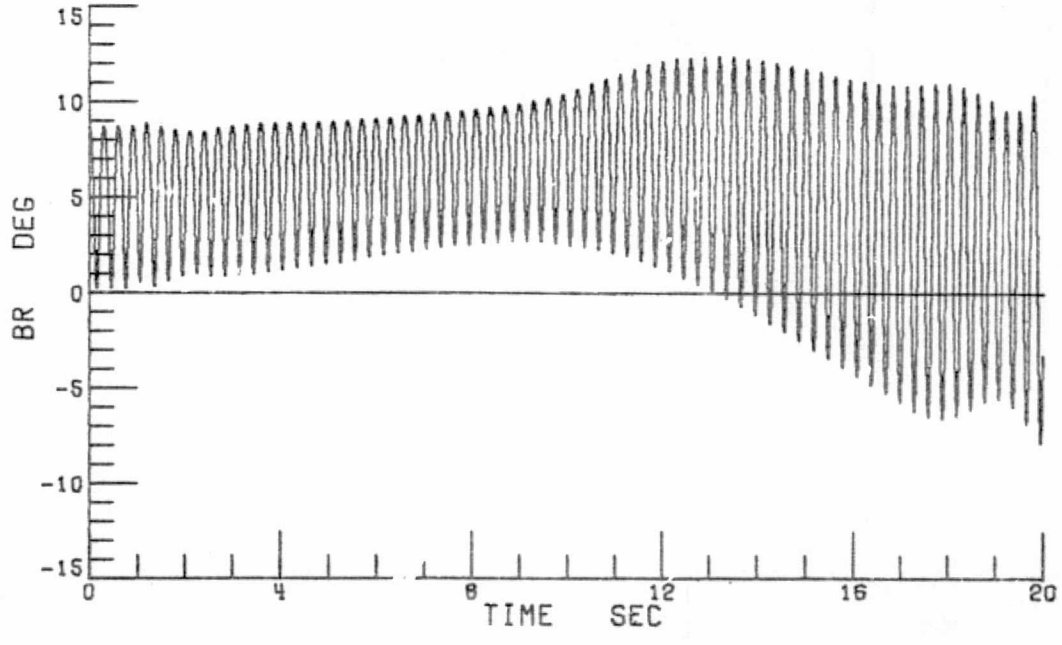

5b X 10s ROTOR

Figure 21.- Concluded.

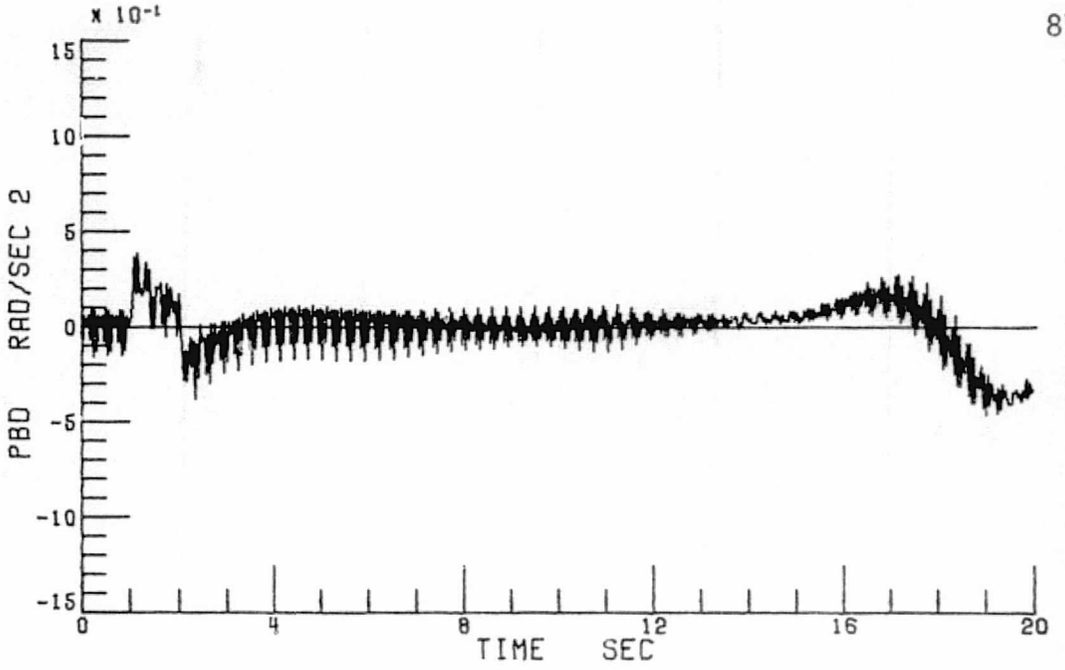

5b X 5s ROTOR, 1/30 SECONDS

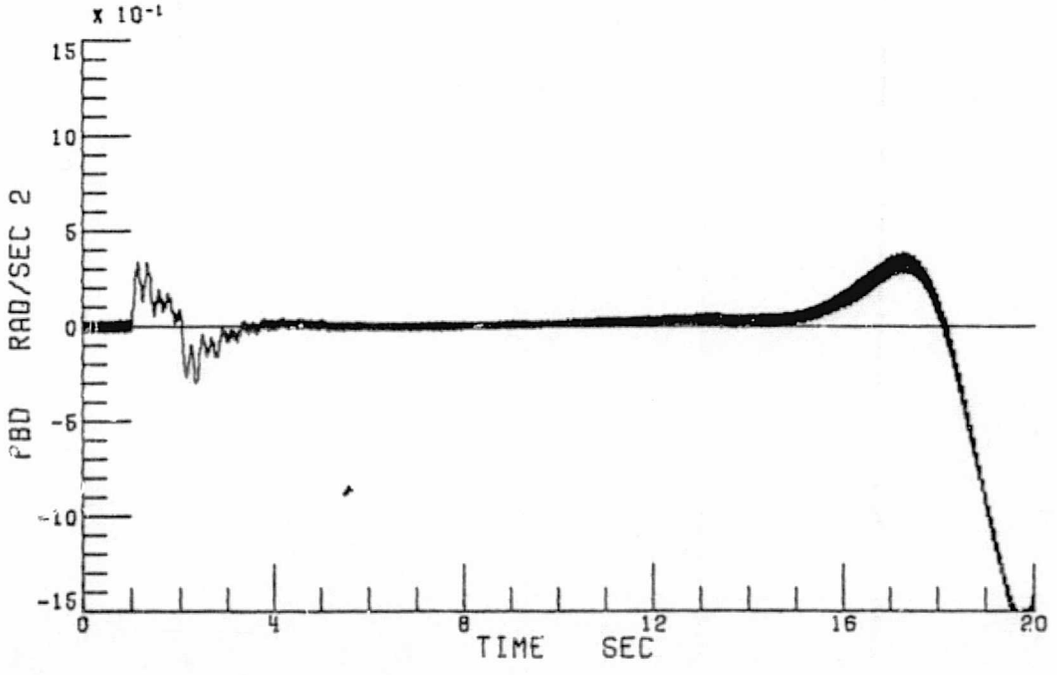

5b X 10s ROTOR, 1/240 SECONDS

Figure 22.- Effect of Increasing Integration Interval to 1/30 Seconds on Vehicle Dynamic Response at 120 Knots for a 5-Blade 5-Blade Segment Rotor.

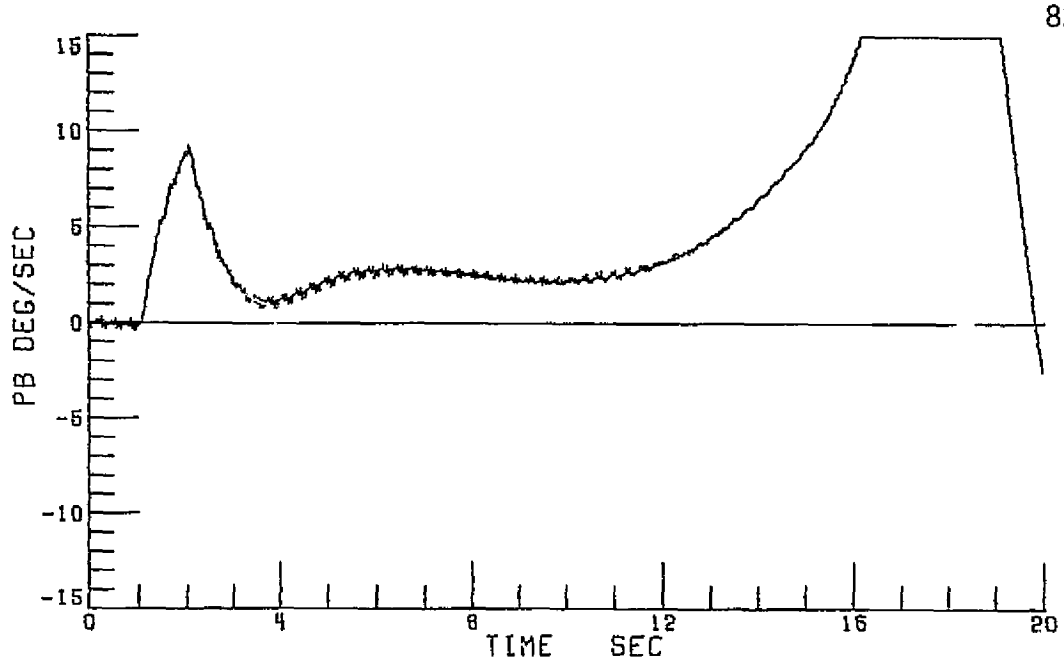

5b X 5s ROTOR, 1/30 SECONDS

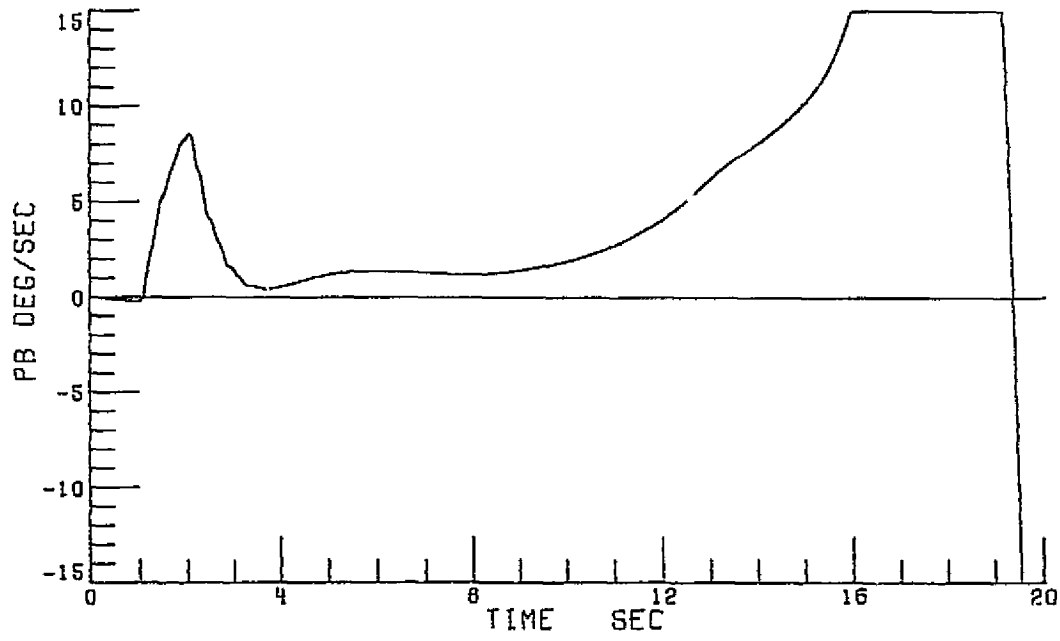

5b X 10s ROTOR, 1/240 SECONDS

Figure 22.- Continued.

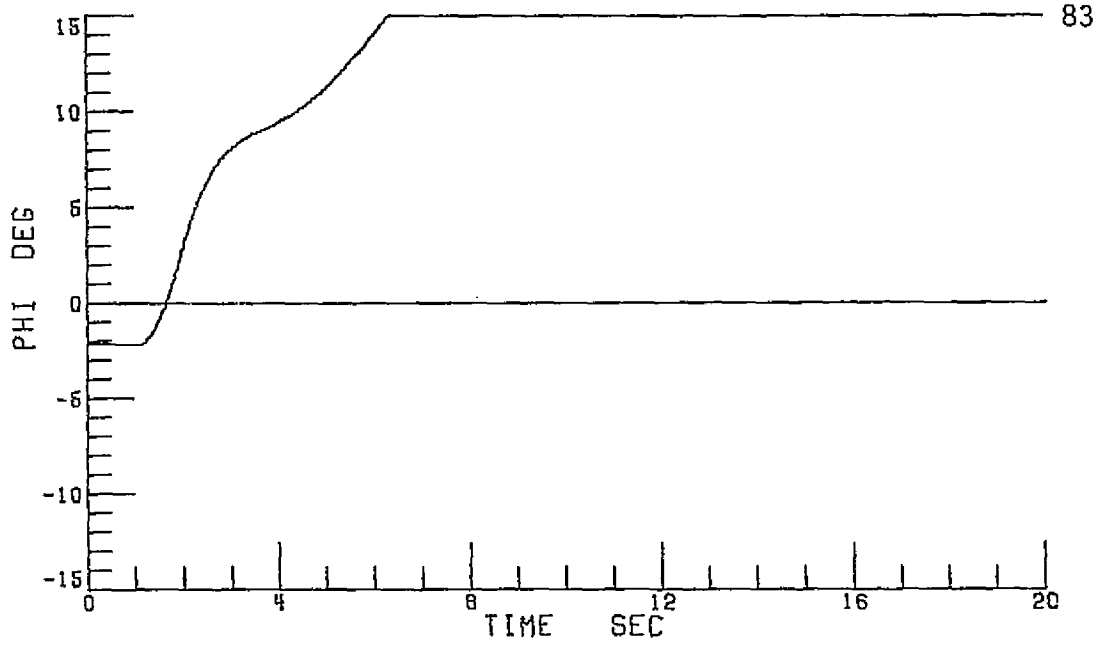

5b X 5s ROTOR, 1/30 SECONDS

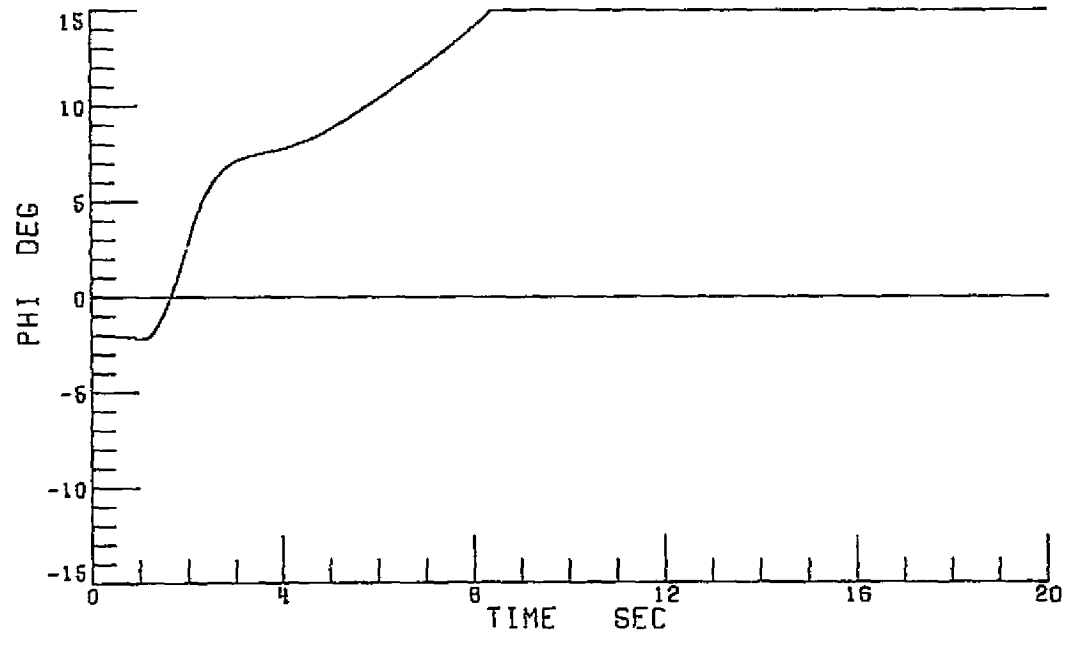

5b X 10s ROTOR, 1/240 SECONDS

Figure 22.- Continued.

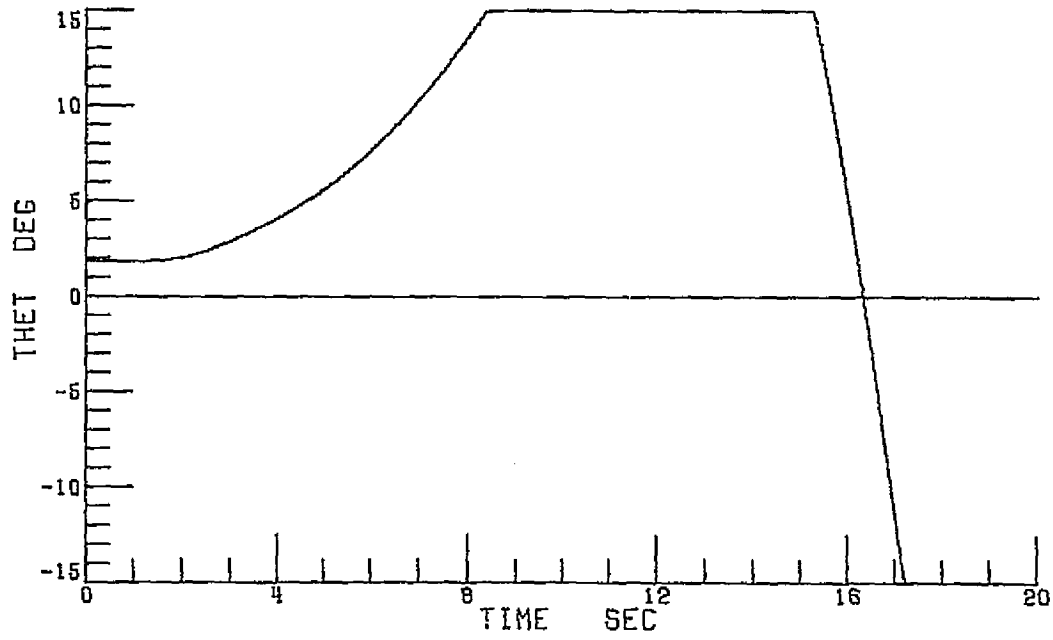

5b X 5s ROTOR, 1/30 SECONDS

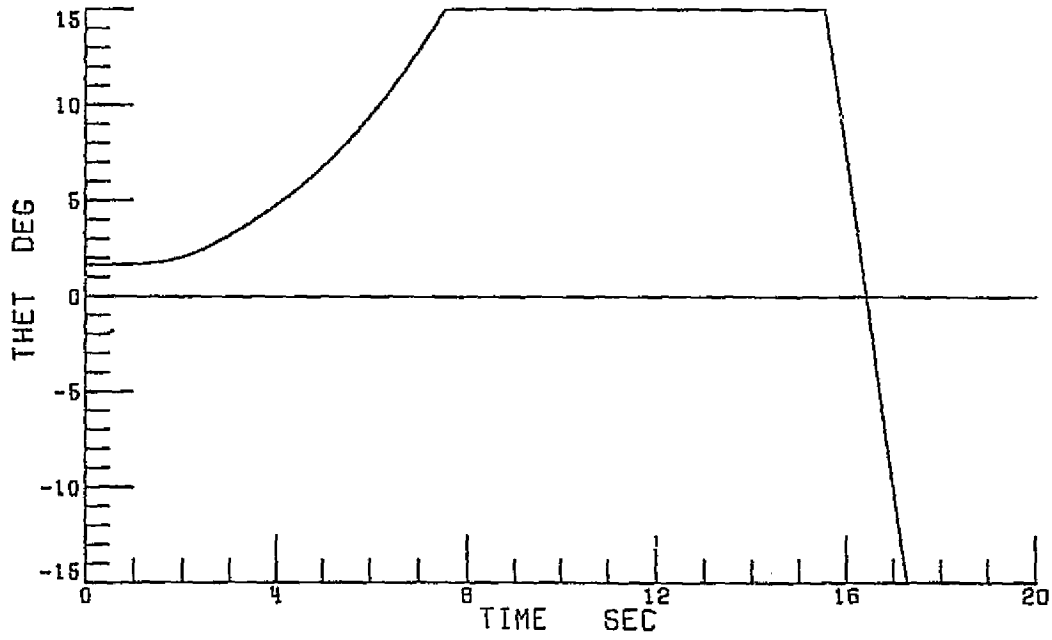

5b X 10s ROTOR, 1/240 SECONDS

Figure 22.- Continued.

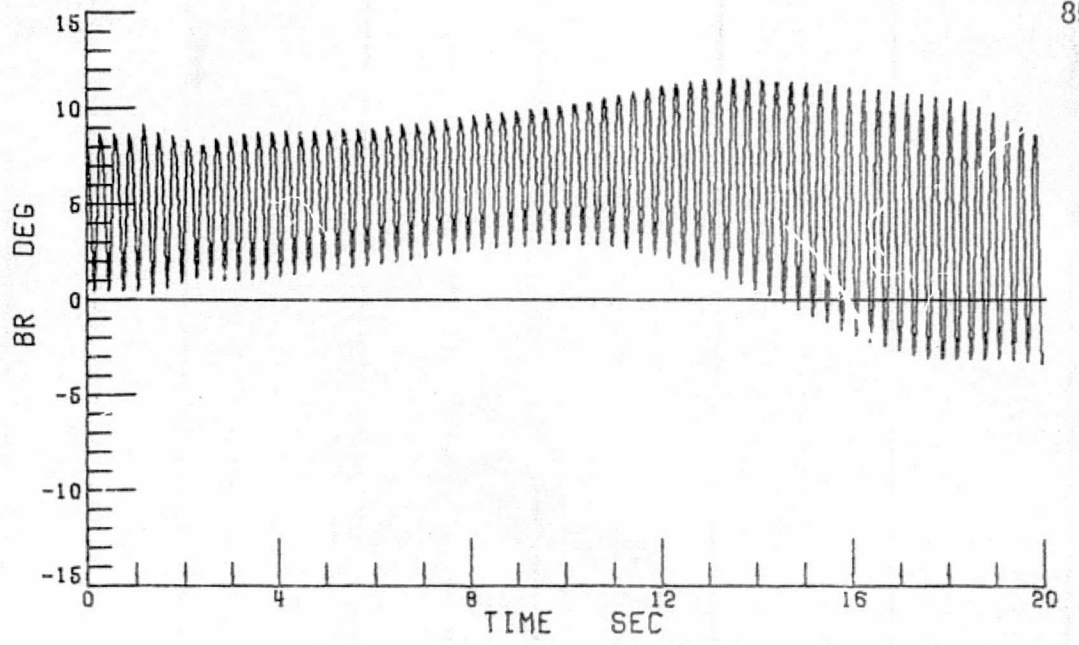

5b X 5s ROTOR, 1/30 SECONDS

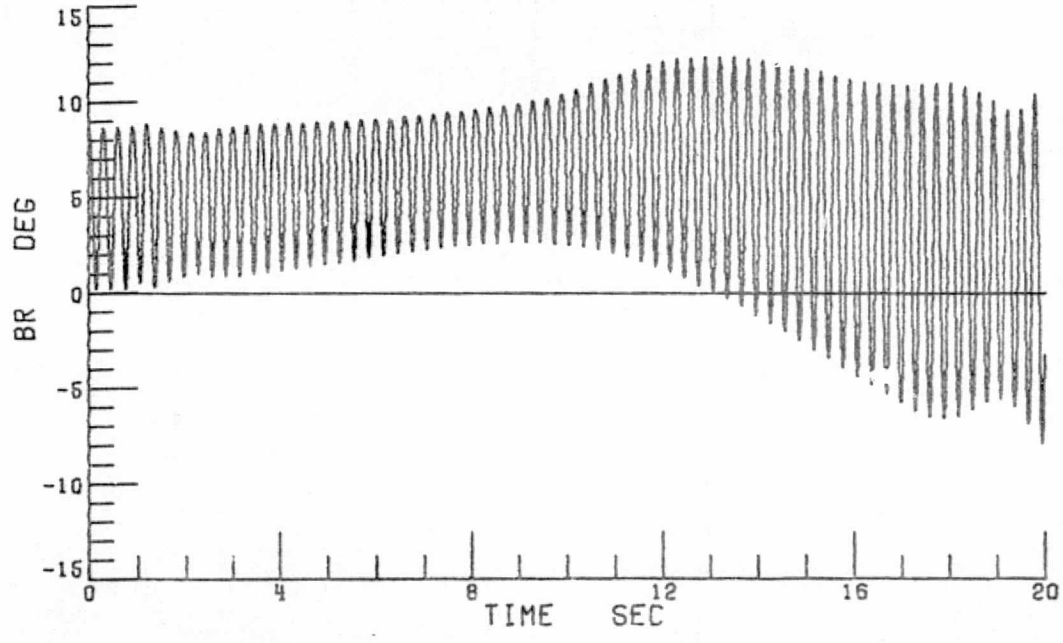

5b X 10s ROTOR, 1/240 SECONDS

Figure 22.- Concluded.

Figure 23 presents the effect of increasing integration interval from 1/240 seconds to 1/30 seconds on vehicle dynamic response at 120 knots for the 3-blade 3-blade segment rotor. In this case the effect of both reduced number of blades and increased integration interval can be seen. As the rotor loads up at high speeds the effects of blade reduction and integration interval continue to amplify each other until an oscillation in roll acceleration occurs which is as large as the effect of the pulse input and in the final seconds of the run the oscillation is double the pulse input. Thus the vehicle equations of motion are continually seeing pulse inputs. Again the roll rate average is higher than what it should be, and the vehicle rolls 15 degrees approximately 3 seconds faster than it should. The pitch angle reaches 15 degrees approximately one second late, and the flapping angle again tends to smooth out instead of following the correct response. Once again the hover case follows the same trends, but to a smaller extent.

Figure 24 presents the effect of increasing integration interval from 1/240 seconds to 1/20 seconds on vehicle dynamic response at 120 knots for the 5-blade 5-blade segment rotor One can easily see that the numerical solution of the total model has broken down and is totally incorrect. Both the vehicle and rotor are highly unstable. The reader should note that the run was stopped at approximately 16 seconds to keep the computer program from sustaining a fatal error.

Figure 25 presents the effect of increasing integration interval from 1/240 seconds to 1/20 seconds on vehicle dynamic response at 120 knots for the 3-blade 3-blade segment rotor. Again, as with the 5-blade 5-blade segment rotor, the vehicle and rotor both go unstable under these conditions, and

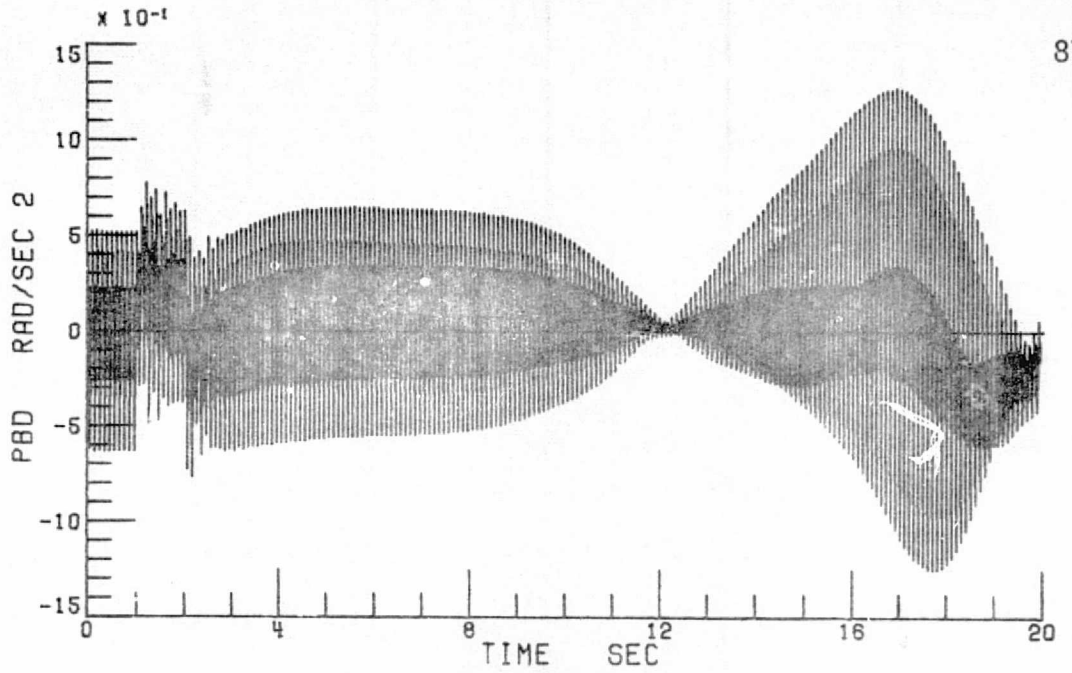

3b X 3s ROTOR, 1/30 SECONDS

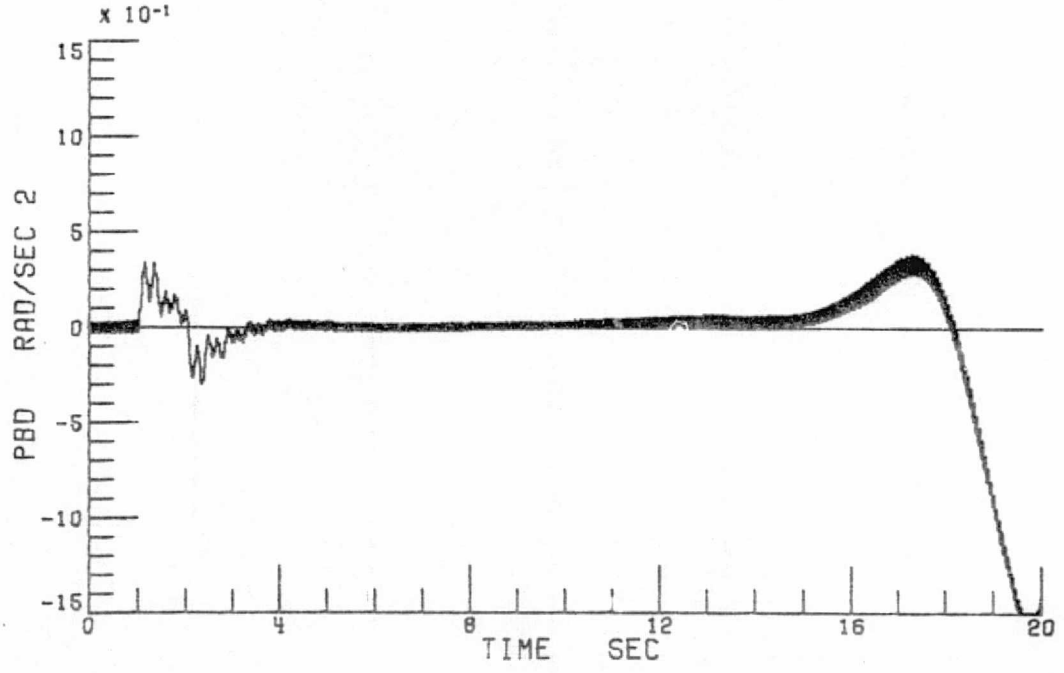

5b X 10s ROTOR, 1/240 SECONDS

Figure 23.- Effect of Increasing Integration Interval to 1/30 Seconds on Vehicle Dynamic Response at 120 Knots for a 3-Blade 3-Blade Segment Rotor.

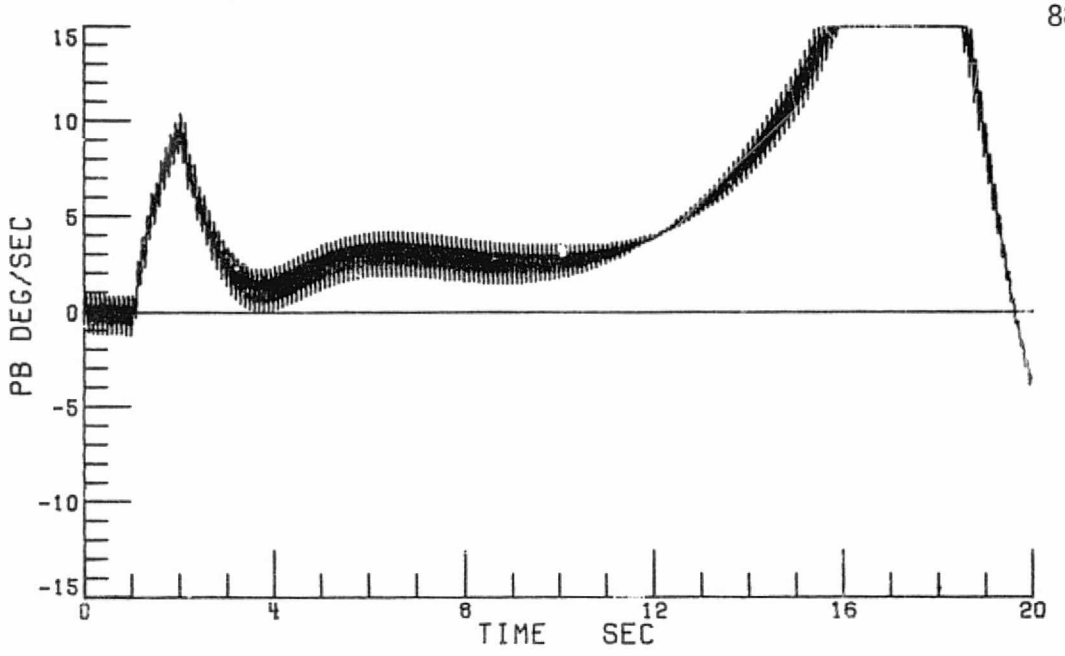

3b X 3s ROTOR, 1/30 SECONDS

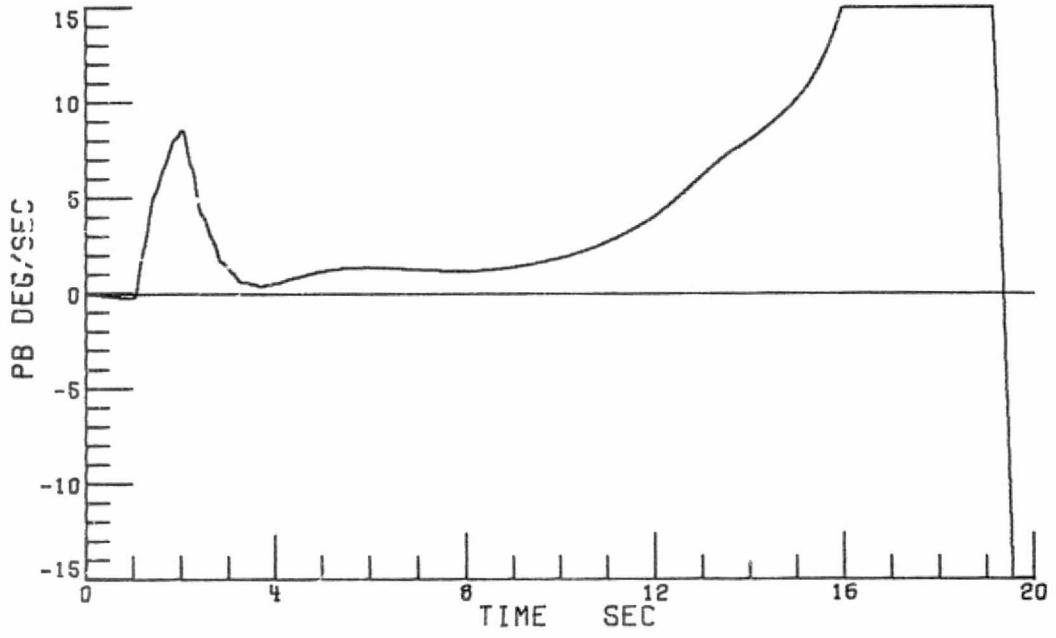

5b X 10s ROTOR, 1/240 SECONDS

Figure 23.- Continued.

L-2

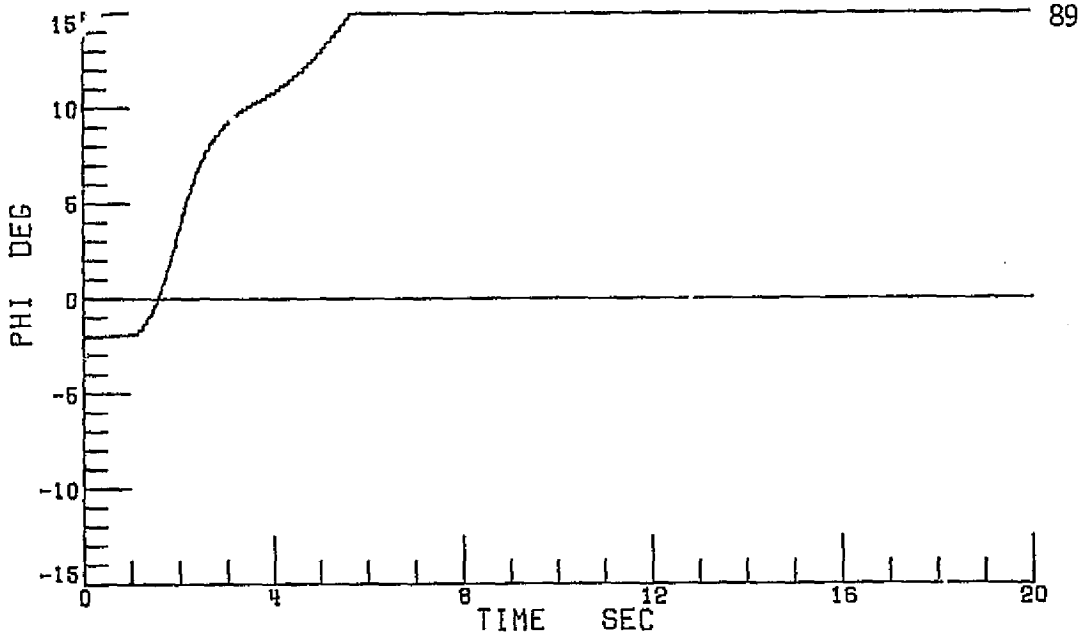

3b X 3s ROTOR, 1/30 SECONDS

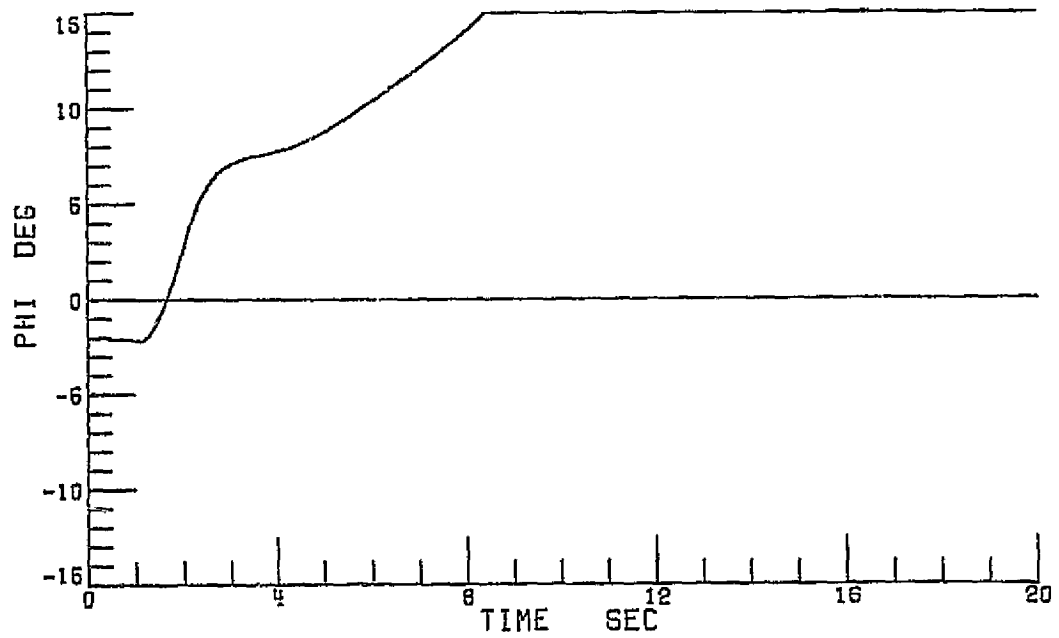

5b X 10s ROTOR, 1/240 SECONDS

Figure 23.- Continued.

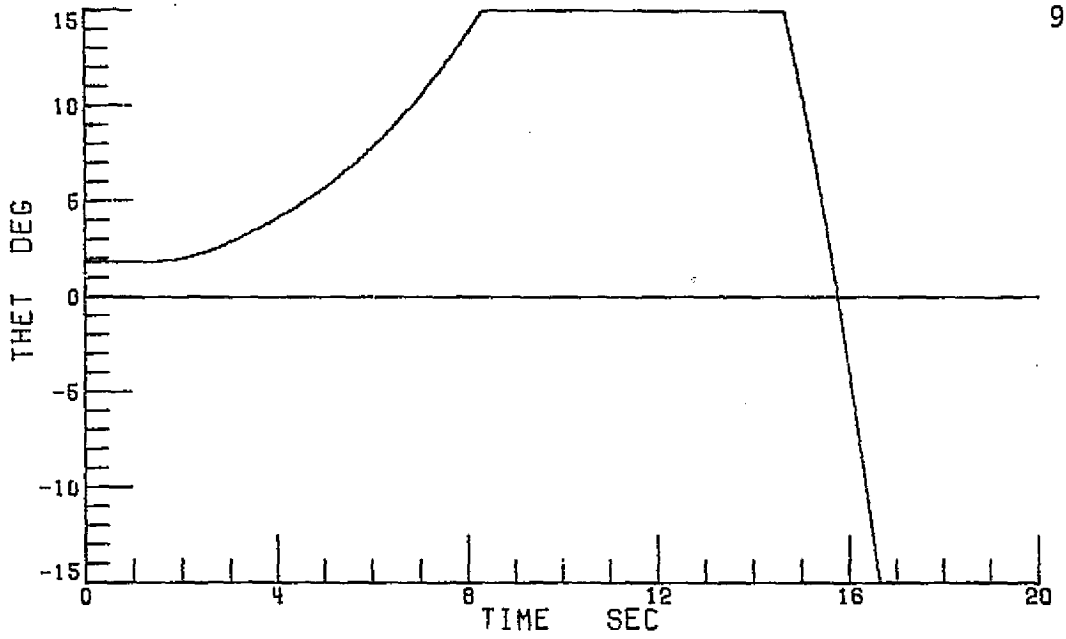

3b X 3s ROTOR, 1/30 SECONDS

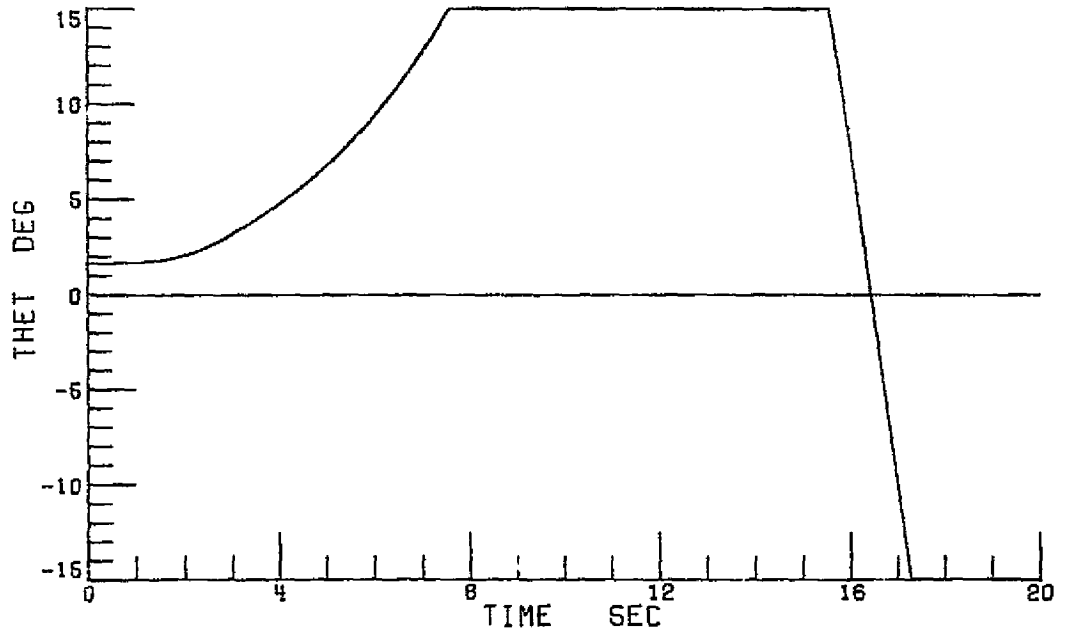

5b X 10s ROTOR, 1/240 SECONDS

Figure 23.- Continued.

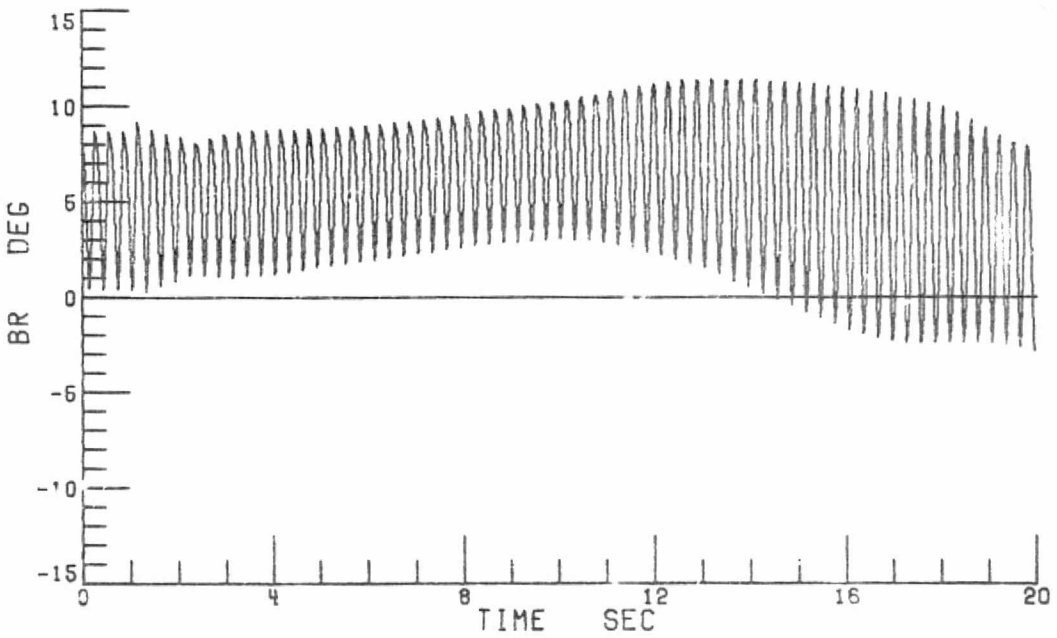

3b X 3s ROTOR, 1/30 SECONDS

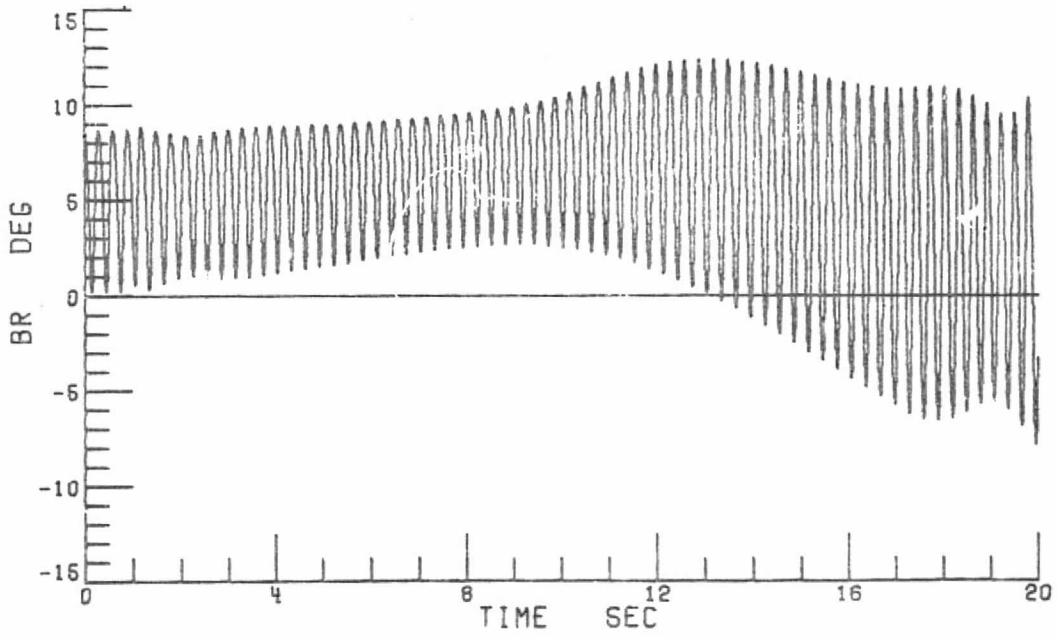

5b X 10s ROTOR, 1/240 SECONDS

Figure 23.- Concluded.

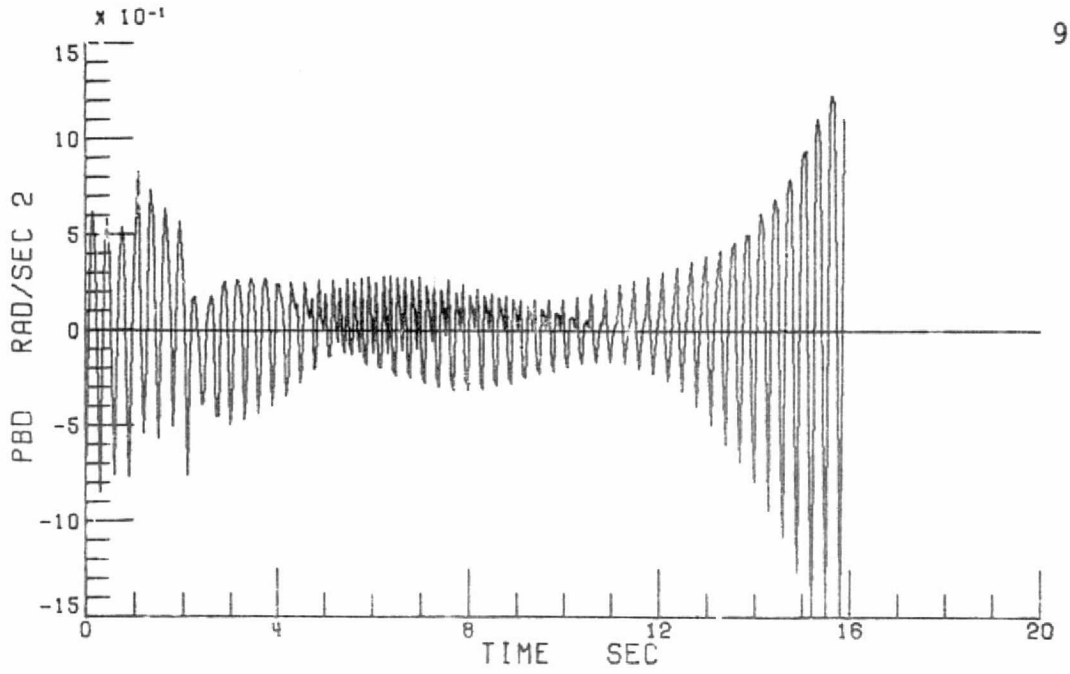

5b X 5s ROTOR, 1/20 SECONDS

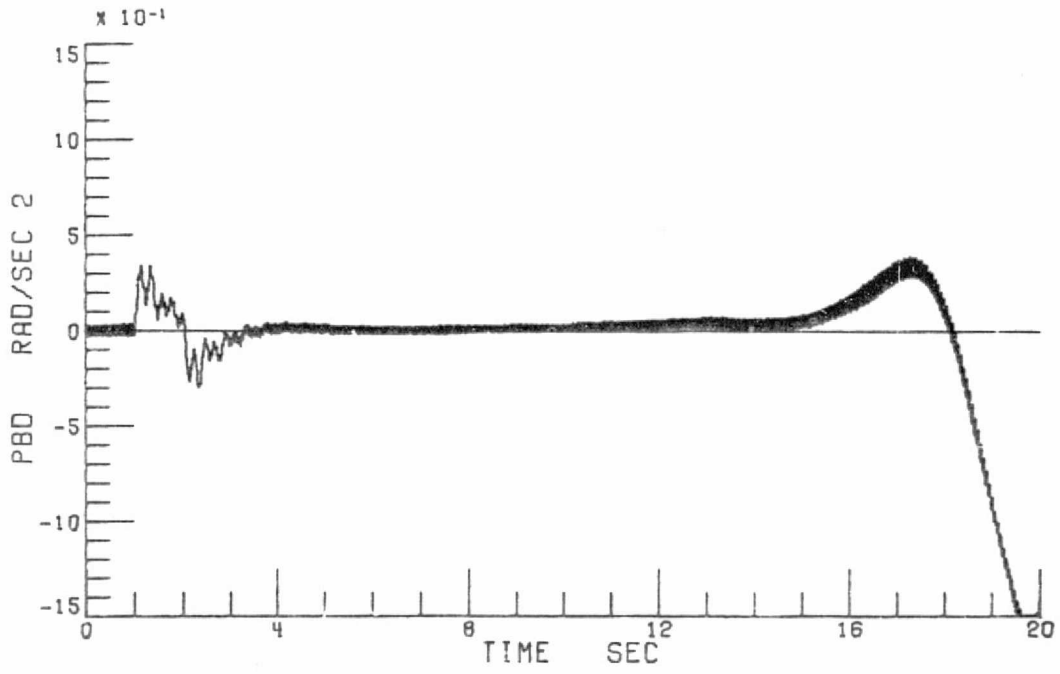

5b X 10s ROTOR, 1/240 SECONDS

Figure 24.- Effect of Increasing Integration Interval to 1/20 Seconds on Vehicle Dynamic Response at 120 Knots for a 5-Blade 5-Blade Segment Rotor.

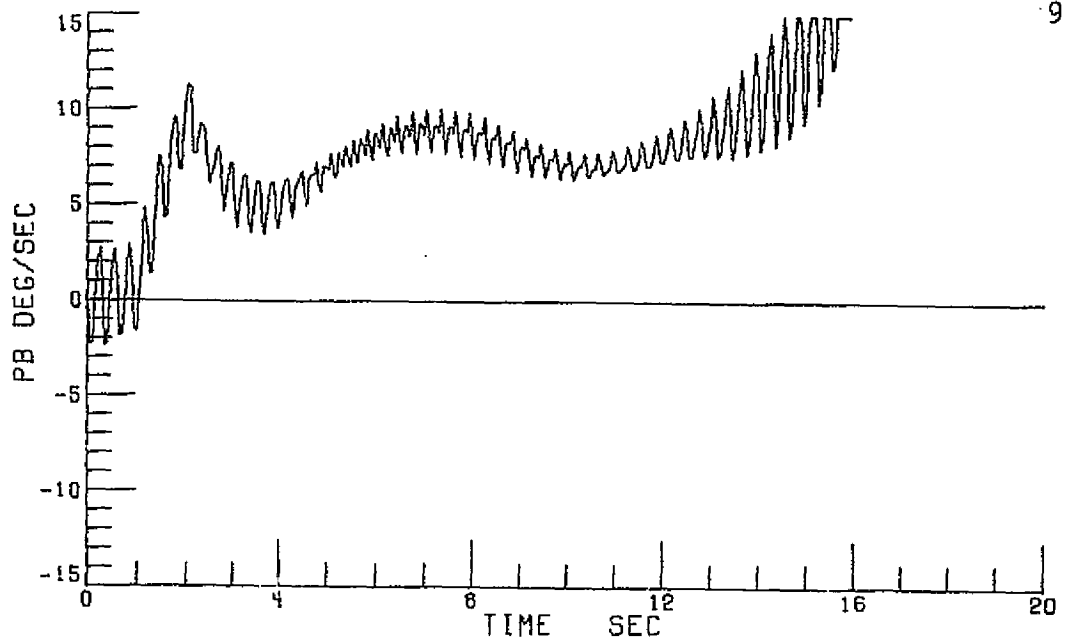

5b X 5s ROTOR, 1/20 SECONDS

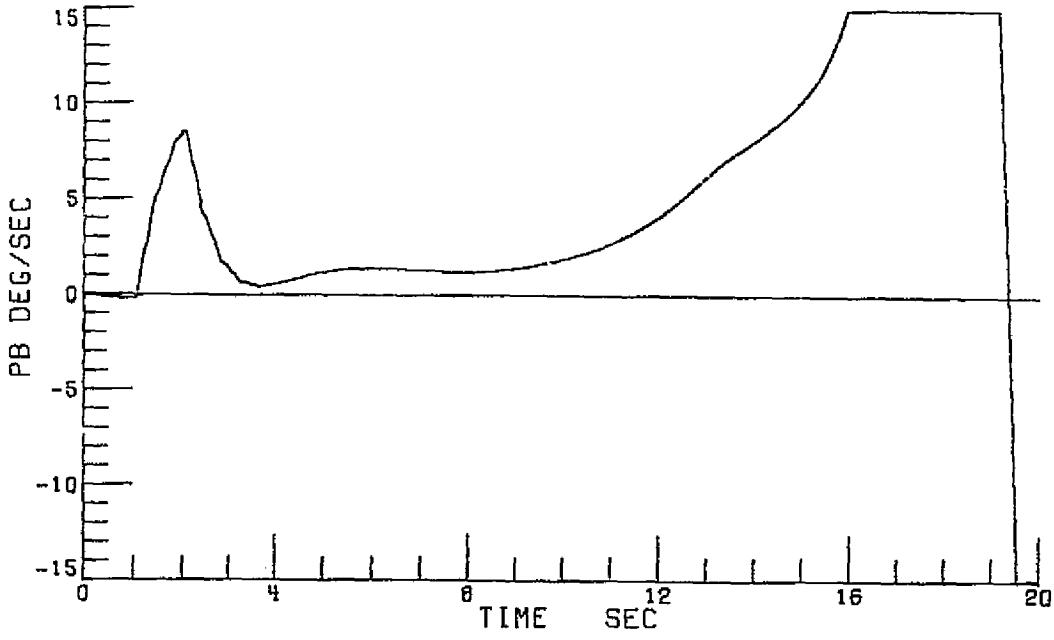

5b X 10s ROTOR, 1/240 SECONDS

Figure 24.- Continued.

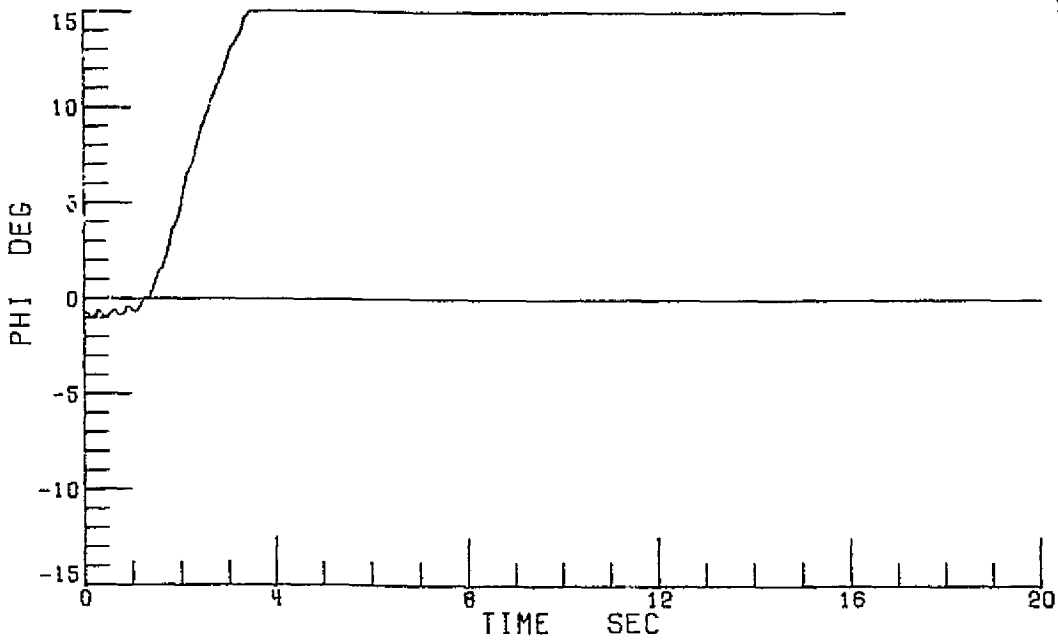

5b X 5s ROTOR, 1/20 SECONDS

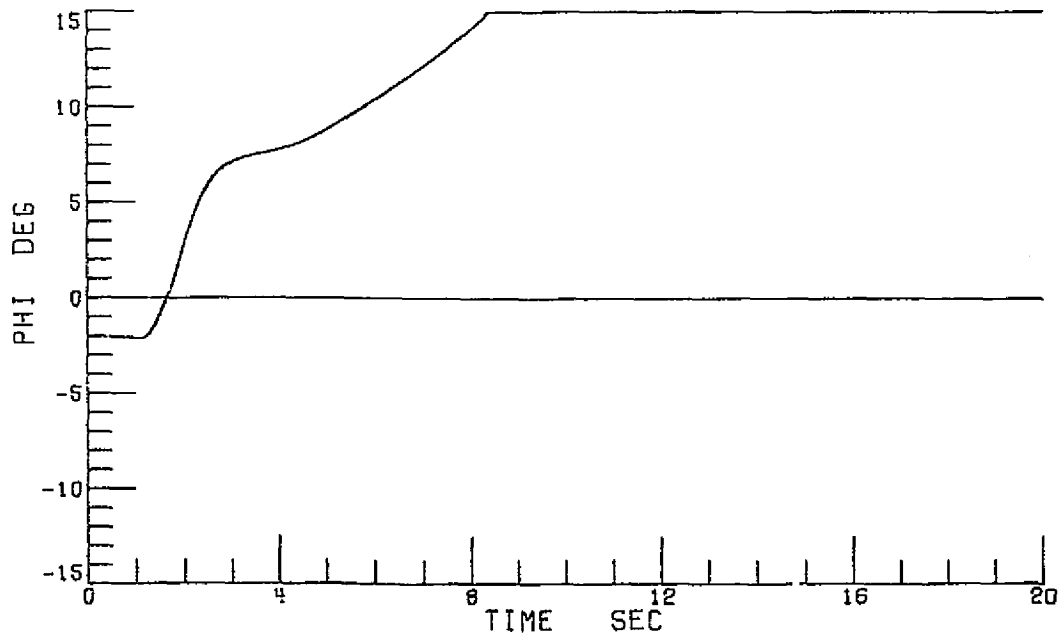

5b x 10s ROTOR, 1/240 SECONDS

Figure 24.- Continued.

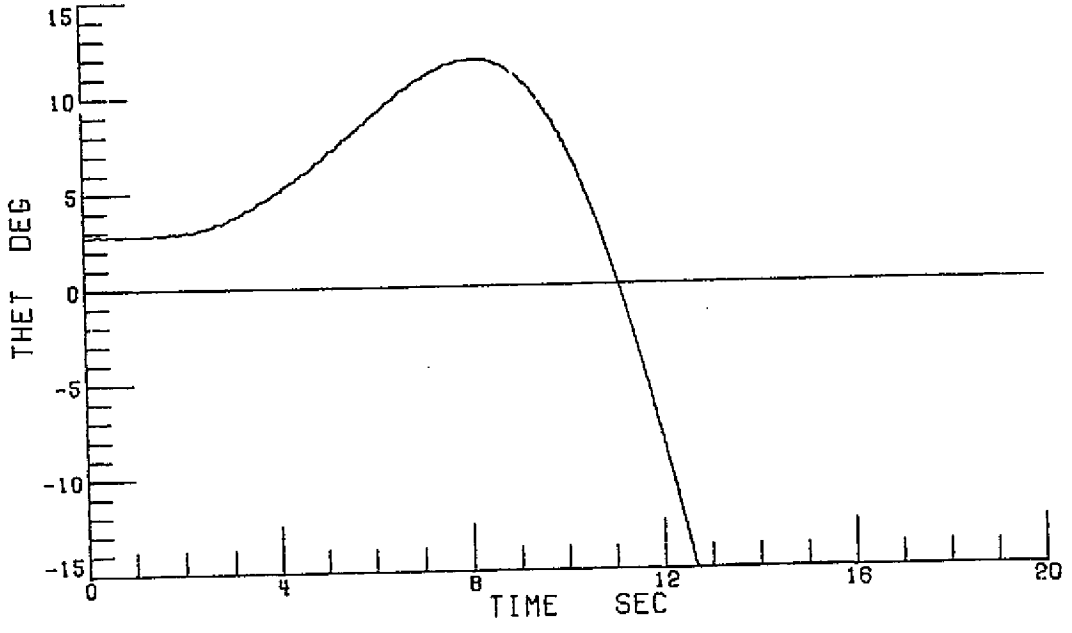

5b X 5s ROTOR, 1/20 SECONDS

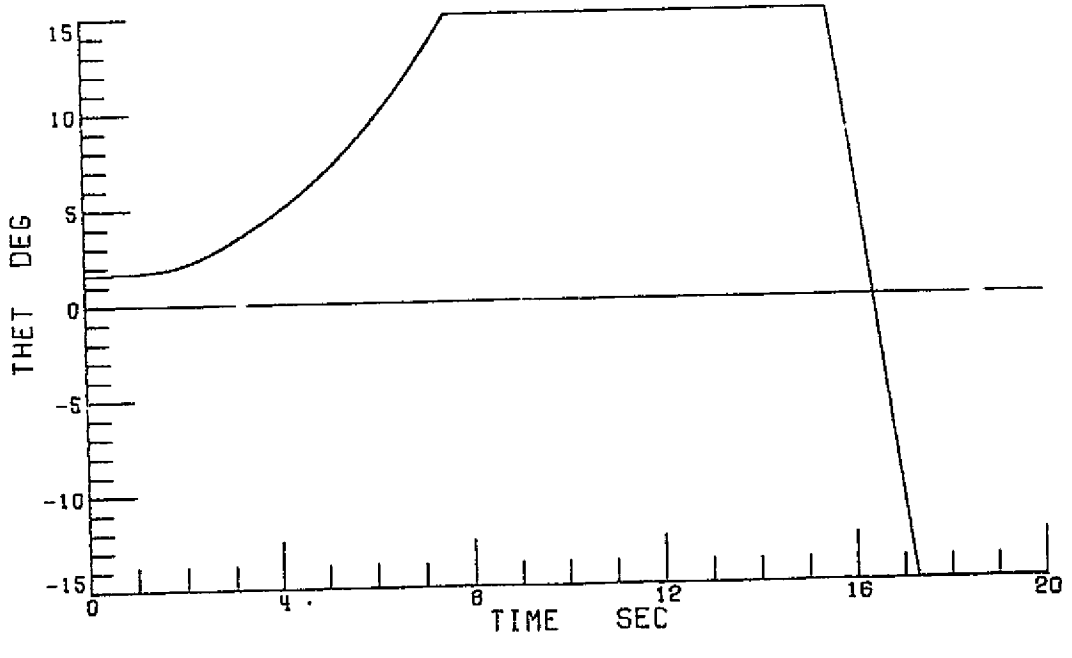

5b X 10s ROTOR, 1/240 SECONDS

Figure 24.- Continued.

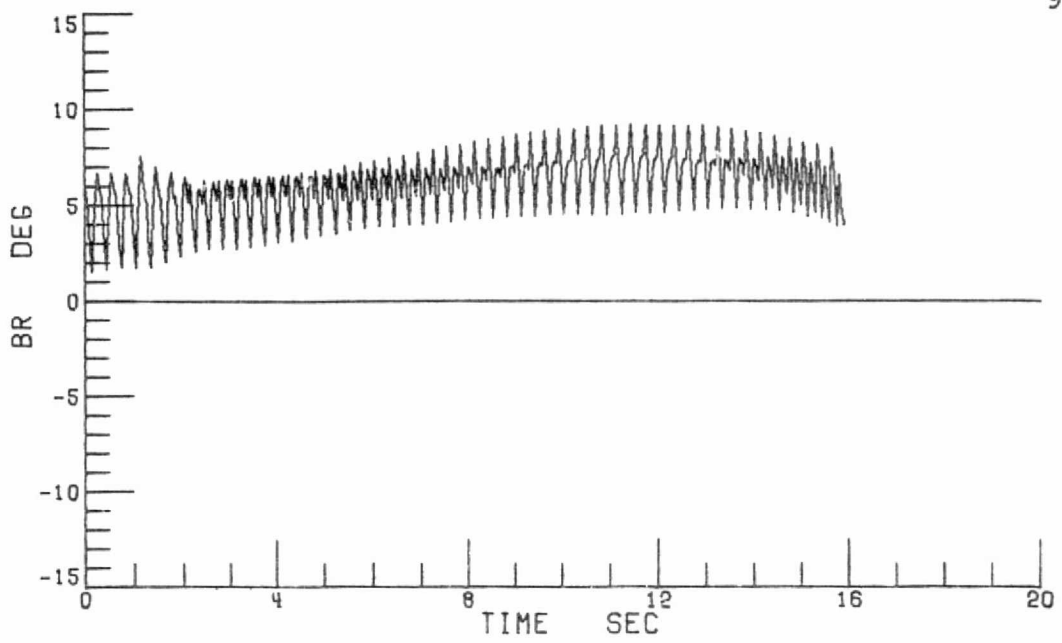

5b X 5s ROTOR, 1/20 SECONDS

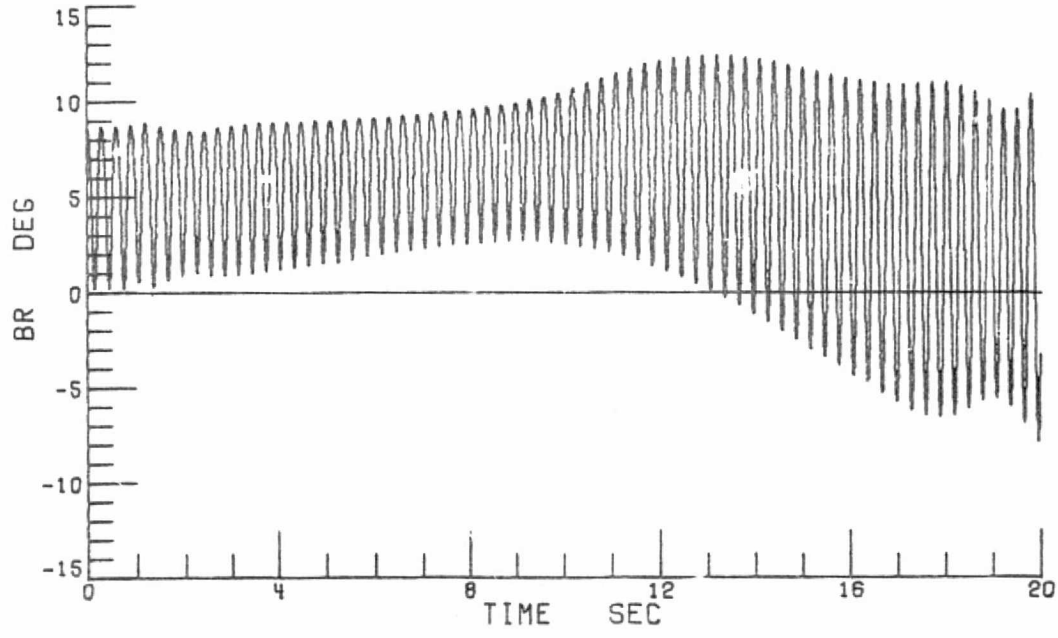

5b X 10s ROTOR, 1/240 SECONDS

Figure 24.- Concluded.

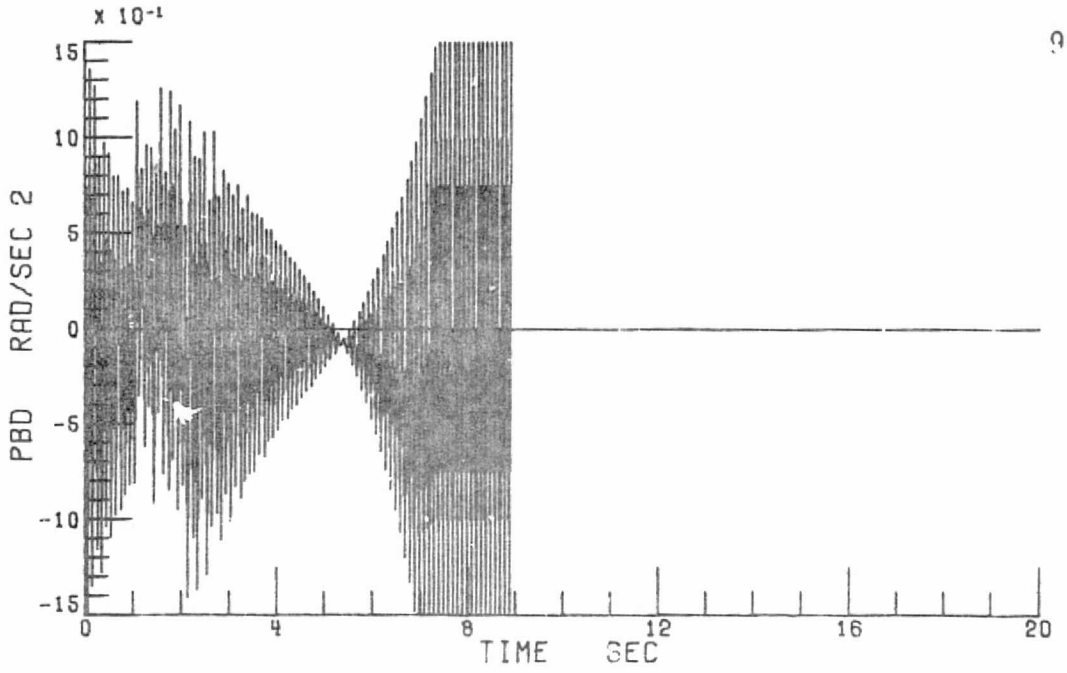

3b X 3s ROTOR, 1/20 SECONDS

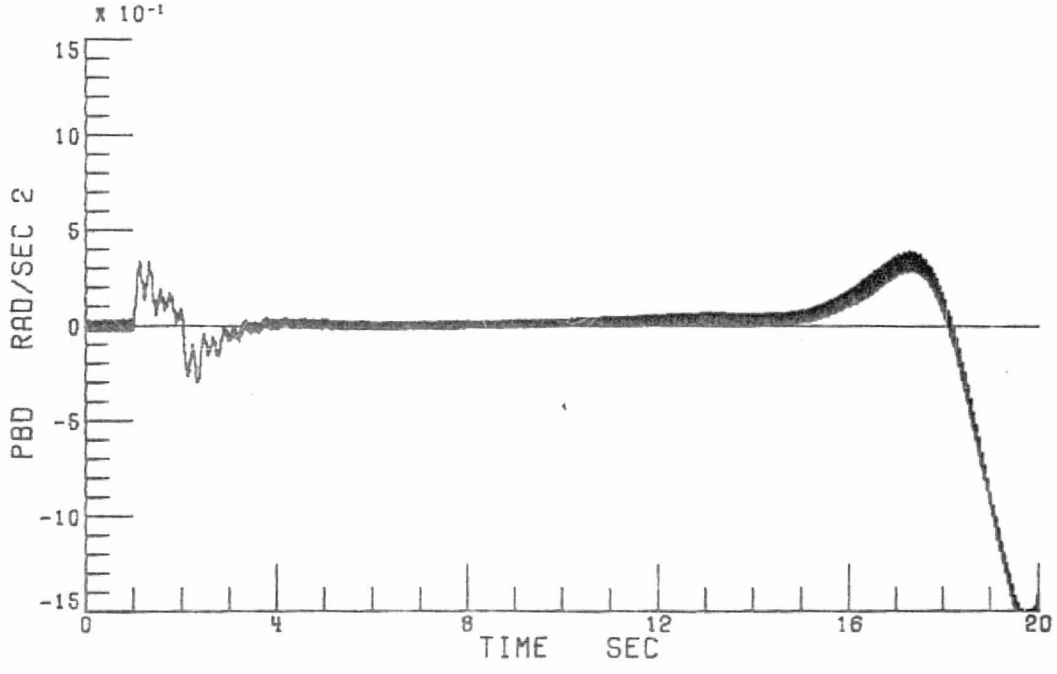

5b X 10s ROTOR, 1/240 SECONDS

Figure 25.- Effect of Increasing Integration Interval to 1/20 Seconds on Vehicle Dynamic Response at 120 Knots for a 3-Blade 3-Blade Segment Rotor.

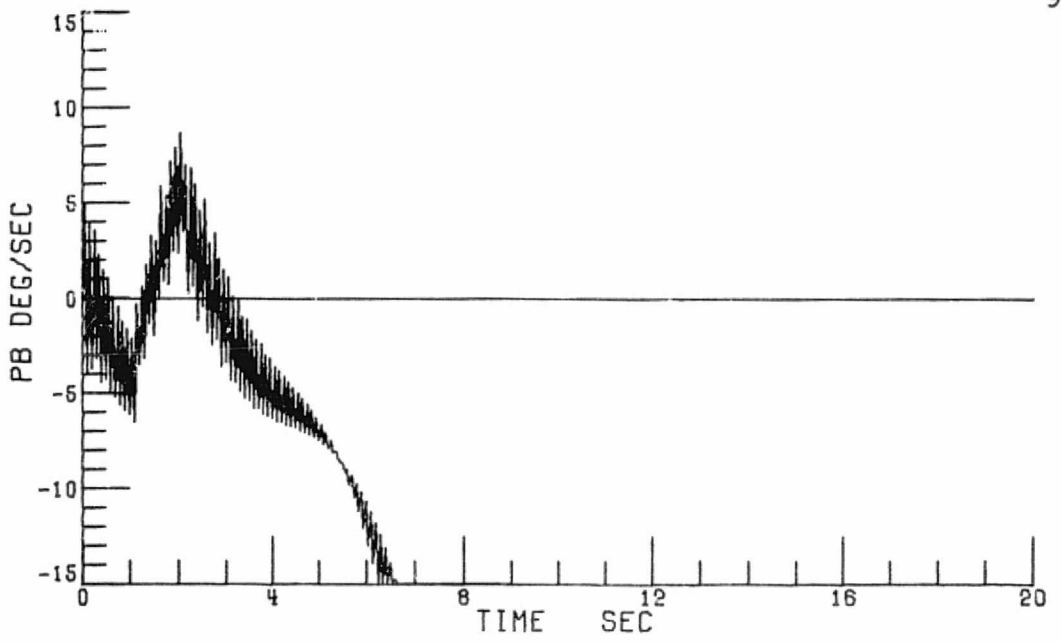

3b X 3s ROTOR, 1/20 SECONDS

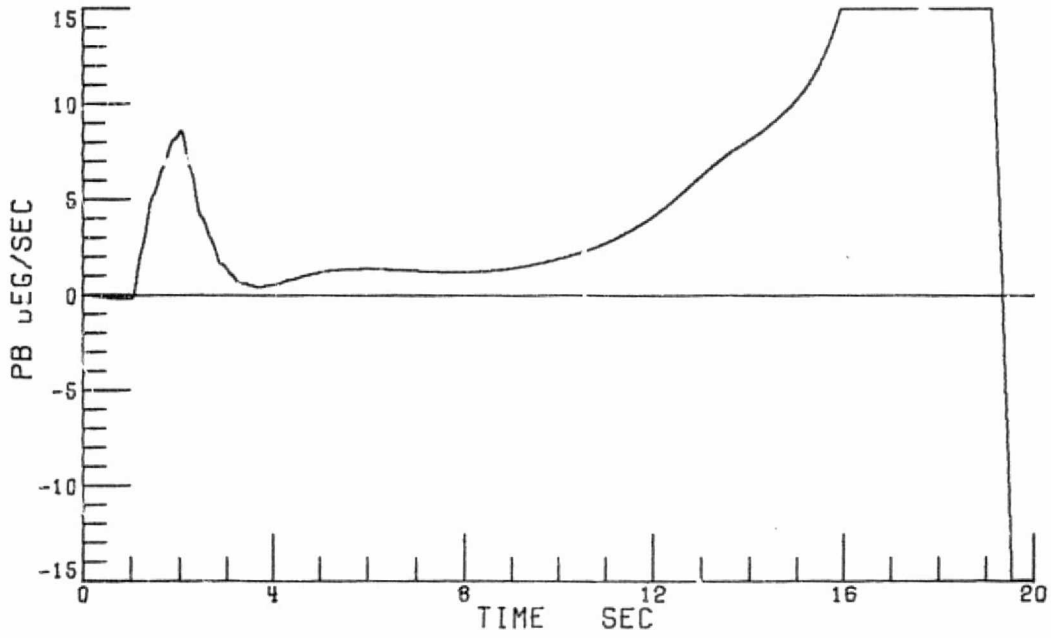

5b X 10s ROTOR, 1/240 SECONDS

Figure 25.- Continued.

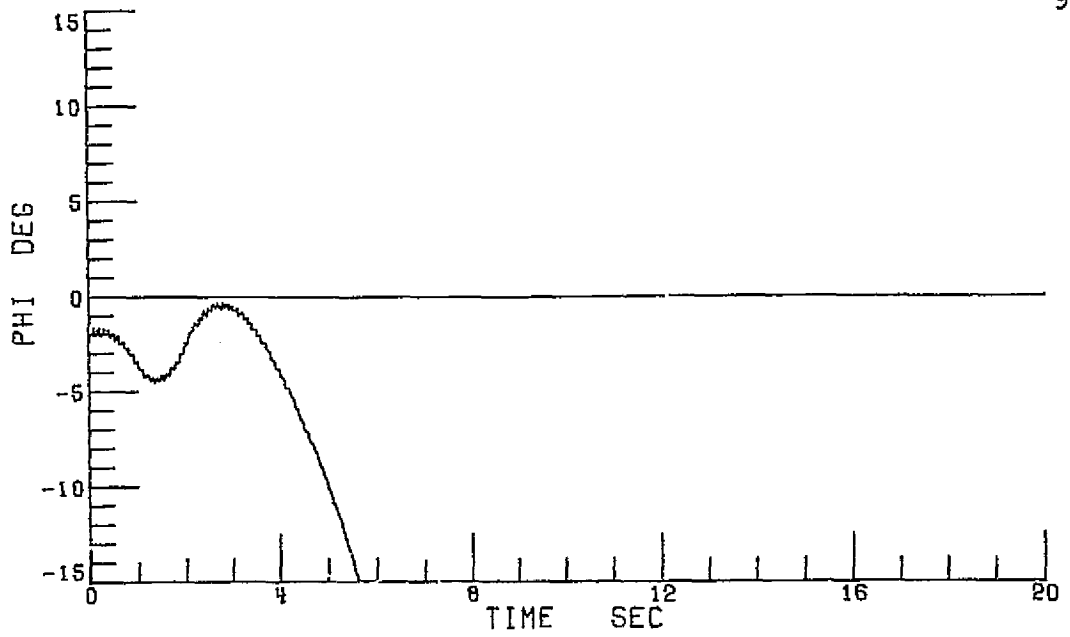

3b X 3s ROTOR, 1/20 SECONDS

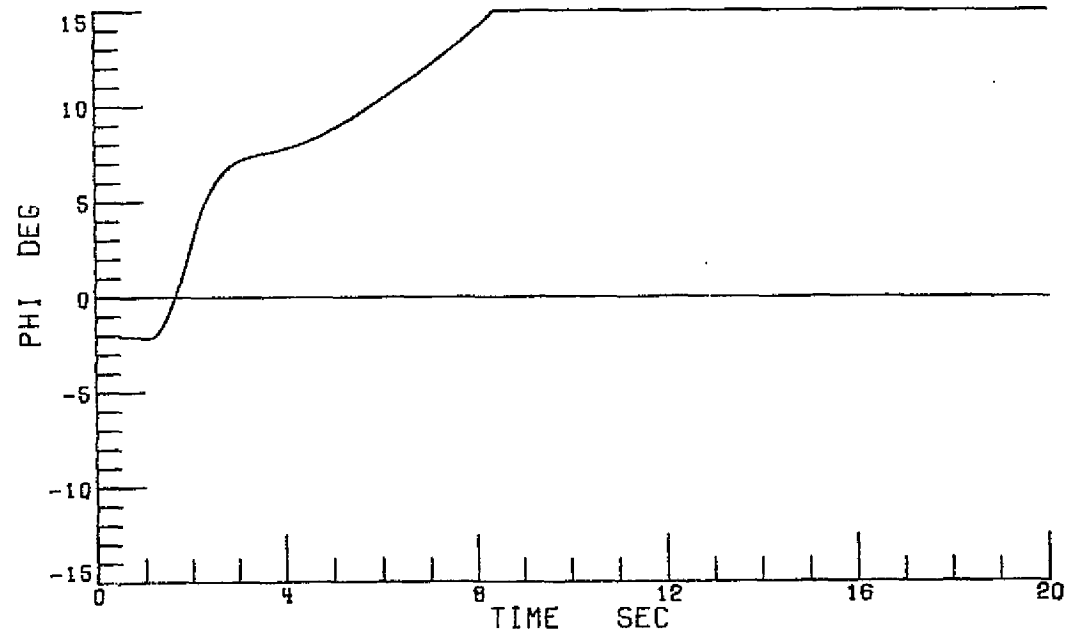

5b X 10s ROTOR, 1/240 SECONDS

Figure 25.- Continued.

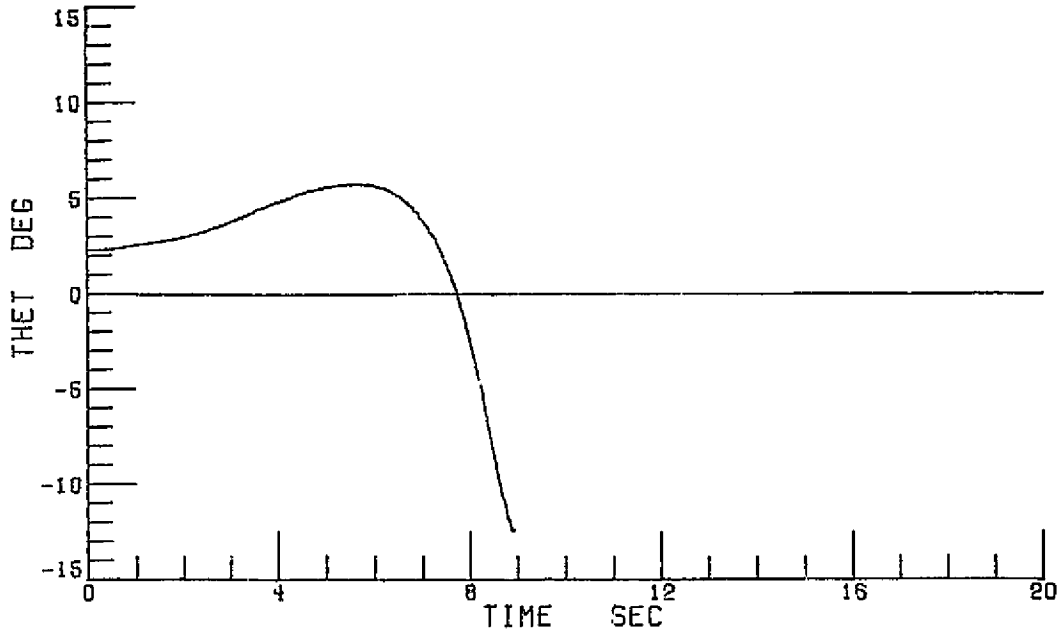

3b X 3s ROTOR, 1/20 SECONDS

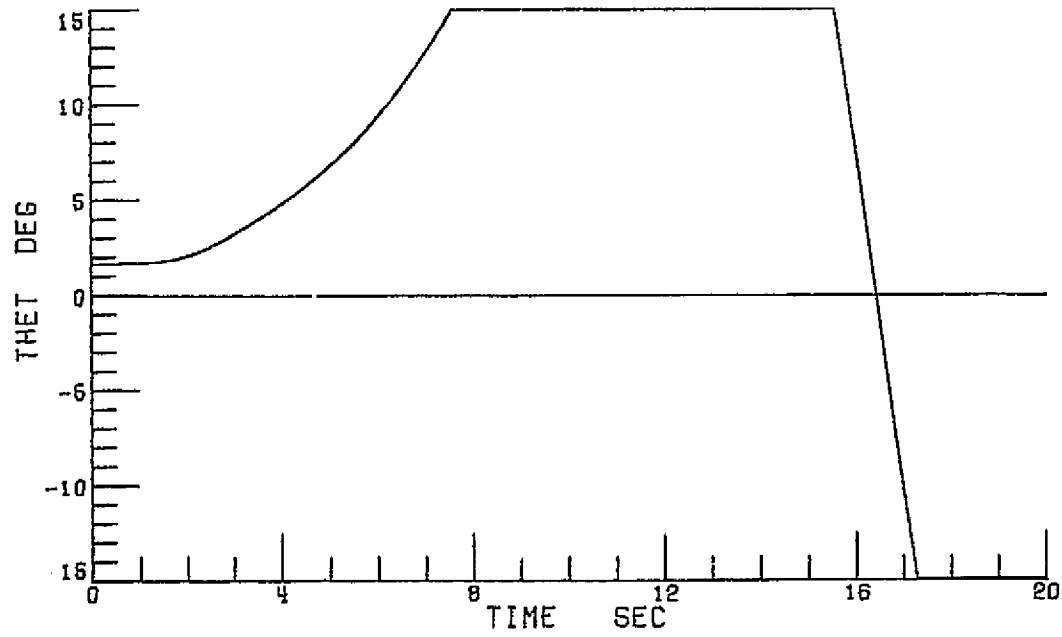

5b X 10s ROTOR, 1/240 SECONDS

Figure 25.- Continued.

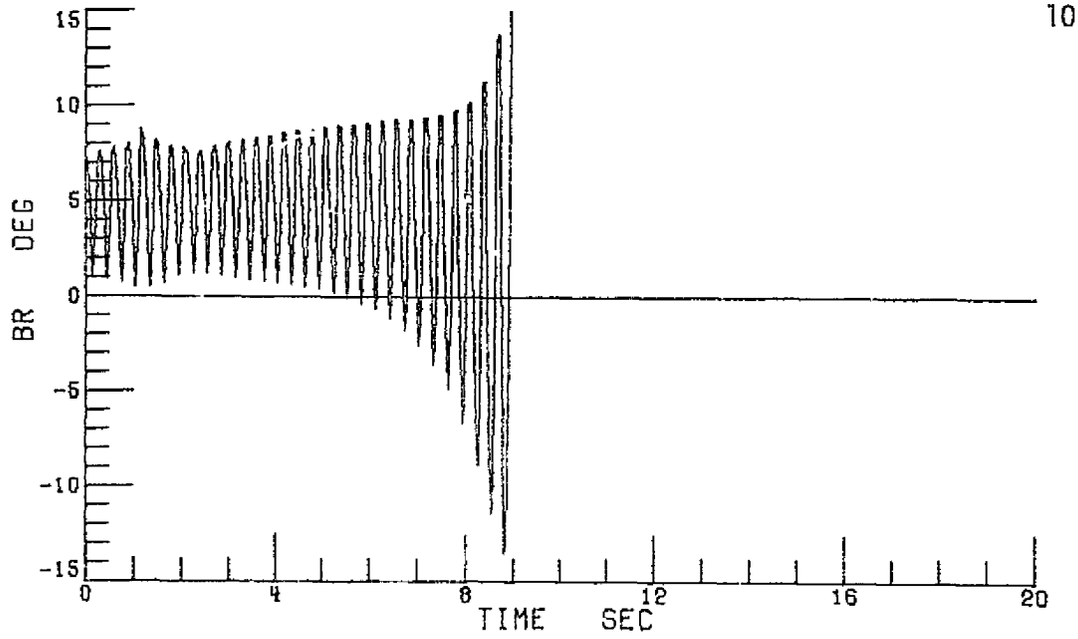

3b X 3s ROTOR, 1/20 SECONDS

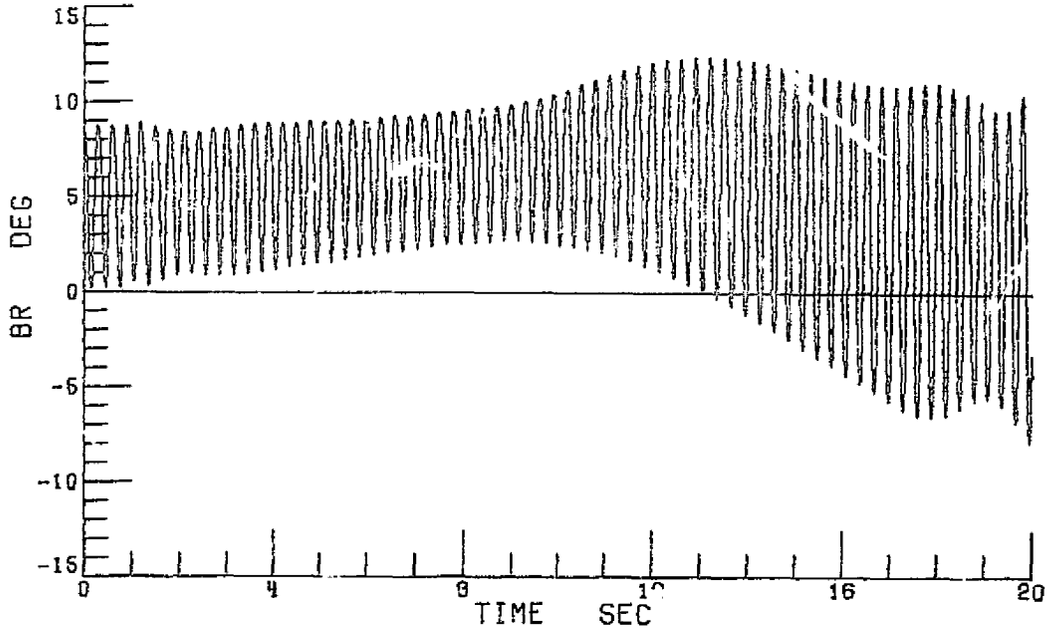

5b X 10s ROTOR, 1/240 SECONDS

Figure 25.- Concluded.

the computer program sustained a fatal error at approximately 9 seconds into the run due to the blade flapping angle going completely unstable.

To summarize, several points are brought out by the dynamic response tests:

(1) Reducing the number of blade segments does not appear to influence the solution to any great extent. This is due to the method used in positioning and determining the lengths of the segments simulated. They always represent equal elemental disk areas, and this tends to distribute the segments toward the high dynamic pressure areas.

(2) Reducing the number of blades tends to amplify the high frequency oscillation of the rotor forces and moments much more than is desirable, and thus affects tne response of the vehicle somewhat as the rotor tends to respond to the number of blades simulated and the tip path plane formed by them.

(3) The most profound effect as would be expected is that of increasing integration interval size. When the integration interval is increased, the blade azimuthal advance angle is also increased therefore decreasing the number of points used to define the rotor forces and moments as the blade sweeps around the azimuth, thus depending on where these points are located, the total forces and moments may tend to be larger or smaller than they should be for the true solution. A second problem arises when the integration interval is increased, and that is loss of accuracy in the numerical integration of the body accelerations and rates. While more sophisticated integration routines are available to allow stretching of the integration interval and retaining accuracy at the same time, they normally require more passes through the equations to update intermediate values of the accelerations and rates thus using up more computing time.

CONCLUSIONS

This paper describes the results of a series of tests designed to examine the effects of degrading a rotating blade element rotor mathematical model in order to fit the model within set computer timing constraints. The three methods of degradation studied were those of reduction of number of blades, reduction of number of blade segments, and increase of integration interval size and thus increase of blade azimuthal advance angle. The tests conducted consisted of static trim comparisons; total rotor force and moment comparisons; index blade force, moment, and angle comparisons for one 360 degree blade sweep; and finally total vehicle dynamic response comparisons for a lateral cyclic control pulse input.

From the data collected the following conclusions were reached:

(1) Reducing blade segments does not appear to influence the solution to any great extent. This is probably due to the method used to determine the blade segment locations. Once the number of blade segments is decided upon, the method positions the blade segments and their size so that equal elemental disk areas are generated. This tends to distribute the blade segments toward the high dynamic pressure areas.

(2) Reducing the number of blades tends to amplify the high frequency content of the body linear and angular accelerations and rates. This is due to the rotor forces and moments oscillating over a wider band. This has two effects. The rotor, and therefore the body, tends to respond to the tip path plane of the number of blades simulated, and the numerical integration formulas used in the integration of the body accelerations and rates tend to respond to the increased amplitude of the high frequency content.

(3) The worst single effect is that of increasing integration interval. This has the double effect of increasing blade azimuthal advance angle and affecting the numerical integrators. When the azimuthal advance angle is increased, the number of points used to define the rotor forces and moments as the blades sweep out the tip path plane is reduced, thus the blades may tend to produce larger or smaller values than the true solution. The second problem arises with the numerical integration formulas one must use for real-time man-in-the-loop simulations. The faster formulas, computationally, are the ones which cannot stand large interval sizes and still retain their accuracy and stability. And the worst problem, is that these two effects tend to amplify each other.

(4) The above effects tend to amplify as the vehicle forward velocity increases and the rotor loads up. Thus while some degradation might be acceptable at low speeds, it may not be suitable at all at higher speeds.

The following recommendations are made:

(1) Do not reduce blade segments less than 3.

(2) Do not reduce blades less than 3.

(3) Do not increase integration interval larger than 1/30 seconds without critically examining the results.

(4) Do not increase azimuthal advance angle larger than 40 degrees.

(5) If the model must be degraded, reduce blade segments first, blades second, and lastly integration interval and azimuthal advance angle.

(6) If any one or combination of the above must be degraded beyond the stated limits to reach real-time, it is recommended that either a different rotor mathematical model be used or a faster computer be used.

REFERENCES

1. Davis, John M.; Bennett, Richard L.; and Blankenship, Barney L.: ROTORCRAFT FLIGHT SIMULATION WITH AEROELASTIC ROTOR AND IMPROVED AERODYNAMIC REPRESENTATION - Volumes I, II, and III. USAAMRDL - TR-74-10A, -10B, -10C, 1974.

2. Niessen, Frank R.: CONTROL THEORY ANALYSIS OF A THREE-AXIS VTOL FLIGHT DIRECTOR. Master's Thesis, The Pennsylvania State University, 1971.

3. Kelly, James R.; Niesson, Frank R.; and Garren, John F., Jr.: A MANUAL - CONTROL APPROACH TO DEVELOPMENT OF VTOL AUTOMATIC LANDING TECHNOLOGY. Presented at the 29th Annual National Forum of the American Helicopter Society, Washington D.C., 1973.

4. Toler, James R.; McIntyre, Walter; and Coffee, Merlin C.: SIMULATION OF HELICOPTER AND V/STOL AIRCRAFT. Volume I - Helicopter Analysis Report. Tech. Rep. NAVTRADEVCEN 1205-1, U.S. Navy, 1963.

5. Baker, E. B.; Hay, I.; and Mitchell, E.E.L.: DEVELOPMENT OF HYBRID COMPUTER PROGRAMS FOR SIMULATION OF COBRA. Volume 1 - Cobra Airframe Simulation. Tech. Rep. ECOM-0387-F2a, U.S. Army, 1969.

6. Houck, Jacob A.; Gibson, Lucille H.; and Steinmetz, G. G.: A REAL-TIME DIGITAL COMPUTER PROGRAM FOR THE SIMULATION OF A SINGLE-ROTOR HELICOPTER. NASA TM X-2872, 1974.

7. Callan, William, M.; Houck, Jacob A.; and DiCarlo, Daniel J.: SIMULATION STUDY OF INTRACITY HELICOPTER OPERATIONS UNDER INSTRUMENT CONDITIONS TO CATEGORY I MINIMUMS. NASA TN D-7786, 1974.

8. Moen, Gene C.; and Yenni, Kenneth R.: SIMULATION AND FLIGHT STUDIES OF AN APPROACH PROFILE INDICATOR FOR VTOL AIRCRAFT. NASA TN D-8051, 1975.

9. Howlett, J.J.: RSRA SIMULATION MODEL - Volumes I & II. Sikorsky Aircraft - SER 72009. NASA/ARMY Contract NAS1-13000, 1974.

10. Cooper, D.E.; and Howlett, J.J.: GROUND BASED HELICOPTER SIMULATION. Presented at Symposium on Status of Testing and Model Techniques for V/STOL Aircraft, American Helicopter Society, Essington, PA, 1972.

A1. Eckhardt, Dave E., Jr.: DESCRIPTION OF LANGLEY RESEARCH CENTER COMPUTER COMPLEX AND SPECIAL FEATURES FOR REAL-TIME SIMULATION APPLICATIONS. Presented at the Eastern Simulation Council Meeting, SCI, NASA Langley Research Center, Hampton, VA, 1968.

APPENDIX A

Langley Research Center's Real-Time Simulation System

The Langley Research Center computer complex consists of three Control Data Corporation (CDC) 6600 computers and two 6400 computers. Two of the CDC 6600 computers are tied to the Real-Time Simulation (RTS) System (Figure A1) which is detailed in Reference A1. Two independent simulation subsystems are provided to support real-time simulation studies. Both of these systems can run concurrently, however, each operates through separate computers. These subsystems are identical in operation and each includes the input/output conversion equipment and control to accommodate multiple simulation jobs simultaneously. Presently three 4-hour shifts per day are run on the RTS system. During the morning shift only one computer is available for real-time simulation studies. Either one large program or two smaller programs are run during this time. On the second and third shifts, two computers are available. Typically two programs are run on one computer, and one large program is run on the second computer.

Each of the simulation subsystems provides the necessary elements of input and output signal conversion, real-time control, program control, and signal distribution to support two real-time simulation jobs simultaneously. Each subsystem contains 80 analog inputs and 960 discrete inputs which are converted and transfered to the computer system by way of the Analog-to-Digital and Discrete Input System, and 192 analog outputs and 960 discrete outputs which are converted from digital output by means of the Digital-to-Analog and Discrete Output System.

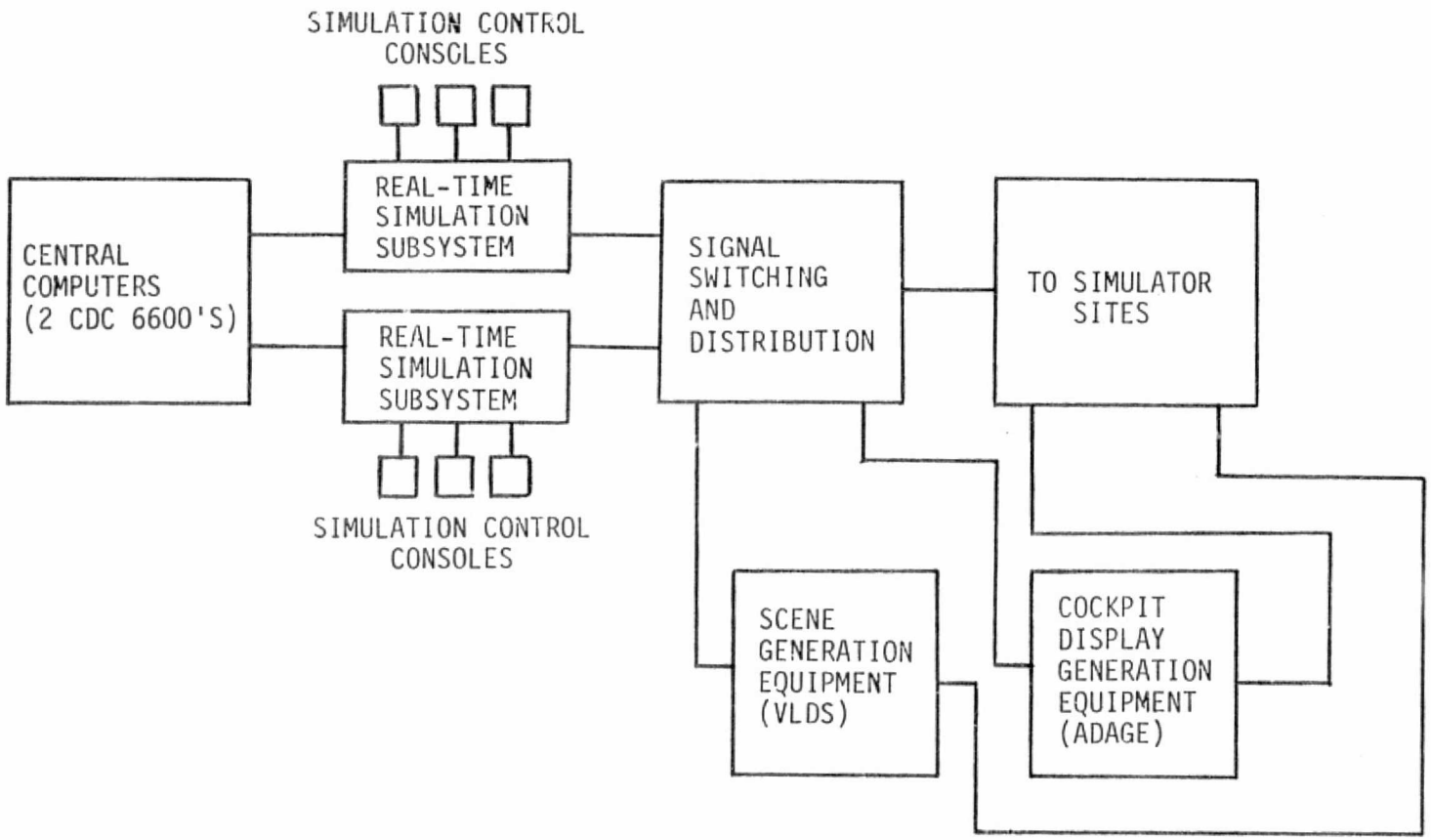

Figure A1.- Langley Research Center's Real-Time Simulation System.

External simulation equipment, such as manned cockpits (Figure A2) with their instrumentation, scene generation equipment, and cockpit display generation equipment are connected to the simulation subsystem by means of analog and discrete patch panels. These panels can be prewired and stored on separate panels allowing for rapid changeover between configurations which distribute the input/output signals to the various simulator sites.

Among the most important aspects of real-time simulation are man-machine communication and the ability to control the simulation program while it is in progress. To provide these capabilities, each subsystem is equipped with three program control stations (Figure A3) consisting of a program control console with function sense switches, potentiometers, indicator lights and connections for analog time-history recorders, and X-Y plotters; a CRT display console; and a typewriter printer. The program control console of each station is connected to the analog/discrete patch panels to provide the real-time functions such as program mode control or special programed functions. The remaining control station equipment, providing service functions such as CRT displays and messages, are connected directly to the computer system.

SIMULATOR SITES

Transport

Terminal Configured Vehicle
Aft Flight Deck

General Aviation

Motion Visual System

Fixed Base 4 - VTOL

Differential Maneuvering Simulator

General Purpose Fixed Base

General Purpose Fighter Cockpit

Figure A2

(a) Typical Program Control Station.

Figure A3.- Operational Control Features.

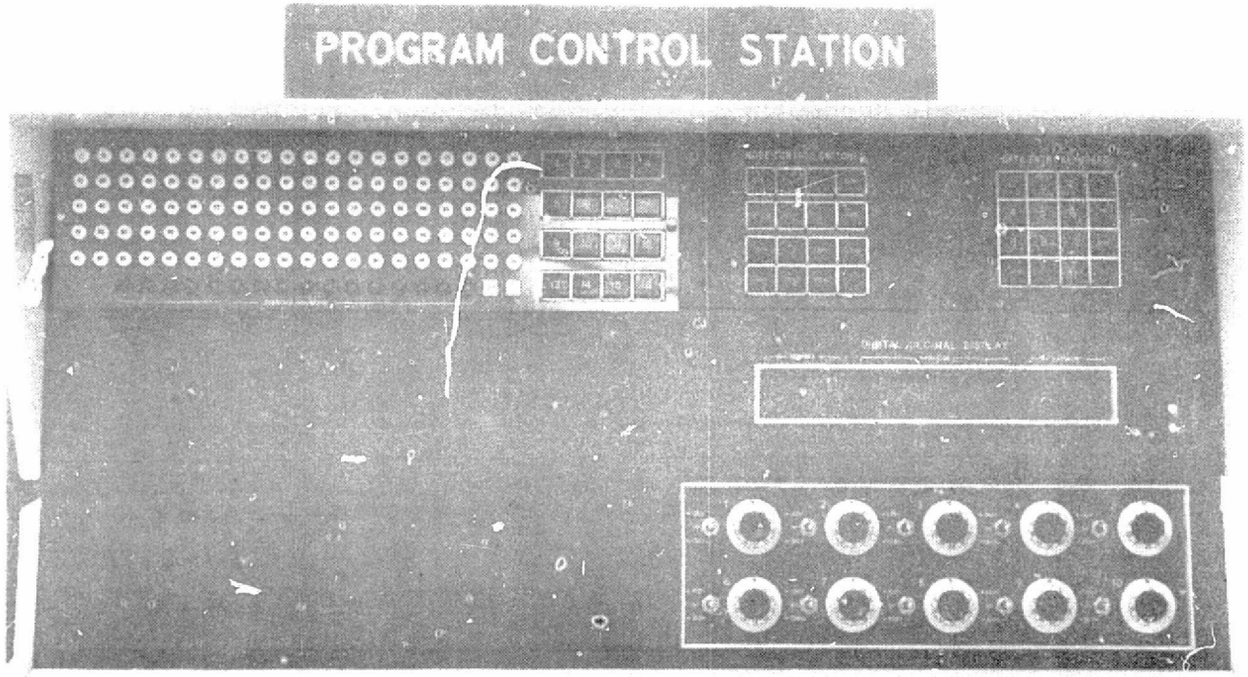

(b) Closeup of Control Panel on the Program Control Console.

Figure A3.- Concluded.

APPENDIX B

Rotor Model Degradation Methods

The following three sections describe the methods used in the degradation of the rotor mathematical model.

A. Blade Reduction

Once the number of blades to be simulated is chosen, the blades are evenly distributed around the disk by use of the following equation:

$$\Delta\Psi_b = \frac{360^0}{b_s}$$

where $\Delta\Psi_b$ is the angle between adjacent blades, starting with blade #1 at 0^0.

b_s is the number of blades to be simulated.

Then the forces and moments are calculated for the blades simulated by the usual equations listed in Reference 9. Next the total rotor forces and moments for the rotor system are calculated in a manner represented by the following general equations:

$$F_T = \frac{b_{mr}}{b_s} \sum_{b=1}^{b=b_s} F_b$$

$$M_T = \frac{b_{mr}}{b_s} \sum_{b=1}^{b=b_s} M_b$$

where F_T represents the total rotor forces.

F_b represents the individual blade forces.

M_T represents the total rotor moments.

M_b represents the individual blade moments.

b_{mr} is the actual number of blades.

b_s is the number of blades simulated.

B. Blade Segment Reduction

First the number of blade segments (n_s) to be simulated is chosen. The positioning of these segments along the blades is determined by the following equations from Reference 9 which are derived based on the assumption of equal annuli area. The reader is directed to Figure B1 for the definitions of the various variables. Distance to Segment Center of Lift:

First Segment

$$y_{2(n=1)} = \left\{ \left[\frac{1 - (\xi + \xi^1)^2}{2n_s} \right] + (\xi + \xi^1)^2 \right\}^{\frac{1}{2}} - \xi$$

Subsequent Segments

$$y_{2(n)} = \left\{ \left[\frac{1 - (\xi + \xi^1)^2}{n_s} \right] + \left(\xi + y_{2(n-1)} \right)^2 \right\}^{\frac{1}{2}} - \xi$$

Distance to Inboard End of Segment from Centerline

$$y_{INB(n)} = \left\{ (\xi + y_{2(n)})^2 - \left[\frac{1 - (\xi + \xi^1)^2}{2n_s} \right] \right\}^{\frac{1}{2}}$$

Distance to Outboard End of Segment from Centerline

$$y_{OUTB(n)} = \left\{ (\xi + y_{2(n)})^2 + \left[\frac{1 - (\xi + \xi^1)^2}{2n_s} \right] \right\}^{\frac{1}{2}}$$

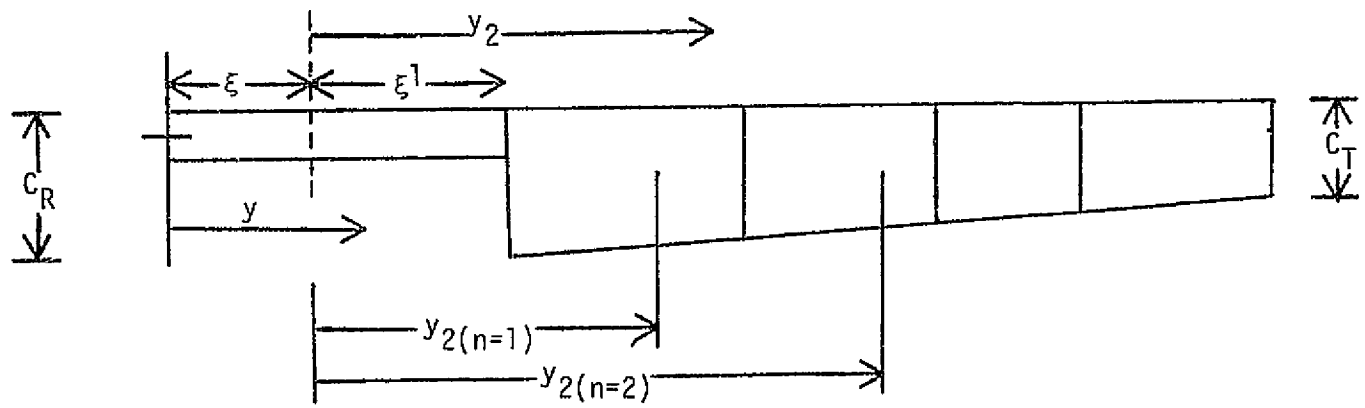

Figure B1.- Blade Segment Definition.

Segment Width

$$\Delta y_{(n)} = y_{OUTB(n)} - y_{INB(n)}$$

Mean Chord of Segment

$$C_{y(n)} = \left[\frac{y_{OUTB(n)} + y_{INB(n)} - 2(\xi + \xi^1)}{2(1 - \xi - \xi^1)}\right] \left[C_T - C_R\right] + C_R$$

C. Integration Interval/Azimuthal Advance Angle Relationship

The user can determine either an integration interval or azimuthal advance angle. Defining one uniquely defines the second assuming a constant rotor speed.

$$\Delta\Psi = 57.3\ \Omega\Delta t$$

where

$\Delta\Psi$ is the azimuthal advance angle.

Δt is the integration interval.

Ω is the rotor rotational speed.